A THEORY OF STATIONARITY AND ASYMPTOTIC APPROACH IN DISSIPATIVE SYSTEMS

Thesis by

Michael T. Rubel

In Partial Fulfillment of the Requirements

for the Degree of

Doctor of Philosophy

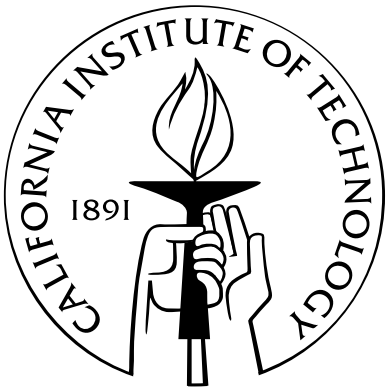

California Institute of Technology

Pasadena, California

2007

(Defended October 6, 2006)

Acknowledgements

First, I would like to acknowledge my research advisor, Prof. Anthony Leonard, for his unwavering support. Prof. Leonard taught subtly and patiently, preferring to ask deceptively simple questions rather than to issue explicit instructions. Our conversations shaped many of the concepts that appear in this thesis.

In addition to Prof. Leonard, my thesis committee also included Prof. Tim Colonius, Prof. Jerrold Marsden, Prof. Dale Pullin, and Prof. Joseph Shepherd, all of Caltech, whose comments and suggestions brought much-needed clarity to the discussion and forged connections to the wider body of scientific discourse. Committee members were kind enough to meet with me as a group on four separate occasions, as well as individually.

I would further like to acknowledge my colleagues in GALCIT's Iris Laboratory, in particular Mr. Daniel Chung, Dr. Vincent Wheatley, Dr. Philippe Chatelain, and Mr. Manuel Lombardini, as well as Prof. Dr. Michael Dellnitz, Chair of Applied Mathematics at the Universität Paderborn, for valuable discussions regarding certain parts of the material.

Financially, this work was supported in large part by the United States Department of Energy (DE-AC03-98EE50506 and through Lawrence Livermore National Laboratory) and also by Caltech. I would like to acknowledge our collaborators including Dr. Rose McCallen of Lawrence Livermore National Laboratories, and Dr. Jules Routbort and the late Dr. Sid Diamond, both of the Department of Energy, for their steadfast support. Dr. Diamond fought tenaciously to keep our program funded, believing as I do that reducing energy consumption, besides being in the national best interest, is essential for the future. A large fraction of energy consumed in the United States goes into overcoming drag on heavy vehicles, making improvement of their aerodynamics an imperative. The

seeds of this research grew out of a realization that conventional fluid flow approximations, based on time integration of model equations, address what is in some sense the wrong question. We still remain far away from being able to predict the drag force on a truck directly, but I hope that this work will prove to be a small step in the right direction.

At a personal level, I would like to acknowledge my family and friends; none of this would have been possible without their love and support. I am deeply grateful for their patience and dedication, particularly during the last few years as my research became an all-consuming affair, occupying days, nights and weekends.

Most of all, I would like to express gratitude to my parents, Laurence and Sandra, who made the well-being of their children their primary goal, and who continually emphasized the importance of education.

Abstract

The approximate dynamics of many physical phenomena, including turbulence, can be represented by dissipative systems of ordinary differential equations. One often turns to numerical integration to solve them. There is an incompatibility, however, between the answers it can produce (i.e., specific solution trajectories) and the questions one might wish to ask (e.g., what behavior would be typical in the laboratory?) To determine its outcome, numerical integration requires more detailed initial conditions than a laboratory could normally provide. In place of initial conditions, experiments stipulate how tests should be carried out: only under statistically stationary conditions, for example, or only during asymptotic approach to a final state. Stipulations such as these, rather than initial conditions, are what determine outcomes in the laboratory.

This theoretical study examines whether the points of view can be reconciled: What is the relationship between one's statistical stipulations for how an experiment should be carried out—stationarity or asymptotic approach—and the expected results? How might those results be determined without invoking initial conditions explicitly?

To answer these questions, stationarity and asymptotic approach conditions are analyzed in detail. Each condition is treated as a statistical constraint on the system—a restriction on the probability density of states that might be occupied when measurements take place. For stationarity, this reasoning leads to a singular, invariant probability density which is already familiar from dynamical systems theory. For asymptotic approach, it leads to a new, more regular probability density field. A conjecture regarding what appears to be a limit relationship between the two densities is presented.

By making use of the new probability densities, one can derive output statistics directly, avoiding the need to create or manipulate initial data, and thereby avoiding the conceptual incompatibility

mentioned above. This approach also provides a clean way to derive reduced-order models, complete with local and global error estimates, as well as a way to compare existing reduced-order models objectively.

The new approach is explored in the context of five separate test problems: a trivial one-dimensional linear system, a damped unforced linear oscillator in two dimensions, the isothermal Rayleigh-Plesset equation, Lorenz's equations, and the Stokes limit of Burgers' equation in one space dimension. In each case, various output statistics are deduced without recourse to initial conditions. Further, reduced-order models are constructed for asymptotic approach of the damped unforced linear oscillator, the isothermal Rayleigh-Plesset system, and Lorenz's equations, and for stationarity of Lorenz's equations.

Contents

List of Figures

List of Tables

Chapter 1

Introduction

1.1 Context of the present work

This study concerns finite systems of ordinary differential equations of the following form:

$$\frac{d\mathbf{Y}}{dt} = \mathbf{f}\left(\mathbf{Y}\right) \tag{1.1}$$

Equations such as (1.1) arise often in dynamics, where they describe how a system changes over time. Both sides of the equations are N-component vectors. The vector $\mathbf{f}(\mathbf{Y})$, for example, has components $f_1(\mathbf{Y})$, $f_2(\mathbf{Y})$, and so on, up to $f_N(\mathbf{Y})$. Notationally, $\mathbf{Y}$ is shorthand for $\mathbf{Y}(\mathbf{Y_0}, t)$.

Components of the *phase vector*[1] $\mathbf{Y}(\mathbf{Y_0}, t)$ collectively represent the state of the system at time t. In a simple mass-spring system, for example, $\mathbf{Y}(\mathbf{Y_0}, t)$ might have two components: position and velocity of the mass. The space of (instantaneous) phase vectors of (1.1) is called its *phase space*. Over time, $\mathbf{Y}(\mathbf{Y_0}, t)$ traces out a *trajectory* through phase space.

Equation (1.1) is accompanied by an *initial condition* vector $\mathbf{Y_0}$ specifying the state of the system at time zero. That is, $Y_i\left(\mathbf{Y_0}, 0\right) = Y_{0i}$, for all $i = 1 \ldots N$. The initial condition marks the starting point of the trajectory through phase space.

The right-hand side of (1.1) is a function $\mathbf{f}(\mathbf{Y})$ that expresses how $d\mathbf{Y}/dt$ can be determined from $\mathbf{Y}$. We assume that $\mathbf{f}(\mathbf{Y})$ is a smooth function, which is often a reasonable assumption for physical systems. In the mass-spring example, $\mathbf{f}(\mathbf{Y})$ would relate the rate of change of position to velocity,

[1] Some authors use the term "state vector" rather than "phase vector," but they have the same meaning here.

and of velocity to the spring force.

We also assume that equation (1.1) admits at least one compact *trapping region* Ω, i.e., a region of phase space that trajectories enter but do not leave. This is a strong assumption, but it is sometimes justified when $\mathbf{f}(\mathbf{Y})$ represents a physical system whose total energy remains bounded. For example, in a damped mass-spring system, any circle of constant energy encloses a trapping region.

Finally, we assume that the *phase-space divergence* of $\mathbf{f}(\mathbf{Y})$,

$$\nabla \cdot \mathbf{f} = \frac{\partial f_i}{\partial Y_i} \tag{1.2}$$

(summation implied on repeated indices), is negative[2] and bounded throughout Ω. This is also a strong assumption—dissipative systems tend to lose energy over time. Unforced physical systems are typically dissipative, but if $\mathbf{f}(\mathbf{Y})$ includes external forcing, it can make (1.2) positive over parts of phase space.

Given the initial condition vector $\mathbf{Y_0}$, equation (1.1) can be *solved* for $\mathbf{Y}(\mathbf{Y_0}, t)$ by integrating forward in time. If $\mathbf{f}(\mathbf{Y})$ is sufficiently simple, then the integration can be performed analytically; if not, one must resort to numerics. Numeric integration produces an approximation to $\mathbf{Y}(\mathbf{Y_0}, t)$ given a specific starting point $\mathbf{Y_0}$. Thus, given a set of ordinary differential equations like (1.1) and a specific starting point $\mathbf{Y_0}$, it is straightforward conceptually—if not always practically—to integrate out the solution trajectory $\mathbf{Y}(\mathbf{Y_0}, t)$.

However, questions about (1.1) do not often seek a specific trajectory. Instead, they ask for generalizations applicable to broad classes of initial conditions: "How does the average speed of the mass in a mass-spring system relate to its peak oscillation amplitude?" "How does the flow rate of water through a pipe vary with pressure?" Or, "What is the average aerodynamic drag on a truck body?"

Such questions are accompanied not by a specific $\mathbf{Y_0}$, but by stipulations about how the test should be conducted. Perhaps initial transients should be allowed to decay before recording measure-

[2]Such systems are usually called *dissipative* in dynamical systems literature. The case $\nabla \cdot \mathbf{f} = 0$ is of particular importance to Hamiltonian problems.

ments, for example; perhaps measurements should only be recorded under statistically stationary conditions. Stipulations of this kind, which must hold from $t = 0$ onward, will be called *experimental conditions* here. They are not always stated explicitly.

There is evidently a mismatch between the questions asked of (1.1) and the answers numerical integration can provide. Numerical integration needs initial conditions, not experimental conditions. The upshot is that there are whole classes of problems for which representative initial conditions must be manufactured artificially. A typical solution procedure might be:

1. make up a pre-initial condition (call it $\mathbf{Y_{00}}$) at random, where experimental conditions might not yet be satisfied,
2. integrate numerically until experimental conditions are satisfied,
3. label the phase vector at that point $\mathbf{Y_0}$ and set $t = 0$,
4. continue to integrate numerically, constructing $\mathbf{Y}(\mathbf{Y_0}, t)$, and
5. repeat again and again, accumulating averages and confidence.

(Repetition can sometimes be avoided by taking long time averages instead,[3] but the distinction is immaterial here.) A well-known problem that requires this kind of treatment, and that will serve to motivate our approach, is the numerical simulation of turbulent flow.

1.2 Motivation in turbulence

When applied to a detailed turbulent flow, numerical integration is known as *direct numerical simulation*, or DNS. DNS begins with a discretization of the Navier-Stokes equations, including boundary conditions, into form (1.1). This means the velocity field $\mathbf{u}(\mathbf{x}, t)$ is written as an inner product of $\mathbf{Y}(\mathbf{Y_0}, t)$ with a vector of basis functions $\boldsymbol{\phi}(\mathbf{x})$:

$$\mathbf{u}(\mathbf{x}, t) = \sum_{i=1}^{N} Y_i(\mathbf{Y_0}, t)\, \boldsymbol{\phi}_i(\mathbf{x}) \tag{1.3}$$

[3]The assumption that time and ensemble averages are equivalent is called the ergodic hypothesis, and it can be rigorously justified in some cases, most famously by Birkhoff (1931) for certain systems satisfying $\nabla \cdot \mathbf{f} = 0$.

For a typical discretization, the right-hand side $\mathbf{f}(\mathbf{Y})$ has quadratic and linear parts; the quadratic part comes from the convection and pressure gradient terms of Navier-Stokes, the linear part from the viscous decay term. The discretization must be fine enough to capture all relevant scales, which tends to inflate N. Kaneda et al. (2003) recently studied turbulence in a 4096^3 periodic box on the Earth Simulator computing system, a feat requiring N of order 10^{11}. For a review of turbulent DNS, see Moin and Mahesh (1998).

The initial condition $\mathbf{Y_0}$ of a turbulent DNS must describe the complete flowfield at $t = 0$. The fine details of $\mathbf{Y_0}$, however, are rarely of interest. Apart from the constraints imposed by experimental conditions, $\mathbf{Y_0}$ may be assigned any reasonable values. Choosing $\mathbf{Y_0}$ values typically involves starting from an even earlier point ($\mathbf{Y_{00}}$, mentioned above), whose components are completely arbitrary, and integrating until transients die out (i.e., until experimental conditions hold). The state that remains at the end of this start-up process becomes $\mathbf{Y_0}$.

It may be the most trusted technique in turbulence prediction, but DNS seems highly inefficient when regarded as a black box (Figure 1.1, top). DNS begins by combining experimental conditions (stationarity or asymptotic approach behavior during the observation period) with a great deal of arbitrary seed data (the components of $\mathbf{Y_{00}}$, sometimes terabytes in size) to create one very large vector ($\mathbf{Y_0}$). This vector is processed in a computationally expensive way (DNS integration), only to be distilled back down onto a small number of degrees of freedom for the outputs (average spectra, correlations, force coefficients, and so on) that—if the initialization was done properly—should be statistically independent of $\mathbf{Y_{00}}$.

One cannot help but wonder whether the arbitrary $\mathbf{Y_{00}}$ data could be eliminated entirely. Might it be possible to obtain the same outputs without actually constructing and manipulating $\mathbf{Y_0}$? Rather than using certain experimental conditions as a basis for choosing $\mathbf{Y_0}$, could the conditions themselves be taken as inputs, as illustrated in Figure 1.1, bottom? If such a procedure were possible, it would answer scientific questions more directly than numerical integration can. Moreover, the size of inputs would be far smaller (no $\mathbf{Y_{00}}$ data), suggesting the possibility of reduced computational effort.

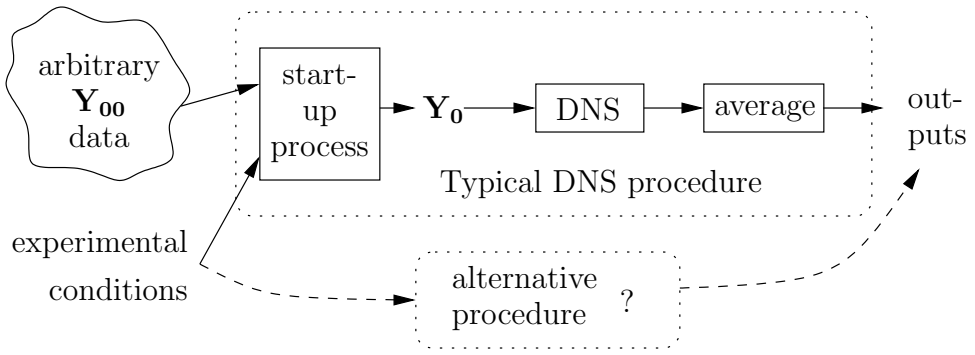

Figure 1.1: Top: Black-box view of DNS. Typically, a great deal of random, arbitrary $\mathbf{Y_{00}}$ data is combined with an experimental condition (such as stationarity), leading to outputs that should be independent of the $\mathbf{Y_{00}}$ data. Bottom: Might some alternative procedure allow the same outputs to be calculated without making use of ultimately irrelevant data?

The question implied in the previous paragraph is this: What is the relationship between experimental conditions and output statistics? Put another way, if the measurement statistics of a system show stationarity or asymptotic approach, what other properties must they show as well? Answering that question will be the primary goal of this study.

1.3 Two experimental conditions

Two types of experimental conditions, mentioned in passing above, stand out in the turbulence DNS literature. The first is stationarity. In this context, stationarity means that $\mathbf{Y}(\mathbf{Y_0}, t)$ is a statistically stationary process during the observation period, which begins at $t = 0$. Common examples include forced turbulence in a periodic box (e.g., Kaneda et al. (2003)) and forced channel flow (e.g., Moser et al. (1999)).

The second type of experimental condition is asymptotic approach. Less well defined than stationarity, asymptotic approach is correspondingly less well represented in the turbulence DNS literature. It is a state of steady decay to some final limit: after initial transients have died away, but while elapsed time still remains finite. The classic problem of unforced turbulence in a periodic box is perhaps the best-known example. Its asymptotic approach begins some time after stirring ends, and it continues indefinitely.

On the other hand, the limit point of asymptotic approach need not be motionless; for forced problems, it might be a state of dynamic equilibrium. For example, consider the acceleration of fluid in a pipe after impulsively pressurizing one end. There is an initial transient, followed by a long, gradual approach to statistically stationary flow. Asymptotic approach might thus describe the process by which a stationary state is achieved.

This study's analysis is based on the following observation: Both stationarity and asymptotic approach conditions ultimately amount to constraints on which parts of phase space may be occupied during measurement. Regions of phase space that correspond to the presence of strong initial transients, for example, should neither be occupied during stationarity nor during asymptotic approach. Stationary conditions exclude regions of gradual, directed change as well.

In the laboratory, such constraints are imposed by selection. An apparatus (e.g., a wind tunnel) is specifically designed to produce, for example, stationary conditions. It makes use of flow straighteners, screens, smooth expansions and contractions, and so on; the net effect of these choices is to enforce stationarity, thereby limiting attention to a certain subset of the phase space. Timing also plays a part; data taken before stationarity is achieved, or after it ends (surely there is an "off" switch!) are summarily discarded.

For analysis, probabilities will be assigned to each point in phase space according to which experimental condition is assumed. To understand the connection to output statistics, however, it is first necessary to review the concept of ensembles and ensemble averaging.

1.4 A word about ensembles

It is customary to describe turbulent behavior in terms of averages over time, space, or most generally,[4] ensemble. In the laboratory, such averages are sometimes repeatable even when other flow features (e.g., individual eddies) are not. Stationarity and asymptotic approach are both examples of average properties.

[4]Both temporal and spatial averaging are special cases of ensemble averaging. The mean over an ensemble of temporally shifted flows (that is, each ensemble member has the form $\mathbf{u}(\mathbf{x}, t-\tau)$ for some value of τ) is equivalent to a time average; that over an ensemble of spatially shifted flows is similarly a space average.

To construct an ensemble average, repeat an experiment governed by (1.1) many times, each time starting from a different $\mathbf{Y_0}$. The distribution of $\mathbf{Y_0}$ points reflects uncertainties about the initial condition. If there is no uncertainty, then the density is Dirac's δ, a distribution whose central moments (i.e., moments taken about the mean) are all zero. More uncertainty means larger-magnitude central moments. The arithmetic mean of all measurements, taken over all realizations and weighted by their frequencies of occurrence, is the ensemble average.

If the initial distribution of $\mathbf{Y_0}$ points is assumed to be continuous and differentiable, then it is possible to describe its motion with a partial differential equation. The relevant theory is due to Liouville. One might reasonably hope to apply this technique to finding averages directly (that is, taking averages over variations in $\mathbf{Y_{00}}$ seed data), but when $\mathbf{f}(\mathbf{Y})$ describes such chaotic behavior as turbulence, this approach tends to fare poorly. Arbitrarily small details of the initial distribution grow rapidly in importance, overwhelming whatever averages were originally of interest.

Another line of attack is needed—one that is not based on taking averages of the governing equations.

1.5 The sample point density

1.5.1 Definition

Let the *sample point density* $\rho(\mathbf{y})$ be a probability density function on $\mathbf{y} \in \Omega$. As a probability density function, it has the normalization property

$$\int_\Omega \rho(\mathbf{y})\, dV = 1. \tag{1.4}$$

and is strictly nonnegative ($\rho(\mathbf{y}) \geq 0$).

The expected value of any *observable* function $\varphi(\mathbf{y})$ with respect to $\rho(\mathbf{y})$ is

$$\langle \varphi(\mathbf{y}) \rangle = \int_\Omega \varphi(\mathbf{y}) \rho(\mathbf{y})\, dV \tag{1.5}$$

The intent of this definition is as follows.

1.5.2 Intent

Consider an experiment on a system obeying (1.1). During each run of the experiment, $\mathbf{Y}(\mathbf{Y_0}, t)$ begins at some initial condition and proceeds forward in time, integrating $\mathbf{f}(\mathbf{y})$ along the way. Meanwhile, *measurements* are recorded for one or more observables $\varphi(\mathbf{y})$. That is, during each run, every $\varphi(\mathbf{y})$ is evaluated at one or more $\mathbf{Y}$. Finally, the recorded values are analyzed statistically, yielding the desired outputs: means, variances, correlations, and so forth.

Generally speaking—particularly for the kinds of problems that motivate this study—the scientist conducting the experiment does not have a full view of the phase space. That is, the number of independent measured observables is usually smaller than N, the number of degrees of freedom in $\mathbf{Y}$. (Numerical experiments are an obvious exception, but the reasoning below still applies.) Suppose, then, that the experiment is also monitored by an omnicient observer having a complete and accurate view of phase space. Further suppose that, each time the scientist records a measurement, the omnicient observer places a mark, a *sample point*, in phase space at the instantaneous location of $\mathbf{Y}(\mathbf{Y_0}, t)$. Apart from measurement error, the omnicient observer can deduce the scientist's recorded values by evaluating each $\varphi(\mathbf{y})$ there.

Over the course of the experiment, the omnicient observer accumulates a cloud of sample points in phase space. The cloud includes points recorded at different times and even during different runs. Averages of the measurement data—that is, output statistics—are, simply, moments of the sample point cloud.

The sample point density $\rho(\mathbf{y})$ is intended to represent the (continuum) density by which the omniscient observer's sample point cloud is distributed. A conjecture has been implied: that the sample points are, in fact, distributed according to an underlying density function. The rationale is that it would otherwise be impossible to reproduce certain experimental results, and results that cannot be replicated fall outside our domain of interest.

Working with a sample point density will be easier than trying to reason about clouds of sample

points. They are related in an obvious way: The mean of the scientist's measurements for any observable should approach the corresponding moment of $\rho(\mathbf{y})$ as the number of samples increases.

1.5.3 Historical note

The preceeding definition and motivation are inspired by a number of ideas in statistical thermodynamics, particularly Boltzmann's ensembles and the Bayesian perspective of Jaynes (1989).

1.6 Problem statement

Cast in terms of $\rho(\mathbf{y})$, the principal question of this thesis (first introduced at the end of Section 1.2) is: What do experimental conditions such as stationarity and asymptotic approach imply about the sample point density?

The answer, as we shall see in Chapters 2 and 3, is that they are assertions regarding broad classes of output statistics. In each case, equations for $\rho(\mathbf{y})$ can be derived by stipulating that those assertions should hold. The approach is similar to a maximum entropy formulation, except that rather than constructing a probability density function by maximizing entropy, we will construct it by enforcing stationarity or asymptotic approach.

A significant second question is: What does the sample point density, thus determined, imply about statistics and reduced-order behavior?

Equation (1.5) gives the beginning of an answer to this question, which will be addressed in Chapter 4 and throughout the examples.

1.7 The expected values of time derivatives

Because $\rho(\mathbf{y})$ has no built-in time dependence, it is not immediately obvious how to apply it to such time-dependent statistical quantities as stationarity or asymptotic approach. In this section we use $\rho(\mathbf{y})$ to compute the expected value of time derivatives, a key prerequisite.

Recall that $\mathbf{Y}(\mathbf{Y_0}, t)$ represents the state of a system evolving from a starting point $\mathbf{Y_0}$ at time zero. The value that would be measured for observable $\varphi(\mathbf{y})$ at time t is $\varphi(\mathbf{Y}(\mathbf{Y_0}, t))$.

Now suppose that, during the course of experiments, in addition to measuring $\varphi(\mathbf{Y}(\mathbf{Y_0}, t))$ at each test point, one also measured $\partial\varphi/\partial t|_{\mathbf{Y}(\mathbf{Y_0},t)}$, the rate at which $\varphi(\mathbf{Y}(\mathbf{Y_0}, t))$ changes along its trajectory (fixed $\mathbf{Y_0}$). How can the average value of $\partial\varphi/\partial t|_{\mathbf{Y}(\mathbf{Y_0},t)}$ be determined from $\rho(\mathbf{y})$?

By the chain rule,

$$\frac{\partial\varphi(\mathbf{Y}(\mathbf{Y_0}, t))}{\partial t} = \left.\frac{\partial\varphi}{\partial y_i}\right|_{\mathbf{Y}(\mathbf{Y_0},t)} f_i(\mathbf{Y}(\mathbf{Y_0}, t)) \tag{1.6}$$

Thus the phase function associated with the time derivative of $\varphi(\mathbf{Y}(\mathbf{Y_0}, t))$, with $\mathbf{Y_0}$ held constant, is $\left.\frac{\partial\varphi}{\partial y_i}\right|_{\mathbf{y}} f_i(\mathbf{y})$. Substituting it into (1.5),

$$\left\langle \frac{\partial\varphi(\mathbf{Y}(\mathbf{Y_0}, t))}{\partial t} \right\rangle = \left\langle f_i(\mathbf{y}) \frac{\partial\varphi(\mathbf{y})}{\partial y_i} \right\rangle = \int_\Omega \rho(\mathbf{y}) f_i(\mathbf{y}) \left.\frac{\partial\varphi}{\partial y_i}\right|_{\mathbf{y}} dV \tag{1.7}$$

Using the product rule, the integrand on the right-hand side of (1.7) is $\partial(f_i\rho\varphi)/\partial y_i - \varphi\partial(\rho f_i)/\partial y_i$ evaluated at $\mathbf{y}$. Substituting this difference into (1.7) and applying the divergence theorem to the first term on the right-hand side leaves

$$\left\langle \frac{\partial\varphi(\mathbf{Y}(\mathbf{Y_0}, t))}{\partial t} \right\rangle = \int_{\partial\Omega} \varphi(\mathbf{y}) \left(\rho\mathbf{f}\cdot\hat{\mathbf{n}}\right) dS - \int_\Omega \varphi(\mathbf{y}) \left(\nabla\cdot(\rho\mathbf{f})\right) dV \tag{1.8}$$

where

- $\partial\Omega$ is the boundary of Ω
- dS is a differential unit of area on $\partial\Omega$
- $\hat{\mathbf{n}}$ is the unit outward normal vector to $\partial\Omega$ at $\mathbf{y}$
- $\rho\mathbf{f}\cdot\hat{\mathbf{n}}$ is $\rho(\mathbf{y}) f_i(\mathbf{y}) \hat{n}_i(\mathbf{y})$
- $\nabla\cdot\rho\mathbf{f}$ is $\frac{\partial}{\partial y_i}\left(\rho(\mathbf{y}) f_i(\mathbf{y})\right)$

In order to invoke the divergence theorem for (1.8), it was necessary to assume that the product $\rho\varphi\mathbf{f}$ is at least C^1 over Ω; there are situations below for which that assumption does not hold.

While it is not essential for the discussion that follows, it should be noted that there is a connection between (1.8) and Liouville's equation for the conservation of probability mass.[5]

Let $R(\mathbf{y}, \tau - t)$ be an auxiliary time-dependent probability density function on Ω satisfying $R(\mathbf{y}, 0) = \rho(\mathbf{y})$. That is, $R(\mathbf{y}, \tau - t)$ is a time-evolving (in τ) PDF that, at the instant $\tau = t$, takes the value $\rho(\mathbf{y})$. Further suppose R obeys Liouville's equation, which governs the convection of probability mass through phase space:

$$\frac{\partial R}{\partial \tau} + \frac{\partial}{\partial y_i}\left(f_i R\right) = 0 \tag{1.9}$$

Then $\partial R/\partial \tau|_{\mathbf{y},\tau=t}$ is $-\,\partial(\rho f_i)/\partial y_i|_{\mathbf{y}}$, which matches the $-\nabla \cdot (\rho \mathbf{f})$ expression in the volume integral of (1.8). Thus if $\rho(\mathbf{y})$ vanishes on $\partial\Omega$, or if Ω is unbounded and $\rho(\mathbf{y})$ decays rapidly, then Liouville's equation provides an alternative way to compute and interpret time-dependent statistics.

1.8 Overview of the thesis

In Chapters 2 and 3, it is shown that the two experimental conditions, stationarity and asymptotic approach, each lead to a different constraint for $\rho(\mathbf{y})$ in phase space. Stationarity leads to a singular $\rho_{\text{stationary}}(\mathbf{y})$, while asymptotic approach leads to a linear partial differential equation for $\rho_{\text{asymptoticapproach}}(\mathbf{y})$, and the former appears to be a long-time limit of the latter. General solutions are found and their qualitative properties are discussed. Numerical solution and approximation techniques are also introduced.

Chapter 4 describes a useful application for the theory: constructing reduced-order models. It also shows how existing reduced-order models can be understood as sets of assumptions about $\rho(\mathbf{y})$.

Over the next several chapters, multiple worked examples of the technique are presented. The examples illustrate the process of defining the problem, finding situationally appropriate $\rho(\mathbf{y})$ functions, and computing useful outputs. Chapter 5 introduces the technique using the trivial system $Y' = -Y$. Chapter 6 examines a simple damped mass-spring system in two dimensions. In Chapter

[5] Some authors reserve the term "Liouville's equation" for when $\mathbf{f}(\mathbf{y})$ is Hamiltonian; we are using it more liberally here.

7, the technique is applied to gas bubbles obeying the isothermal Rayleigh-Plesset equation. Then, in Chapter 8, we consider Lorenz's dynamical system in three dimensions, compute appropriate density functions, and use them to construct reduced-order models. Chapter 9 presents Burgers' equation, where we predict the energy spectrum in the Stokes limit analytically.

Chapter 2

Theory of stationarity

Two experimental conditions, stationarity and asymptotic approach, were introduced in Chapter 1. In this chapter, the first of these conditions is translated into specific, quantitative constraints on $\rho(\mathbf{y})$. Analogous constraints for asymptotic approach are derived in Chapter 3. For clarity, when $\rho(\mathbf{y})$ refers to a stationary process, it will sometimes be labeled $\rho_{\text{stationarity}}(\mathbf{y})$.

For motivation, we begin with a naïve translation of statistical stationarity into partial differential equations on $\rho(\mathbf{y})$. Initial attempts to solve those equations will fail, but they will serve as a natural introduction to established results from dynamical systems theory.

2.1 Stationarity

A stationary process is one whose probability density is time-invariant. For continuous $\rho(\mathbf{y})$, this is equivalent (see Eq. 2.4, recall Liouville's theorem) to requiring that

$$\left\langle \frac{\partial \varphi\left(\mathbf{Y}(\mathbf{Y_0}, t)\right)}{\partial t} \right\rangle = 0 \tag{2.1}$$

for *all* continuously differentiable phase functions $\varphi(\mathbf{y})$. Substituting from (1.8), equation (2.1) requires that

$$\int_{\partial\Omega} \varphi(\mathbf{y}) \left(\rho \mathbf{f} \cdot \hat{\mathbf{n}}\right) \, dS - \int_{\Omega} \varphi(\mathbf{y}) \left(\nabla \cdot (\rho \mathbf{f})\right) \, dV = 0 \tag{2.2}$$

If equation (2.2) holds for *all* continuously differentiable $\varphi(\mathbf{y})$, then it holds *in particular* for

those that are zero everywhere on $\partial\Omega$. Thus one necessary requirement for stationarity is that:

$$\int_{\Omega} \varphi(\mathbf{y}) \left(\nabla \cdot (\rho \mathbf{f})\right) \, dV = 0 \tag{2.3}$$

for all continuously differentiable $\varphi(\mathbf{y})$ taking the value zero on $\partial\Omega$. It follows from a basic lemma of variational calculus (see e.g., Weinstock (1974)) that this implies that

$$\frac{\partial}{\partial y_i} \left(f_i(\mathbf{y})\rho(\mathbf{y})\right) = 0 \qquad \forall \mathbf{y} \in \Omega \tag{2.4}$$

Substituting result (2.4) back into equation (2.2) leaves only the boundary term:

$$\int_{\partial\Omega} \varphi(\mathbf{y}) \left(\rho \mathbf{f} \cdot \hat{\mathbf{n}}\right) \, dS = 0 \tag{2.5}$$

Functions that are continuously differentiable over Ω are continuously differentiable over the smooth surface $\partial\Omega$ as well. Applying the same lemma there,

$$\rho(\mathbf{y}) f_i(\mathbf{y}) \hat{n}_i(\mathbf{y}) = 0 \qquad \forall \mathbf{y} \in \partial\Omega \tag{2.6}$$

Taken together, necessary conditions for stationarity (in the sense of 2.1) are (2.4) and (2.6). Moreover, substituting them into (1.8) gives exactly zero for any $\varphi(\mathbf{y})$, so the conditions are sufficient as well.

2.2 Naïve stationarity solution

A naïve attempt will now be made to solve the equations derived in the previous section. The attempt will fail, but it will do so in an instructive way.

Equation (2.4) is a first-order linear partial differential equation for $\rho(\mathbf{y})$; (2.6) is its boundary condition. We treat the latter first, as its implications are immediate. Equation (2.6) stipulates that one or more of the following conditions must hold for all $\mathbf{y} \in \partial\Omega$:

1. $\rho(\mathbf{y}) = 0$

2. $\mathbf{f}(\mathbf{y}) = 0$

3. $\mathbf{f}(\mathbf{y})$ is orthogonal to $\hat{\mathbf{n}}(\mathbf{y})$

We shall return to these shortly.

A general solution to (2.4) may be constructed by the method of characteristics. Characteristic curves of (2.4), denoted here as $\mathbf{Z}(\mathbf{Z_0}, s)$, coincide exactly with solution trajectories of (1.1), the original system of ordinary differential equations. That is, they satisfy

$$\frac{\partial Z_i}{\partial s} = f_i\left(\mathbf{Z}\left(\mathbf{Z_0}, s\right)\right) \tag{2.7}$$

with $Z_i(\mathbf{Z_0}, 0) = Z_{0i}$, an initial condition given at any point along the trajectory. The time-like characteristic parameter has been denoted s rather than t to distinguish it from physical time, but insofar as mathematics is concerned, the two are identical.

Along characteristic curves (2.7), equation (2.4) for $\rho(\mathbf{y})$ becomes

$$\frac{d\rho}{ds} + \left(\nabla \cdot \mathbf{f}\right)\rho = 0 \tag{2.8}$$

for $\rho(\mathbf{Z}(\mathbf{Z_0}, s))$ with $\mathbf{Z_0}$ held constant.

Equation (2.8) has the analytical solution

$$\rho(\mathbf{Z}(\mathbf{Z_0}, s)) = \rho(\mathbf{Z_0}) \exp\left(-\int_0^s \nabla \cdot \mathbf{f}|_{\mathbf{Z}(\mathbf{Z_0}, s')}\, ds'\right) \tag{2.9}$$

When $\nabla \cdot \mathbf{f}$ is a constant, (2.9) simplifies to

$$\rho(\mathbf{Z}(\mathbf{Z_0}, s)) = \rho(\mathbf{Z_0}) \exp\left(-\left(\nabla \cdot \mathbf{f}\right) s\right) \tag{2.10}$$

To understand solutions (2.9) and (2.10) in the context of boundary conditions and the $\rho(\mathbf{y})$ normalization requirement (1.4), it is helpful to express Ω as the direct sum of two subsets. The

first, $\mathcal{R} \subset \Omega$, consists only of points $\mathbf{y}$ that are *not* accessible in finite time from any trajectory crossing $\partial\Omega$. The second, $\mathcal{R}^c$, is the complement to $\mathcal{R}$. That is, for any $\mathbf{y} \in \mathcal{R}^c$, there is one trajectory that crosses $\partial\Omega$ and reaches $\mathbf{y}$ in a finite period of time.

Conceptually, $\mathcal{R}$ is where the mathematically interesting behavior of $\mathbf{f}(\mathbf{y})$ occurs. It is the set on which stationary points, periodic orbits, and strange attractors are located. In dynamical systems terminology, $\mathcal{R}$ is the union of all chain-recurrent sets of $\mathbf{f}(\mathbf{y})$. For dissipative problems, the Lebesgue measure of $\mathcal{R}$ is zero—it is not empty, but it accounts for a vanishingly small fraction of the total volume of Ω (proof in Appendix C).

For all $\mathbf{y} \in \mathcal{R}^c$, there is a trajectory that reaches $\mathbf{y}$ from $\partial\Omega$ after finite time (definition of $\mathcal{R}^c$. Because Ω was assumed to be a trapping region, the trajectory crosses $\partial\Omega$ only once. Thus for all $\mathbf{y} \in \mathcal{R}^c$, one can place $\mathbf{Z_0}$ on $\partial\Omega$. The inner product $\mathbf{f} \cdot \hat{\mathbf{n}}$ cannot be zero where the trajectory crosses $\partial\Omega$ (for it to cross the boundary requires a nonzero normal velocity relative to the boundary), so by (2.6), $\rho(\mathbf{Z_0}) = 0$ there. It follows from (2.9) that stationarity requires $\rho(\mathbf{y}) = 0$ over the entirety of $\mathcal{R}^c$, and thus over Ω by continuity.

2.3 Stationarity solution is not smooth

Recall, however, that $\rho(\mathbf{y})$ must still satisfy the normalization requirement (1.4). Obviously, the trivial solution $\rho(\mathbf{y}) = 0$ does not suffice. It follows that *there is no solution for* $\rho_{\text{stationarity}}(\mathbf{y})$ *on the space of* C^1 *functions on* Ω. Thus if a stationarity solution exists, it violates the assumption of continuous differentiability.

In fact, invariant probability measures do exist for our situation, but they are neither continuous nor differentiable; they are singular on $\mathcal{R}$ and zero everywhere else. Such measures are of significant interest in ergodic theory and are discussed at length below.

2.4 Background from statistical thermodynamics

By the middle of the nineteenth century, understanding of heat transfer, though largely phenomenological, had reached a level of engineering maturity. Using only caloric theory and intuition, Carnot had deduced fundamental limits on the efficiency of heat engines. Gases behaved predictably under changes in temperature, pressure, and volume.

What remained a mystery was the nature of heat itself. Early theories, which treated it as a kind of fluid, did not adequately describe such phenomena as friction heating. It was the subsequent discovery of statistical thermodynamics, with work by Boltzmann, Gibbs, Clausius, Maxwell, and many others, that finally identified heat as a statistical property of small-scale motion.

In statistical thermodynamics, a macroscopic system is described by the dynamics of its molecules, leading to a system of ordinary differential equations—in the form of (1.1)—having a very *very* large N. The components of $\mathbf{Y}$ specify the locations and momenta of all particles, and $\mathbf{f}$ describes their dynamics. The initial condition is unknown, and just as for turbulence, its details are generally neither knowable nor of practical importance.

The key to making the description manageable is restricting attention to certain cases by taking clues from the macroscopic world. If the system is assumed to be closed—that is, configured so that no energy or matter can flow in our out—then whatever the enormously complicated N dimensional behavior, one can rest assured that total energy will be conserved. Such a system is called Hamiltonian, and it can always be expressed with *canonical* variables for which $\nabla \cdot \mathbf{f} = 0$.

Boltzmann postulated that over a sufficiently long period of time, such a thermodynamic system in equilibrium would visit every point in phase space having its same initial energy[1] (his *H theorem*). The idea was initially quite controversial; it took decades for a satisfactory proof (Birkhoff, 1931) to emerge. The approach suggests constructing a probability density that is uniform on a surface of constant energy—a *Liouville measure*—that can be used to derive such important results as the equipartition theorem. The distribution may also be found by maximizing entropy, or $-\rho \log(\rho)$, subject to energy constraints. This approach eventually led to the study of informa-

[1] This property is now understood to hold *almost* everywhere rather than everywhere.

tion and information-theoretic entropy (Shannon, 1948), then to the maximum entropy principle of Jaynes (1957), whose Bayesian point of view strongly influenced this study.

As the subsequent success of statistical thermodynamics became better established—one might now say, given the weight of experimental evidence, incontrovertibly so—interest has turned to dissipative ($\nabla \cdot \mathbf{f} < 0$) and nonequilibrium situations. Such situations admit more complicated dynamical behavior, but some of the same ideas can be applied.

We are certainly not the first to contemplate applying ergodic theory to turbulent flow, but it is an exceptionally hard problem. As a starting point, the reader is referred to e.g., Gallavotti and Cohen (1995), van Veen and Kida (2006), and Temam (1991).

2.5 SRB: invariant measures for dissipative systems

The first step for making progress on dissipative systems is to find a replacement for the Liouville measure. Sinai (1972) found an invariant *Gibbs measure* for a special class of dissipative systems having strange attractors. His ideas were further refined and extended by Bowen and Ruelle (1975) and Ruelle (1976), leading to what has become known as the *SRB measure*, an invariant probability measure μ_{SRB} that is singular on the attractor (in $\mathcal{R}$). The most important property of SRB measures is that they are *physical*. A physical measure μ is one under which time averages approaches phase averages:

$$\lim_{T\to\infty} \frac{1}{T} \int_0^T \varphi\left(\mathbf{Y}(\mathbf{Y_0}, t)\right)\, dt = \int \varphi \, d\mu \tag{2.11}$$

and for which $\mathbf{Y_0}$ can be anywhere on a set of positive Lebesgue measure. Some authors refer to (2.11) as the "SRB property."

Thus SRB measures allow ergodic theory to be extended to certain dissipative systems with strange attractors. Previously, even though such systems were sometimes described in an ergodic way—comparing, for example, long-time averages of a simulation with those of an experiment—they were technically outside the realm of ergodic theory, whose foundations rested with certain Hamiltonian systems in dynamic equilibrium.

The question of precisely which systems have SRB measures remains open. They were originally derived for a specific class of systems having a special mathematical structure, but over time, they have been proven to exist for more general problems as well (Young, 2002), (Gallavotti and Cohen, 1995). Ruelle (2004) gives a whimsical discussion.

If a system is known to have an SRB measure, then one may find it by constructing the appropriate invariant measure of the system—a measure relative to which the motion induced by $\mathbf{f}(\mathbf{y})$ is an identity. Details of this process are the domain of Perron-Frobenius theory, which is outside our intended scope; it involves finding the eigensystem of the transfer operator associated with $\mathbf{f}$. The Ruelle-Perron-Frobenius theorem makes certain guarantees regarding the eigenvectors that allow it to function as a probability measure.

Approximate numerical techniques for finding such measures must do so in a discrete way. Dellnitz and Junge (1999) divide phase space into small boxes and express the transfer operator as a discrete matrix. Eigenvectors corresponding to eigenvalues of magnitude one are invariant measures; those corresponding to lesser eigenvalues still close to unity are called almost-invariant and represent states that tend to be occupied continuously for a long period of time (but not indefinitely).

2.6 Connection to stationarity density

As we are also considering probability measures in phase space and invariance (in the form of statistical stationarity), it seems natural to expect a connection. In fact, there seem to be several.

First, in Section 2.3, it was shown that are no C^1 probability density functions that satisfy the requirement for stationarity, given by (2.1). However, a singular, invariant measure like $\mu_{\mathrm{SRB}}(\mathbf{y})$, when it exists, does satisfy that requirement.

Perron-Frobenius theory may be used to find μ_{SRB} when it exists, but the general stationarity solution (2.9) suggests an alternative way to construct it: as a limit function. Let us suppose that the conditions of Chapter 1 hold, and that furthermore,

$$\hat{\varphi}(\mathbf{Y_0}) = \lim_{T\to\infty} \frac{1}{T} \int_0^T \varphi(\mathbf{Y}(\mathbf{Y_0}, t))\, dt \tag{2.12}$$

exists and is independent of $\mathbf{Y_0} \in \Omega$. (This is a strong assumption, of course.)

Let the density function $\rho_T(\mathbf{y})$, be defined along characteristics as

$$\rho_T(\mathbf{Z}(\mathbf{Z_0}, s)) = \begin{cases} \frac{\sigma_T(\mathbf{Z_0})}{T} \exp\left(- \int_0^T \nabla \cdot \mathbf{f}|_{\mathbf{Z}(\mathbf{Z_0}, s')} \, ds' \right) & s < T \\ 0 & s > T \end{cases} \tag{2.13}$$

where $\sigma_T(\mathbf{Z_0}) : \mathbf{Z_0} \in \partial\Omega$ is an arbitrary real-valued nonnegative integrable function on $\partial\Omega$.

For all finite T, one may compute $\int_\Omega \varphi(\mathbf{y}) \, \rho_T(\mathbf{y}) \, dV$ by integrating over $\mathcal{R}^c$ rather than Ω, because the set on which they differ has zero measure, and (2.13) is zero there. Thus the integration may be carried out over streamtubes as described in Appendix A. That is,

$$\begin{aligned} &\int_\Omega \varphi(\mathbf{y}) \, \rho_T(\mathbf{y}) \, dV \\ &\qquad = \int_{\mathcal{R}^c} \varphi(\mathbf{y}) \, \rho_T(\mathbf{y}) \, dV \\ &\qquad = \int_{\partial\Omega} \int_0^T \varphi(\mathbf{Z}(\mathbf{Z_0}, s)) \rho_T(\mathbf{Z}(\mathbf{Z_0}, s)) \, \mathcal{J}(\mathbf{Z_0}, s) \, ds \, dS \\ &\qquad = \int_{\partial\Omega} - \mathbf{f} \cdot \hat{\mathbf{n}}|_{\mathbf{Z_0}} \, \sigma_T(\mathbf{Z_0}) \left(\frac{1}{T} \int_0^T \varphi(\mathbf{Z}(\mathbf{Z_0}, s)) \, ds \right) dS \end{aligned} \tag{2.14}$$

Taking the limit as $T \to \infty$ and making use of assumption (2.12), the term in parentheses approaches $\hat{\varphi}(\mathbf{Z_0})$, which exists and is independent of $\mathbf{Z_0}$ by assumption. Thus

$$\int_\Omega \varphi(\mathbf{y}) \, \rho_T(\mathbf{y}) \, dV = \hat{\varphi} \int_{\partial\Omega} - \mathbf{f} \cdot \hat{\mathbf{n}}|_{\mathbf{Z_0}} \, \sigma_T(\mathbf{Z_0}) \, dS \tag{2.15}$$

Now suppose boundary values of $\sigma_T(\mathbf{Z_0})$ are normalized so that

$$\int_{\partial\Omega} - \mathbf{f} \cdot \hat{\mathbf{n}}|_{\mathbf{Z_0}} \, \sigma_T(\mathbf{Z_0}) \, dS = 1 \tag{2.16}$$

Then the SRB property (2.11) is satisfied.

Under the aforementioned assumptions regarding $\mathbf{f}$ and normalization requirement (2.16), one

may therefore take

$$\rho_{\text{stationary}}(\mathbf{Z}(\mathbf{Z_0}, s)) = \lim_{T\to\infty} \begin{cases} \frac{\sigma_T(\mathbf{Z_0})}{T} \exp\left(-\int_0^T \nabla \cdot \mathbf{f}|_{\mathbf{Z}(\mathbf{Z_0}, s')}\, ds'\right) & s < T \\ 0 & s > T \end{cases} \tag{2.17}$$

This expression is singular arbitrarily close to $\mathcal{R}$ and zero everywhere else. So long as (2.16) holds, $\sigma_T(\mathbf{Z_0})$ may take any nonnegative values on the boundary. Notice too that expression (2.17) is defined even when (2.12) does not hold, although in that case its moments might not be independent of $\sigma_T(\mathbf{z_0})$ (and might not correspond to any particular time average).

At a point attractor, (2.17) approaches a Dirac delta function. At periodic attractors, it is infinite on the attractor and zero everywhere else. On strange attractors, it is an SRB measure. Henceforth, expression (2.17) will be taken as the stationarity density, though one should bear in mind that there may be easier ways to construct it and that, owing to the arbitrary nature of $\sigma_T(\mathbf{Z_0})$, moments derived from it will not necessarily be unique.

Because (2.17) is zero away from $\mathcal{R}$, and $\mathcal{R}$ does not intersect $\partial\Omega$ (by definition, it contains no points accessible from the boundary in finite time, thus in particular it contains no points accessible from the boundary in zero time), moments computed from the limit function (2.17) do not change under continuous deformation of $\partial\Omega$. So long as Ω remains a trapping region, it may be translated anywhere in the basin of attraction. In this sense, for the stationary density, the answer does not depend on the choice of trapping region.

2.7 Remark: stationarity in the laboratory

Ultimately, one may conclude from the previous discussion that if an experiment is conducted under perfectly stationary conditions, then its sample point density $\rho_{\text{stationary}}(\mathbf{y})$ must be singular on $\mathcal{R}$, a set of negligible volume inside Ω. Indeed, such a density might describe the sample points of a system that has achieved perfect stationarity after running an infinitely long period of time.

Practical considerations impose another constraint, however, that did not enter into the analysis

above and that leads to a logical problem with the previous line of reasoning: no experiment runs indefinitely. Thus region $\mathcal{R}$ is never entered from outside during a real experiment. Furthermore, no experiment begins *inside* $\mathcal{R}$ either: Assuming that the process that creates the initial condition is continuous, its probability of being inside any particular set of measure zero is nil.

It follows that the probability of finding a laboratory system inside $\mathcal{R}$, or $\Pr(\mathbf{y} \in \mathcal{R})$, should be zero, not one as would be concluded from $\rho_{\text{stationary}}(\mathbf{y})$. Conversely, the probability of finding a laboratory system in $\mathcal{R}^c$ should be one, not zero. The apparent inconsistency can be resolved by noting that $\rho(\mathbf{y})$ specifically represents the density of sample points—states occupied by the system while data are being recorded. Thus laboratory systems may approach stationarity, but they never actually achieve it.[2] Their expected rates of change never reach zero, and they remain in a state of asymptotic approach forever. (For sufficiently long-running experiments, $\rho_{\text{stationary}}(\mathbf{y})$ still might give an excellent approximation, of course.)

This topic will be revisited in section 3.7, where long-time limits of asymptotic approach are compared to stationarity.

[2]Dissipative systems never achieve stationarity in the laboratory. No such claim is being made for nondissipative systems, of course.

Chapter 3

Theory of asymptotic approach

Two experimental conditions, stationarity and asymptotic approach, were introduced in Chapter 1. In this chapter, the second of these conditions is translated into specific, quantitative constraints on $\rho(\mathbf{y})$. Analogous constraints for stationarity were derived in Chapter 2. For clarity, when $\rho(\mathbf{y})$ refers to an experiment involving asymptotic approach, it will sometimes be labeled $\rho_{\mathrm{asymptoticapproach}}(\mathbf{y})$.

Some of the chapter's more lengthy derivations appear in the appendices.

3.1 Asymptotic approach

While stationarity is the most common criterion for selecting $\mathbf{Y_0}$, there are important nonstationary problems as well. The first real turbulent DNS, due to Orszag and Patterson (1972), simulates the canonical problem of unforced turbulent flow decaying in a periodic box. Its only truly stationary state, $\mathbf{u}(\mathbf{x}, t) = 0$, is trivial. Moreover, even nominally stationary conditions—when produced in a laboratory, numerical or otherwise—might be more accurately characterized as late-time asymptotic approach.

Unfortunately, where stationarity is a well-defined mathematical concept, "asymptotic approach" is vague. There is no definitive test for it. After beginning from a suitably random $\mathbf{Y_{00}}$, Orszag and Patterson (1972) wait until small scales decorrelate. Hughes et al. (2001) also start from a physically realizable random state, but report data from nondimensional time 4.16 onward, including spectra at nondimensional time 6.47, by which point several statistics appear to be decaying smoothly. The choices are qualitatively reasonable, but the justification does not appear to be quantitative.

Because there is no single, universally-agreed-upon criterion to identify the onset of asymptotic approach, there is more than one logical choice for the conditions on $\langle \partial\varphi(\mathbf{Y}(\mathbf{Y_0}, t))/\partial t \rangle$, and hence more than one reasonable choice for the equation governing $\rho_{\text{asymptoticapproach}}(\mathbf{y})$. It would be tempting—but misleading—to regard any choice made under such arbitrary conditions as a modeling assumption. The difference is that asymptotic approach criteria do not represent unknowns, but rather choices that are consciously made in the laboratory (specifically, details of the start-up procedure and data-collection schedule). The choice here cannot be ambiguous, but it is no more arbitrary than it would be in the laboratory.

3.2 Details of the domain

There are two mathematical details to cover before approaching asymptotic approach in earnest.

First, the following constraint, which was introduced in Section 2.7, will need to be imposed:

$$\Pr(\mathbf{y} \in \mathcal{R}) = 0 \tag{3.1}$$

Physically, equation (3.1) stipulates that a negligible fraction of experiments begins on $\mathcal{R}$, and that no experiment runs indefinitely. Mathematically, it prevents the solution from degenerating into an unphysical idealized limit. Constraint (3.1) will be imposed by requiring that the fraction of probability mass within an ϵ-neighborhood of $\mathcal{R}$ approaches zero as ϵ approaches zero.

Next, recall that the derivation of equation (1.8) assumed continuous differentiability of $\rho\varphi\mathbf{f}$ on Ω when applying the divergence theorem. That assumption would not hold if $\rho(\mathbf{y})$ were singular on $\mathcal{R}$, which from the stationary case seems to be a possibility. Our workaround is to construct a weak solution by adjusting the domain to create an ϵ-neighborhood around $\mathcal{R}$, as follows.

At every $\mathbf{y} \in \mathcal{R}^c$, there is exactly one boundary-crossing trajectory that reaches $\mathbf{y}$ in finite time. Let the finite time at which the trajectory reaches $\mathbf{y}$ be denoted $s_b(\mathbf{y})$.

Let $T(\mathbf{Z_0}) \in (0, \infty)$ be a continuously differentiable function on $\partial\Omega$, and let $\mathcal{Q}^c \subset \mathcal{R}^c$ consist of those $\mathbf{y} \in \mathcal{R}^c$ for which $s_b(\mathbf{y}) < T(\mathbf{Z_0})$ (Figure 3.1). As $\min T(\mathbf{Z_0}) \to \infty$, the difference between $\mathcal{Q}^c$

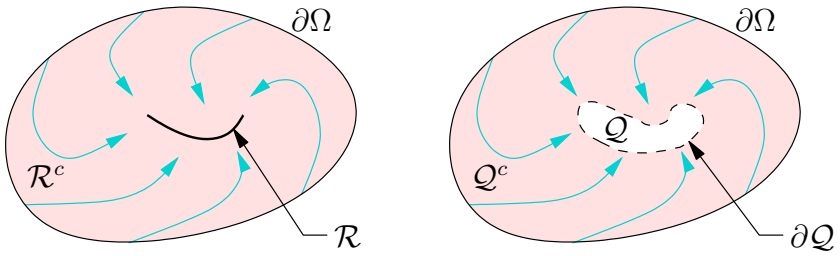

Figure 3.1: Illustration of the difference between sets $\mathcal{Q}$ and $\mathcal{R}$, $\mathcal{Q}^c$ and $\mathcal{R}^c$. $\mathcal{R}^c$ includes all points accessible from the boundary in finite time; $\mathcal{Q}^c$ includes only those accessible from the boundary in time less than $T(\mathbf{Z_0})$. In both cases, the direct sum of the set and its complement is Ω.

and $\mathcal{R}^c$ (more precisely, the Lebesgue measure of the complement of their intersection) approaches zero. Let $\mathcal{Q}$ consist of all points in Ω that are not in $\mathcal{Q}^c$. It follows that $\mathcal{R} \subset \mathcal{Q}$.

If there is no singular behavior away from $\mathcal{R}$, then the divergence theorem can be applied over $\mathcal{Q}^c$ (or any connected subset of $\mathcal{Q}^c$ having a smooth boundary), although there is an inner boundary that must be taken into account. In the analysis below, $\rho(\mathbf{y})$ is computed over $\mathcal{Q}^c$ rather than over Ω. If condition (3.1) holds, however, then as $\min T(\mathbf{Z_0}) \to \infty$, moments of $\rho(\mathbf{y})$ over Ω become independent of its behavior on $\mathcal{Q}$, so what remains is a weak solution over Ω.

Applied over $\mathcal{Q}^c$ rather than Ω, equation (1.8) appears almost unchanged:

$$\left\langle \frac{\partial\varphi(\mathbf{Y}(\mathbf{Y_0},t))}{\partial t} \right\rangle = \int_{\partial\mathcal{Q}^c} \varphi(\mathbf{y})\,(\rho\mathbf{f}\cdot\hat{\mathbf{n}})\;dS - \int_{\mathcal{Q}^c} \varphi(\mathbf{y})\,(\nabla\cdot(\rho\mathbf{f}))\;dV \tag{3.2}$$

Remember, however, that the boundary $\partial\mathcal{Q}^c$ now has *two* parts: an outer part coinciding with $\partial\Omega$, as before, and a new inner part coinciding with $\partial\mathcal{Q}$ (but of opposite orientation).

3.3 Asymptotic approach as a minimization problem

Stationarity required that equation (2.1)

$$\left\langle \frac{\partial\varphi(\mathbf{Y_0},t)}{\partial t} \right\rangle = 0$$

hold for all continuously differentiable phase functions $\varphi(\mathbf{y})$ on Ω, now on $\mathcal{Q}^c$ instead. This meant that any measurement was likely to be growing and decaying in equal measure; its expected rate of change was precisely zero.

For asymptotic approach, however, the expected rate of change is not zero. It is a small value that might be different for each $\varphi(\mathbf{y})$. An observable whose expected value decays exponentially, for example, has an expected rate of change of $-\theta \langle\varphi\rangle$, where θ is a rate constant. Another observable might decay according to a power law. The common characteristic of asymptotic approach is not form, but speed. Under asymptotic approach, no initial transients remain, and so no observable changes faster (on average) than absolutely necessary.

Because $\langle \partial\varphi/\partial t \rangle$ has dimensions of φ over time, dividing it by any norm of φ leaves a rate, a quantity having units of inverse time. A small-magnitude rate corresponds to gradual change, and a zero rate corresponds to no change—which is to say statistical stationarity, a regime that was covered in Chapter 2.

An upper bound on the expected rate of change, valid for all $\varphi(\mathbf{y})$, is derived below. For systems undergoing asymptotic approach (as opposed to those already at statistical equilibrium) this bound cannot be made exactly zero, but it can be minimized. Minimization is subject to the two constraints already cited: the normalization requirement of (1.4) and the requirement that asymptotic approach still be in progress, expressed in (3.1). Together, these lead to a quantitative criterion for the sample point density $\rho_{\text{asymptoticapproach}}(\mathbf{y})$ during asymptotic approach. This criterion will not be the only possible choice—asymptotic approach is not a precisely defined concept—but the minimized solution captures any qualitative definition reasonably well.

Equation (3.2) gives the expected rate of change of a phase function over $\mathcal{Q}^c$. Its value remains unchanged if $\varphi(\mathbf{y})$ is displaced by some constant φ_0. That is, identically,

$$\left\langle \frac{\partial\varphi(\mathbf{Y}(\mathbf{Y_0}, t))}{\partial t} \right\rangle = \int_{\partial\mathcal{Q}^c} (\varphi(\mathbf{y}) - \varphi_0)\, (\rho\mathbf{f} \cdot \hat{\mathbf{n}})\; dS - \int_{\mathcal{Q}^c} (\varphi(\mathbf{y}) - \varphi_0)\, (\nabla \cdot (\rho\mathbf{f}))\; dV \tag{3.3}$$

It is always possible to choose φ_0 in a way that eliminates the first (boundary) term in (3.3).

That is because there are three mutually exclusive possibilities:

1. $\int_{\partial\mathcal{Q}^c} \rho\mathbf{f}\cdot\hat{\mathbf{n}}\,dS \neq 0$

2. $\int_{\partial\mathcal{Q}^c} \rho\mathbf{f}\cdot\hat{\mathbf{n}}\,dS = 0$ because $\rho\mathbf{f}\cdot\hat{\mathbf{n}} = 0$ almost everywhere on $\partial\mathcal{Q}^c$

3. $\int_{\partial\mathcal{Q}^c} \rho\mathbf{f}\cdot\hat{\mathbf{n}}\,dS = 0$, but $\rho\mathbf{f}\cdot\hat{\mathbf{n}} \neq 0$ over a non-negligible part of $\partial\mathcal{Q}^c$

In the first and second cases, the surface integral in (3.3) can be eliminated by taking

$$\varphi_0 = \begin{cases} 0 & \int_{\partial\mathcal{Q}^c} \rho\mathbf{f}\cdot\hat{\mathbf{n}}\,dS = 0 \\ \frac{\int_{\partial\mathcal{Q}^c} \varphi(\mathbf{y})\rho\mathbf{f}\cdot\hat{\mathbf{n}}\,dS}{\int_{\partial\mathcal{Q}^c} \rho\mathbf{f}\cdot\hat{\mathbf{n}}\,dS} & \text{otherwise} \end{cases} \tag{3.4}$$

The third possibility, as shown in Appendix C (Section C.3), would violate (3.1) and so can be safely disregarded. With (3.4), equation (3.3) reduces to a volume integral:

$$\left\langle \frac{\partial\varphi(\mathbf{Y}(\mathbf{Y_0},t))}{\partial t} \right\rangle = \int_{\mathcal{Q}^c} \left(\varphi(\mathbf{y}) - \varphi_0\right)\left(\nabla\cdot(\rho\mathbf{f})\right)\,dV \tag{3.5}$$

The next step is to bound (3.5) in a way that isolates its φ-dependence. There are many ways to split and bound an integral, of course; the approach below is simply one among many reasonable choices. The lack of uniqueness here is an unfortunate consequence of ambiguity inherent in the definition of asymptotic approach; ambiguity follows from first principles. It will be shown in Section 3.5, however, that other choices at this point would ultimately lead to the same predictions, provided that certain conventions are observed.

By the Cauchy-Schwartz inequality,

$$\left\langle \frac{\partial\varphi(\mathbf{Y}(\mathbf{Y_0},t))}{\partial t} \right\rangle^2 \leq \left(\int_{\mathcal{Q}^c} \left(\varphi(\mathbf{y}) - \varphi_0\right)^2\,dV\right)\left(\int_{\mathcal{Q}^c} \left(\nabla\cdot(\rho\mathbf{f})\right)^2\,dV\right) \tag{3.6}$$

Unless $\varphi(\mathbf{y})$ is constant on $\mathcal{Q}^c$ (in which case its expected time derivative is trivially zero, obviating the need to bound it), the first integral on the right-hand side of equation (3.6) is positive.

Thus for any nontrivial $\varphi(\mathbf{y})$, it is true that

$$\frac{\left\langle \frac{\partial \varphi(\mathbf{Y}(\mathbf{Y_0},t))}{\partial t} \right\rangle^2}{\int_{\mathcal{Q}^c} \left(\varphi(\mathbf{y}) - \varphi_0\right)^2 \, dV} \leq \int_{\mathcal{Q}^c} \left(\nabla \cdot (\rho \mathbf{f})\right)^2 \, dV \tag{3.7}$$

or equivalently

$$\left\langle \frac{\partial}{\partial t} \left(\frac{\varphi(\mathbf{Y}(\mathbf{Y_0},t))}{\left(\int_{\mathcal{Q}^c} \left(\varphi(\mathbf{y}) - \varphi_0\right)^2 \, dV\right)^{1/2}} \right) \right\rangle^2 \leq \int_{\mathcal{Q}^c} \left(\nabla \cdot (\rho \mathbf{f})\right)^2 \, dV \tag{3.8}$$

The left-hand side of (3.7) is a (squared) nondimensional rate of decay associated with $\varphi(\mathbf{y})$. The right-hand side is an upper bound independent of $\varphi(\mathbf{y})$. Thus to minimize the expected rate of decay for all observables, one ought to minimize κ, defined as

$$\kappa = \int_{\mathcal{Q}^c} \left(\frac{\partial}{\partial y_i} \rho(\mathbf{y}) f_i(\mathbf{y}) \right)^2 \, dV \tag{3.9}$$

with respect to the function $\rho(\mathbf{y})$.

In the next section, we obtain $\rho_{\text{asymptoticapproach}}(\mathbf{y})$ by minimizing (3.9) subject to constraints (1.4) and (3.1).

3.4 The minimized asymptotic approach solution

Constrained minimization of κ, as defined in (3.9), is a straightforward problem of variational calculus; it leads to a differential equation (and boundary condition) from which a $\rho(\mathbf{y})$ corresponding to asymptotic approach may be found.

Details of the derivation are omitted here, but are included for completeness in Appendix D. The end result, from (D.12) and (D.13), is that $\rho(\mathbf{y})$ satisfies the second-order parabolic linear partial differential equation:

$$f_i(\mathbf{y}) \frac{\partial}{\partial y_i} \left(\frac{\partial}{\partial y_j} \left(\rho(\mathbf{y}) f_j(\mathbf{y}) \right) \right) = -\frac{\lambda}{2} \qquad \forall y \in \mathcal{Q}^c \tag{3.10}$$

along with the boundary condition

$$\left(\frac{\partial}{\partial y_j}\left(\rho(\mathbf{y})f_j(\mathbf{y})\right)\right)\left(f_i(\mathbf{y})\hat{n}_i(\mathbf{y})\right) = 0 \qquad \forall y \in \partial\mathcal{Q}^c \tag{3.11}$$

where λ is a Lagrange multiplier associated with normalization requirement (1.4).

Because equation (3.10) is parabolic, it has only one family of characteristics, which, unsurprisingly, coincides with trajectories of the original system. As in the stationary case, the characteristics satisfy

$$\frac{\partial Z_i}{\partial s} = f_i\left(\mathbf{Z}\left(\mathbf{Z_0}, s\right)\right) \tag{3.12}$$

with $Z_i(\mathbf{Z_0}, 0) = Z_{0i}$, an initial condition given at any point along the trajectory. We choose to place $\mathbf{Z_0}$ on $\partial\Omega$. Again, the time-like characteristic parameter has been denoted s rather than t to distinguish it from physical time.

A detailed analysis along characteristics, taking into account requirement (3.1), is included for reference in Appendix E. Its final conclusion is that

$$\rho_{\text{asymptoticapproach}}(\mathbf{Z}(\mathbf{Z_0}, s)) = \frac{\lambda}{2M(\mathbf{Z_0}, s)} \int_s^\infty M(\mathbf{Z_0}, s')\ s'\, ds' \tag{3.13}$$

where $M(\mathbf{Z_0}, s)$ is given by (E.3).

The dynamical significance of (3.13) is that, relative to other nonstationary probability densities on the same domain, it minimizes a norm of the expected rate of change of all possible measurement statistics. In other words, among all non-invariant probability measures over Ω, it is the one that is most nearly invariant (as measured by a reasonable, but not necessarily unique, norm).

3.5 Alternative bounds for the asymptotic approach integral

In Section 3.3, integral (3.5) gave the mean rate of asymptotic approach for any observable. We chose to bound it using the Cauchy-Schwartz inequality, but many other reasonable choices exist. For example, we could have chosen to bound it using some other Hölder inequality, or to multiply

and divide by a positive function of $\rho(\mathbf{y})$ before splitting the integral. How might a different choice have affected the outcome?

It is shown in Section E.3 that a wide class of alternatives would have left the characteristic solution intact, changing only the growth rate of ρ with s.

3.6 Numerical techniques for the asymptotic approach density

The most straightforward, albeit inefficient, way to compute $\rho_{\text{asymptoticapproach}}(\mathbf{y})$ is by numerical integration of (3.13) along trajectories; it is this technique that is applied in Chapters 5, 6, 7, and 8.

The numerical integration technique takes place on a rectangular grid that is uniform in each phase-space direction. The grid is oriented and scaled so that it completely covers Ω, and so that no grid point falls exactly on $\mathcal{R}$. Each grid point outside Ω is assigned the value zero; each grid point inside Ω is assigned a value for $\rho_{\text{asymptoticapproach}}(\mathbf{y})$ by the following algorithm. First, the value of s at the grid point is computed by integrating outward along its trajectory (in the $-\mathbf{f}(\mathbf{Y})$ direction) with an implicit fourth-order Runge-Kutta algorithm. Integration terminates when $\mathbf{Y}$ reaches $\partial\Omega$. Then, integration proceeds inward (in the $+\mathbf{f}(\mathbf{Y})$ direction) from the grid point, meanwhile accumulating the integrand of (3.13). Because the integrand first grows and then decays exponentially, integration can be terminated after a finite period of time, for example after the integrand decreases beyond a small fraction of its peak value. Because $\nabla\cdot\mathbf{f}$ is bounded and negative on Ω, the remainder can be rigorously estimated. Finally, the solution must be scaled (by adjusting λ) to satisfy (1.4).

Once $\rho_{\text{asymptoticapproach}}(\mathbf{y})$ is known at gridpoints, its moments and conditional moments may be computed directly. One can immediately derive expected values, reduced-order models as discussed in Chapter 4, or even approximate $\rho_{\text{stationary}}(\mathbf{y})$ by taking conditional expectations on large s or ρ, as discussed in Section 3.7. This last technique is applied in Chapter 8.

When $\nabla\cdot\mathbf{f}$ is constant, the asymptotic approach density field can also be computed by conventional finite-difference methods, provided that λ is first computed analytically via (E.15). To

construct a finite-difference solution, one approximates the partial differential operator of (3.10) on the solution grid using any conventional stencil, yielding a sparse system of linear algebraic equations. The system's solution vector is $\rho_{\text{asymptoticapproach}}(\mathbf{y})$. The solutions in Chapters 5 and 6 were validated by comparing to second-order centered finite-difference solutions computed in this way.

Because (3.10) is linear and parabolic, there are many other well-known techniques, such as the Galerkin method, that could potentially be applied to solving it. None, however, would be suitable for high-dimensional problems such as DNS of a turbulent flow, because it remains impractical to grid a high-dimensional space.

Nevertheless, progress can be made, even for high-dimensional problems, because ultimately only a few moments of $\rho_{\text{asymptoticapproach}}(\mathbf{y})$ are generally of interest. It is unnecessary to work out the density in its entirety. Moments computed by Monte Carlo techniques—randomly selecting and integrating along a relatively small number of trajectories—should eventually converge. (This, it might be argued, is precisely what DNS does.) Certain asymptotic approximations appear to work as well, although their development remains in progress at time of writing.

Finally, sometimes one is simply lucky: Chapter 9 presents an exact solution for the energy spectrum of the truncated one-dimensional Burgers' equation in the Stokes' limit.

3.7 Conjectured relationship to stationarity

Over the course of asymptotic approach, a system gradually approaches its limit state. Based on the examples in Chapters 5, 6, 7, 8, and 9, that limit state would appear to be stationarity. Whether a system approaches a single stationary point, a periodic orbit, or a strange attractor, the approach ends at $\mathcal{R}$, which is precisely the support set of $\rho_{\text{stationary}}(\mathbf{y})$.

It is only natural to ask, then, whether the two are equivalent. In other words: is the limit density of $\rho_{\text{asymptoticapproach}}(\mathbf{y})$, conditioned upon large time, physical (as defined in Equation 2.11)? Is it, under the right conditions, an SRB measure?

To answer this question, it is evidently necessary to pin down what is meant by "conditioned on large time." Recall that within $\mathcal{R}^c$, $s_b(\mathbf{y})$ measures time elapsed since crossing the boundary. Thus

an expectation conditioned on $s_b(\mathbf{y}) > T$ rejects any point within T time units of the boundary. Points that remain represent systems that have undergone asymptotic approach for at least T time units. As $T \to \infty$, the rejected set approaches all of $\mathcal{R}^c$.

Thus the question is whether

$$\rho_{\text{asymptoticapproach}|\text{longtime}}(\mathbf{Z}(\mathbf{Z_0}, s)) = \lim_{T\to\infty} \begin{cases} \frac{\rho_{\text{asymptoticapproach}}(\mathbf{Z}(\mathbf{Z_0},s))}{\int_{\partial\Omega}\int_T^\infty \rho_{\text{asymptoticapproach}}(\mathbf{Z}(\mathbf{Z_0},s'))\mathcal{J}(\mathbf{Z_0},s')\,ds'\,dS} & s > T \\ 0 & s < T \end{cases} \tag{3.14}$$

satisfies (2.11)—that is, that its moments coincide with those of $\rho_{\text{stationary}}(\mathbf{y})$ from (2.17).

Unfortunately, we do not yet have a satisfactory proof that (3.14) satisfies (2.11), and must treat it as a conjecture. However, on the basis of the following observations, we believe that the conjecture is plausible:

1. Both $\rho_{\text{asymptoticapproach}|\text{longtime}}(\mathbf{y})$ and $\rho_{\text{stationary}}(\mathbf{y})$ are zero on all $\mathbf{y} \in \mathcal{R}^c$, and singular on $\mathcal{R}$.

2. For a suitable choice of $\sigma_T(\mathbf{z_0})$, isosurfaces of functions in the limit sequences of $\rho_{\text{stationary}}(\mathbf{y})$ and $\rho_{\text{asymptoticapproach}|\text{longtime}}(\mathbf{y})$ coincide.

The first observation shows that if moments differ, the difference can only be due to differences in the distribution of probability mass on $\mathcal{R}$, a set of measure zero. The second observation makes us suspect that it is always possible to choose a $\sigma_T(\mathbf{Z_0})$ for which there is no such difference.

A proof that the two are equivalent would be significant, both theoretically and practically. It would provide a convenient way to construct an SRB measure, avoiding Perron-Frobenius theory, and it is based on a relatively well-behaved function. The asymptotic approach density $\rho_{\text{asymptoticapproach}}(\mathbf{y})$ is singular on $\mathcal{R}$, but integrably so. Furthermore, it is finite over $\mathcal{R}^c$ and solves a linear, parabolic equation. Its boundary condition, in the case of constant phase-space divergence, is simply a constant. Thus there is reason to believe $\rho_{\text{asymptoticapproach}}(\mathbf{y})$ can be analytically approximated in a straightforward way, even when strange attractors are present. At present, SRB measures are highly singular and therefore somewhat more difficult to construct, especially for high-dimensional systems.

We make use of the above conjecture in Chapter 8 to produce long-time limit statistics of Lorenz's equations. Lorenz's attractor is known to possess an SRB measure, so if the conjecture is true, then it is approximated by the long-time limit. For practical reasons, we compute the density conditioned on large ρ rather than on large T; the two are equivalent. Convergence is investigated numerically in Section 8.5.

Chapter 4

Application to reduced-order modeling

4.1 Overview

The motivation for this chapter is twofold. On one hand, it presents a particularly nice application for the sample point density $\rho(\mathbf{y})$: constructing reduced-order models. At the same time, it demonstrates the basic equivalence of model assumptions and sample-point-density constraints.

The objective of reduced-order modeling is to represent a relatively large, N-dimensional system of ordinary differential equations like (1.1) with a smaller M-dimensional one ($M << N$). We will refer to the M components of the simpler system as *model variables*, and to the right-hand side of the corresponding evolution equations as a *model*.[1] One set of model variables might admit many different models; for example, a wide variety of large-eddy simulation (LES) models have been proposed, most of which operate over the same set of model variables (the filtered velocity field).[2]

Usually the term "modeling" connotes approximation; the simpler system's solution is not expected to predict the full system perfectly for all values of $\mathbf{Y_0}$. There also exist problems (such as linear ones) for which simpler systems do hold exactly; while these would not normally fall under the rubric of modeling, the reasoning below should also apply to them.

Given a system of ODEs like (1.1), constructing a model by this method is a five-step process.

[1] The term "model," as used throughout this chapter, refers exclusively to the reduced-order kind; we assume that $\mathbf{f}(\mathbf{y})$ is already known in its entirety, but is too complicated to apply directly. In other contexts, "model" sometimes means that $\mathbf{f}(\mathbf{y})$ itself is unknown.

[2] One might object that LES is not a pure form of reduced-order modeling because it is inextricably tied to specifics of the discretization.

It leads to a system of M ordinary differential equations:

$$\frac{d\mathbf{W}}{dt} = \mathbf{g}(\mathbf{W}) \tag{4.1}$$

for $\mathbf{W}(\mathbf{W_0}, t)$, which is a vector of model variables. The model is $\mathbf{g}(\mathbf{W})$. Steps are listed briefly below, followed by more in-depth discussions of each.

1. Obtain $\rho(\mathbf{y})$ by one of the methods discussed in Chapters 2 or 3.

2. Decide how the model variables will relate to $\mathbf{y}$ by choosing M functions $\varphi_{w_i}(\mathbf{y})$, $i = 1 \ldots M$. Construct a vector function $\boldsymbol{\varphi}_\mathbf{w}(\mathbf{y})$ having these as components.

3. Using $\rho(\mathbf{y})$, compute the conditional expected value $\langle \partial\boldsymbol{\varphi}_\mathbf{w}/\partial t \mid \boldsymbol{\varphi}_\mathbf{w}(\mathbf{y}) = \mathbf{W}\rangle$.

4. Solve the model system, which is simply (4.1) with the conditional expression in the previous step substituted for $\mathbf{g}(\mathbf{W})$. The initial condition is $\mathbf{W_0} = \boldsymbol{\varphi}_\mathbf{w}(\mathbf{Y_0})$.

5. Compute the nondimensional standard deviation of $\partial\boldsymbol{\varphi}_\mathbf{w}/\partial t$, also conditioned on $\boldsymbol{\varphi}_\mathbf{w}(\mathbf{y}) = \mathbf{W}$, which serves as a local uncertainty estimate. Good models can be defined as those whose expected uncertainty is much less than 1 everywhere, or at least whose average uncertainty is much less than 1.

There is no hand-waving; once model variables have been chosen and $\rho(\mathbf{y})$ has been computed, the model follows directly, along with specific uncertainty estimates. Each of the above steps is discussed in a different section below.

4.2 Obtain the sample point density

The appropriate sample point density $\rho(\mathbf{y})$ depends on the conditions being modeled. These were discussed at length in Chapters 2 and 3. If one is modeling an experiment conducted under stationary conditions—for example, under constant forcing, with initial transients allowed to decay

before taking data—then $\rho_{\text{stationary}}(\mathbf{y})$ is the appropriate density. To model an experiment involving asymptotic approach, use $\rho_{\text{asymptoticapproach}}(\mathbf{y})$. Some situations call for using a more restricted density based on conditional probabilities.

4.3 Choose the model variables

In choosing the M model variables, the modeler has almost complete freedom. A complicated mechanical system having flexibility and many degrees of freedom (large N) might be modeled as a rigid body of $M = 9$ (position and momentum of the center of mass, and angular momentum). A fluid flow requiring N modes for DNS might neglect small spatial scales, truncating away N-M high-wavenumber modes (LES), or fluctuating perturbations (RANS). A fixed volume of gas having a large number of molecules, all moving and interacting chaotically, might be reduced to $M = 2$: the average enthalpy and entropy.

Mathematically, choosing model variables means expressing the M-dimensional model phase vector $\mathbf{w}$ in terms of the N-dimensional full phase vector $\mathbf{y}$. This is accomplished by means of a vector function $\boldsymbol{\varphi}_{\mathbf{w}}(\mathbf{y})$ mapping $\mathbb{R}^N$ to $\mathbb{R}^M$. The mapping must be differentiable.

In the rigid-body approximation example, $\boldsymbol{\varphi}_{\mathbf{w}}(\mathbf{y})$ is simply an average taken over mass. Its first three components are the mass-average position, $\int \mathbf{x}\, dm / \int dm$. For large-eddy simulation, $\boldsymbol{\varphi}_{\mathbf{w}}(\mathbf{y})$ applies a spatial filter at each large-scale grid location. For the body of gas, the first component (enthalpy) is the total energy, and the second (entropy) is related to the volume of phase space the system would eventually explore.

Once $\rho(\mathbf{y})$ has been computed and a suitable vector function $\boldsymbol{\varphi}_{\mathbf{w}}(\mathbf{y})$ has been selected, the remainder of the process is strictly mechanical.

4.4 Compute the conditional expected velocity

The next step is to compute the conditional expected velocity $\langle \partial \boldsymbol{\varphi}_{\mathbf{w}} / \partial t \mid \boldsymbol{\varphi}_{\mathbf{w}}(\mathbf{y}) = \mathbf{W} \rangle$. This is usually straightforward. The phase function corresponding to $\partial \boldsymbol{\varphi}_{\mathbf{w}} / \partial t$ in the direction of trajectories

is

$$\frac{\partial \boldsymbol{\varphi}_{\mathbf{w}}(\mathbf{Y}(\mathbf{Y_0}, t))}{\partial t} = \mathbf{f} \cdot \nabla \boldsymbol{\varphi}_{\mathbf{w}}|_{\mathbf{Y}(\mathbf{Y_0}, t)} \tag{4.2}$$

For details on working out the conditional probability, see Appendix B. Essentially,

$$\langle \partial \boldsymbol{\varphi}_{\mathbf{w}}/\partial t \mid \boldsymbol{\varphi}_{\mathbf{w}}(\mathbf{y}) = \mathbf{W} \rangle = \lim_{\Delta w \to 0} \frac{\int_{\mathcal{S}} \mathbf{f} \cdot \nabla \boldsymbol{\varphi}_{\mathbf{w}}|_{\mathbf{y}} \, \rho(\mathbf{y}) \, dV}{\int_{\mathcal{S}} \rho(\mathbf{y}) \, dV} \tag{4.3}$$

when $\mathcal{S}$ is the region of Ω satisfying $|\mathbf{w} - \boldsymbol{\varphi}_{\mathbf{w}}(\mathbf{y})| < \Delta w$.

4.5 Solve the model system

Expression (4.3) is precisely the average $d\mathbf{W}/dt$ of systems matching $\boldsymbol{\varphi}_{\mathbf{w}}(\mathbf{y}) = \mathbf{W}$ at the time of measurement. If $\rho(\mathbf{y})$ is the true sample point density, then (4.3) gives the best possible choice for $\mathbf{g}(\mathbf{W})$ in (4.1), in the sense that the expected deviation from any other choice would be larger. (A basic property of the arithmetic mean is that it minimizes expected deviation). To do better would require a larger M, or at least a better choice of model variables.

Thus the model system is

$$\frac{d\mathbf{W}}{dt} = \langle \partial \boldsymbol{\varphi}_{\mathbf{w}}/\partial t \mid \boldsymbol{\varphi}_{\mathbf{w}}(\mathbf{y}) = \mathbf{W} \rangle \tag{4.4}$$

with initial condition $\mathbf{W_0} = \boldsymbol{\varphi}_{\mathbf{w}}(\mathbf{Y_0})$.

Constructing a model in this way avoids the need to engage in the kinds of phenomenological or empirical arguments common to model-building. The model has a clear statistical meaning.

4.6 Predict the expected deviation

The last part of this exercise—one that is otherwise rarely possible in the world of reduced-order modeling—is to predict statistically how the actual system will deviate from the model. Recall that the model makes use of the mean value of $\partial \boldsymbol{\varphi}_{\mathbf{w}}/\partial t$ over all realizations, but the actual $\partial \boldsymbol{\varphi}_{\mathbf{w}}/\partial t$ for

a particular realization depends on the full $\mathbf{Y}$, which is not generally known. For each $\mathbf{W}$, there is an entire distribution of possible $\partial\boldsymbol{\varphi}_{\mathbf{W}}/\partial t$. With $\rho(\mathbf{y})$, however, one can obtain any moment of the $\partial\boldsymbol{\varphi}_{\mathbf{W}}/\partial t$ distribution, and the mean is not the only useful moment. Many might be of interest—for example, if the distribution is unimodal for some time and then suddenly becomes bimodal, a bifurcation is suggested. Similarly, if the distribution is heavily skewed, or otherwise peaks far away from the mean, then most realizations will not obey the model (because the model only predicts average behavior).

The usual measure of deviation is variance. The variance of interest here is

$$\operatorname{var}(\mathbf{W}) = \left\langle \left(\frac{\partial\boldsymbol{\varphi}_{\mathbf{W}}}{\partial t} - \left\langle \frac{\partial\boldsymbol{\varphi}_{\mathbf{W}}}{\partial t} \right\rangle \right)^2 \,\middle|\, \boldsymbol{\varphi}_{\mathbf{W}}(\mathbf{y}) = \mathbf{W} \right\rangle \tag{4.5}$$

with time derivatives from (4.2). Because $\boldsymbol{\varphi}_{\mathbf{W}}(\mathbf{y})$ is a vector, the square implies a dot product.

A distribution of small variance is concentrated near its mean; one of large variance has a wide variety of likely realizations. At one extreme, the variance might be zero, in which case the model's $d\mathbf{W}/dt$ prediction is always correct at $\mathbf{W}$; at the other, the variance might be large, in which case a given realization's $d\mathbf{W}/dt$ would likely differ. Thus the variance $\operatorname{var}(\mathbf{W})$ from (4.5) gives a measure of uncertainty that a system at $\mathbf{W}$ will do what the model predicts.

To make sense of the variance's magnitude, it is customary to take its square root, leaving the standard deviation, a quantity having the same dimensions as $\partial\boldsymbol{\varphi}_{\mathbf{W}}/\partial t$. The standard deviation should then be normalized. A reasonable choice is to normalize it by the magnitude of $\langle \partial\boldsymbol{\varphi}_{\mathbf{W}}/\partial t \mid \boldsymbol{\varphi}_{\mathbf{W}}(\mathbf{y}) = \mathbf{W} \rangle$, assuming the latter is not zero (it is only zero at stationary points of the model). Thus at a given $\mathbf{W}$, the nondimensional standard deviation is:

$$\operatorname{dev}(\mathbf{W}) = \frac{\left\langle \left(\frac{\partial\boldsymbol{\varphi}_{\mathbf{W}}}{\partial t} - \left\langle \frac{\partial\boldsymbol{\varphi}_{\mathbf{W}}}{\partial t} \right\rangle \right)^2 \,\middle|\, \boldsymbol{\varphi}_{\mathbf{W}}(\mathbf{y}) = \mathbf{W} \right\rangle^{\frac{1}{2}}}{\left| \left\langle \frac{\partial\boldsymbol{\varphi}_{\mathbf{W}}}{\partial t} \,\middle|\, \boldsymbol{\varphi}_{\mathbf{W}}(\mathbf{y}) = \mathbf{W} \right\rangle \right|} \tag{4.6}$$

Where $\operatorname{dev}(\mathbf{W})$ is small compared to 1, the model performs reliably; where it is large compared to 1, the model performs poorly.

Other measures of deviation can also be applied, such as the expected magnitude of velocity orthogonal to the direction of travel. That measure discounts differences in speed along the trajectory, which might be less important than differences that tend to fork the trajectory.

4.7 Global deviation and the choice of model variables

Deviation measures from the previous section are local; they represent uncertainty in the model at a particular $\mathbf{W}$. To compare different choices of model variables, a global measure is required. A reasonable choice would be the average nondimensional standard deviation (given by 4.6) taken over all $\mathbf{W}$. A set of model variables having a deviation (4.6) that is smaller on average would be objectively better than a competing set.

Naturally, one wonders whether it would be possible to choose an optimal set of model variables for a problem—that is, whether one could analytically minimize the average of (4.6) over Ω with respect to the choice of model variables (at fixed M). Intuitively, such a technique ought to be possible—whether it would be practical is a separate question—but at time of writing no generally satisfactory technique has been found.

4.8 Equivalence of model assumptions and sample-point-density moments

The preceding sections show that a model can be deduced from moments of the sample point density $\rho(\mathbf{y})$ in a straightforward way. The converse, however, is also interesting, as it gives basic insight into the nature of modeling.

The most unsettling feature of existing reduced-order models is that there are so many to choose from. Even more unsettling, different models can make qualitatively different predictions, particularly for chaotic situations such as turbulence. Models are typically compared by examining their behavior under certain well-known—but ultimately arbitrary—test problems. A model that performs well on one test problem might perform poorly on another. It is sometimes unclear how

a model-based solution ought to be interpreted. Is the unphysically large "wake" behind a blunt object predicted by RANS an (incorrect) prediction of time-averaged streamlines, or is it a mathematical artifact? An LES solution presumes that large scales evolve similarly when the filtered fields coincide at one point in time. Turbulence, however, is chaotic. Large scales depart rapidly under the slightest of subgrid perturbations. What, then, does an LES solution actually signify? Also, how should models should be constructed in the first place? Do they represent an approximation to the equations of motion? If so, then why are terms invariably left over (the *closure problem* of turbulence)?

The answers to many of these questions become clearer when they are posed in terms of the sample point density. Most reduced-order models can be interpreted as a $\mathbf{g}(\mathbf{W})$ for (4.1), because given $\mathbf{W}$, each predicts a corresponding $d\mathbf{W}/dt$. Turbulence models based on LES and URANS are of this form[3]. In light of (4.4), then, the predicted $d\mathbf{W}/dt$ may be interpreted as a conditional moment of $\rho(\mathbf{y})$, a $\langle \partial\boldsymbol{\varphi}_\mathbf{w}/\partial t \mid \boldsymbol{\varphi}_\mathbf{w}(\mathbf{y}) = \mathbf{W}\rangle$. From the sample point density point of view, therefore, *every reduced-order model is equivalent to a set of assumptions regarding moments of the sample point density.*

Because the sample point density is not determined solely by the governing equations, but also by the experimental conditions (stationary or asymptotic approach), an immediate consequence is that models are not simply approximations to the governing ODEs, but rather approximations to the conditions under which experiments take place. To put it in concrete terms, a turbulence closure for LES like that of Smagorinsky (1963) is not merely a statement about Navier-Stokes, but an assertion that data will only be taken when conditions allow the closure assumption to hold, i.e., under approximate stationarity. Intuitively, that makes sense: The model obviously would not hold for highly nonstationary conditions, such as while a wind tunnel is being abruptly powered off.

This point of view also sheds light on the closure problem. Because $\rho(\mathbf{y})$ depends on the apparatus design, start-up process, and sampling schedule—not merely on the governing equation—(1.1) does not provide enough information to determine any moment of the distribution of $\partial\boldsymbol{\varphi}_\mathbf{w}/\partial t$. There

[3]Models based on steady RANS are different because for these, $d\mathbf{W}/dt$ is zero by construction. Instead, expected Reynolds stresses are assumed. The conclusion in italics still holds.

simply isn't enough information to close the reduced-order equations; they are underdetermined. On the other hand, once $\rho(\mathbf{y})$ is known, the equations can be closed by the methods of this chapter without further difficulty.

Finally, the methods of this chapter allow models to be compared in absolute terms. If $\rho(\mathbf{y})$ is physically correct, then for a given choice of model variables, the model given by (4.4) is optimal. The expected mean square difference between $\mathbf{g}(\mathbf{W})$ and the actual rates of change of any realization's model variables is a global minimum, and the expected mean square difference would be larger for any other model. Thus existing models may be compared by examining the norm of the difference between their predictions and those from the conditional expected velocity of (4.3).

Reduced-order models will play a part in several of the example problems, including a damped linear oscillator in Chapter 6, the Rayleigh-Plesset equation in Chapter 7, and Lorenz's equations in Chapter 8.

Chapter 5

Example: one-dimensional linear decay

5.1 Introduction

Consider the trivial one-dimensional linear system

$$\frac{dY}{dt} = -Y \tag{5.1}$$

when Ω is the set $Y : Y \in [1, 1]$.

System (5.1) represents the simplest kind of first-order decay. For example, $Y(Y_0, t)$ would describe the voltage across a capacitor being discharged through a resistor; Y_0 is the initial voltage, and t is time in units of RC. This particular application is neither intended to be representative nor typical; it is too simple to justify the conceptual overhead of our technique. Rather, our goal in this chapter is to render the abstractions introduced in Chapters 2 and 3 in concrete terms.

Solution trajectories of (5.1) have the form

$$Y(Y_0, t) = Y_0 \exp(-t) \tag{5.2}$$

In this case, the set $\mathcal{R}$ has only one element, the origin $Y = 0$. All other points in the interval $[-1, 1]$ belong to $\mathcal{R}^c$. The outer boundary $\partial\Omega$ consists of two points, $Y = -1$ and $Y = 1$, and the phase-space divergence is -1 everywhere.

5.2 Solutions

We begin with the solution for stationary conditions, followed by that for experiments undergoing asymptotic approach.

Because the solution for stationary conditions is singular on $\mathcal{R}$ and zero elsewhere, generalized functions are required to represent it. In Section 2.3, we saw that a solution may be found by taking certain limits. Here, the answer is obvious:

$$\rho_{\text{stationary}}(y) = \delta(y) \tag{5.3}$$

where $\delta(y)$ is Dirac's delta function. Thus to obtain the expected value of any observable $\varphi(y)$ under stationary conditions, simply take $\varphi(0)$. The expected voltage of the system (5.1) under stationary conditions, for example, is zero.

Because $\nabla \cdot \mathbf{f} = -1$, the appropriate asymptotic approach solution is given by (E.14). In order to satisfy (1.4), λ must be $1/2$. Thus

$$\rho_{\text{asymptoticapproach}}(Z(Z_0, s)) = \frac{1}{4}(s+1) \tag{5.4}$$

whether Z_0 is $+1$ or -1. Using (5.2) and $|Z_0| = 1$, (5.4) is equivalent to

$$\rho_{\text{asymptoticapproach}}(y) = \frac{1}{4}\left(\log\left(\frac{1}{|y|}\right) + 1\right) \tag{5.5}$$

A plot of this function appears in Figure 5.1.

With $\rho_{\text{asymptoticapproach}}(y)$, one may derive the expectation value of any observable during approach to the origin. In this case, the system is so simple that such an application might seem contrived, but it helps to illustrate the thought process. We now use $\rho_{\text{asymptoticapproach}}(y)$ to compute the expected value $\langle y^2 \rangle$ during asymptotic approach.

The mean square value of Y during experiments is an observable having the phase function

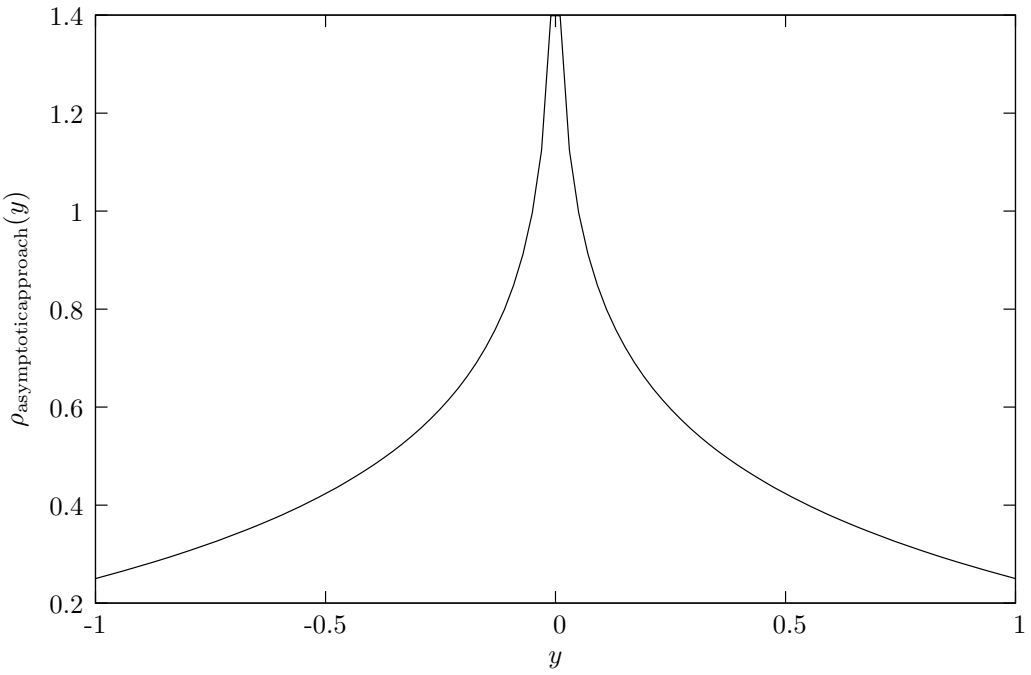

Figure 5.1: The asymptotic approach solution $\rho_{\text{asymptoticapproach}}(y)$ given by Equation (5.5) for system (5.1) on the domain $y \in [-1:1]$.

$\varphi(y) = y^2$. Its expected value is

$$\langle y^2 \rangle = \int_\Omega \varphi\rho \, dV = \int_{-1}^{1} y^2 \frac{1}{4} \left(\log(\frac{1}{|y|}) + 1 \right) \, dy = \frac{2}{9} \tag{5.6}$$

The root mean square value of Y during asymptotic approach experiments on this interval is therefore about 0.47. One should not read too far into this result, as other legitimate ways to bound integral (3.5) would give somewhat different numbers. Nevertheless—and this is remarkable, considering nothing has been said about initial conditions; only the equation, interval of interest, and assumption of asymptotic approach—the answer does match experience. A series of experiments designed to study system (5.1) asymptotically decaying on the interval $[-1:1]$ might, reasonably, have such an RMS value for y.

The preceding result could also have been found by integration along characteristics. By the

transformation of variables given in Appendix A:

$$\begin{aligned}\langle y^2 \rangle &= \int_\Omega \varphi\rho \, dV \\ &= \int_{\partial\Omega} \int_0^\infty \varphi\rho\mathcal{J} \, ds \, dS \\ &= 2\int_0^\infty (\exp(-s))^2 \left(\frac{1}{4}(s+1)\right)(\exp(-s)) \, ds \\ &= \frac{1}{2}\int_0^\infty (\exp(-s))^3 (s+1) \, ds = 2/9\end{aligned} \tag{5.7}$$

The transformation will be of greater utility in more than one dimension.

5.3 Arriving at the asymptotic approach density

One might reasonably ask what course of experiments could give rise to a $\rho_{\text{asymptoticapproach}}(y)$ such as the one derived above. As always, there are infinitely many ways to produce a given sample point density; what follows is one specific possibility.

Suppose that the following experiment were repeated many times. Starting from exactly $Y_0 = \pm 1$ (with equal likelihood) at $t = 0$, the system of (5.1) is allowed to run until some finite but variable t_{end}, with measurements taken at regular intervals during the asymptotic approach. What distribution of t_{end} would produce the $\rho_{\text{asymptoticapproach}}(y)$ above? That is, what density function $\mu(t_{\text{end}})$ of experiment durations would correspond to $\rho_{\text{asymptoticapproach}}(y)$?

The density of measurements for a particular t_{end} grows exponentially in time. Normalized and expressed in terms of y, it is $1/(2t_{\text{end}}|y|)$ for $\exp(-t_{\text{end}}) < |y| \leq 1$, otherwise zero. Therefore $\mu(t_{\text{end}})$ would need to satisfy

$$\int_{-\log(|y|)}^\infty \frac{1}{2t_{\text{end}}|y|}\mu(t_{\text{end}}) \, dt_{\text{end}} = \rho_{\text{asymptoticapproach}}(y) \tag{5.8}$$

The right-hand side may be taken from (5.5).

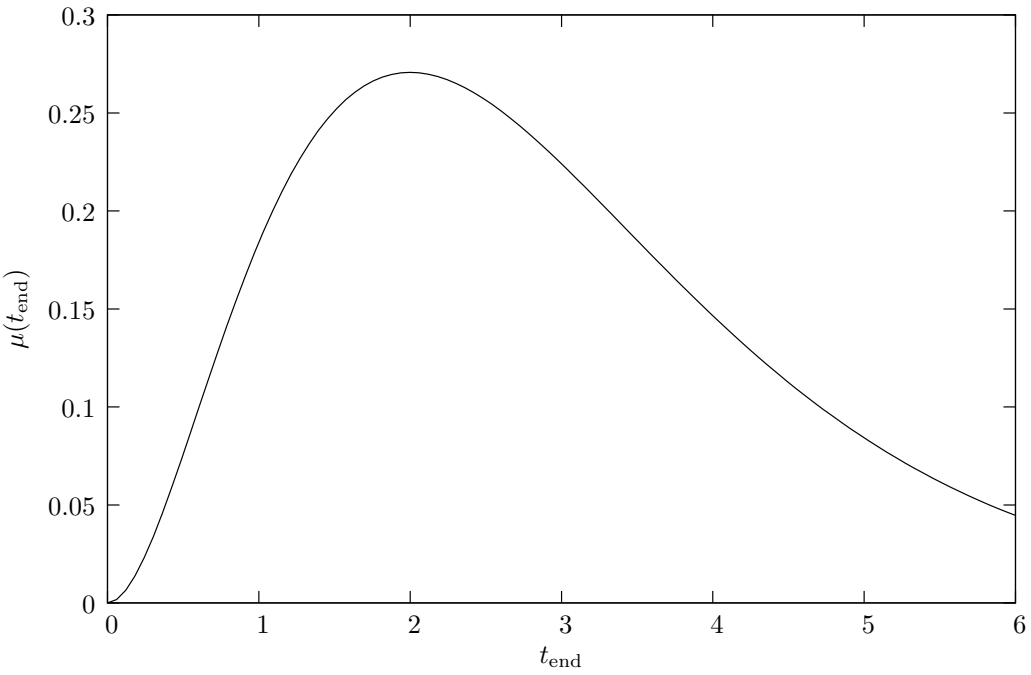

Figure 5.2: $\mu(t_{\text{end}})$, a distribution of experiment durations that would give rise to the asymptotic approach density $\rho_{\text{asymptoticapproach}}(y)$ of (5.5) if each experiment starts from $Y_0 = \pm 1$ and measurements are taken at uniform intervals. The distribution, from (5.9), has a mode of 2 and a mean of 3.

Solving (5.8) for $\mu(t_{\text{end}})$, the duration of experiments would be distributed as

$$\mu(t_{\text{end}}) = \frac{1}{2} t_{\text{end}}^2 \exp(-t_{\text{end}}) \tag{5.9}$$

A plot of the t_{end} distribution appears in Figure 5.2.

Chapter 6

Example: damped linear oscillator

6.1 Introduction

In this chapter, we consider the two-dimensional linear system

$$\frac{d}{dt}\begin{pmatrix} Y_1 \\ Y_2 \end{pmatrix} = \begin{pmatrix} -\frac{1}{2} & 1 \\ -1 & -\frac{1}{4} \end{pmatrix}\begin{pmatrix} Y_1 \\ Y_2 \end{pmatrix} \tag{6.1}$$

when Ω is the unit disk. A phase portrait of (6.1) appears as Figure 6.1.

System (6.1) describes a damped linear oscillator (damping coefficient of $-1/4$) such as a mass-spring system, but it includes an additional damping due to position (the $-1/2$ in the upper left-hand corner) to make the phase portrait more interesting. It is harder to rationalize the $-1/2$ in terms of physical effects; it could come from a change of variables or some sort of elastic-plastic behavior.

That Ω should be a unit disk is based on the following reasoning, which applies even in more complicated situations: if there were no damping, flow would be everywhere tangent to circles centered on the origin, which represent surfaces of constant energy. Their shape is determined entirely by the off-diagonal terms. Thus a circle is the only shape that remains a trapping region under different damping characteristics (even in the limit of small damping). The choice of radius, however, remains arbitrary.

System (6.1) is dissipative. Its phase-space divergence $\nabla \cdot \mathbf{f}$ is everywhere constant at $-3/4$. There is a spiral point at the origin, which is the only point not accessible from the boundary in

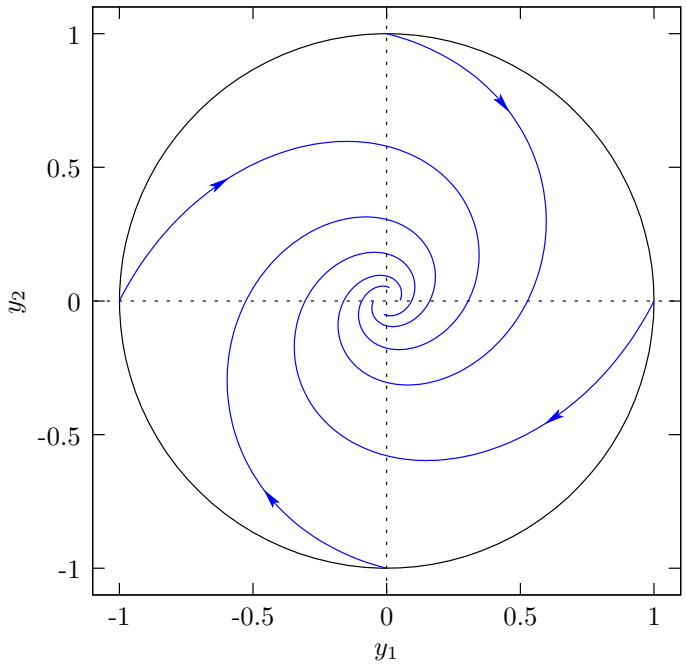

Figure 6.1: Phase portrait of system (6.1). Trajectories approach the origin after infinite time. The boundary circle indicates $\partial\Omega$.

finite time. Thus $\mathcal{R}$ is the point $(0, 0)$, and all other points in Ω belong to $\mathcal{R}^c$, a punctured disk in y_1, y_2 space.

6.2 Solutions

As in the previous example, the only stationary density is a delta function at the origin, now in two dimensions:

$$\rho_{\text{stationary}}(\mathbf{y}) = \frac{\delta\left(\sqrt{y_1^2 + y_2^2}\right)}{\pi\sqrt{y_1^2 + y_2^2}} \tag{6.2}$$

Thus the expected value of any observable $\varphi(\mathbf{y})$ under stationary conditions is exactly $\varphi(\mathbf{0})$. This is a typical situation for unforced problems.

Because $\nabla \cdot \mathbf{f}$ is constant, the decaying solution is given by (E.14). From (E.15),

$$\lambda = \frac{(\nabla \cdot \mathbf{f})^3}{\int_{\partial\Omega} \mathbf{f} \cdot \hat{\mathbf{n}}\, dS} = \frac{(-3/4)^3}{-3\pi/4} = \frac{9}{16\pi} \tag{6.3}$$

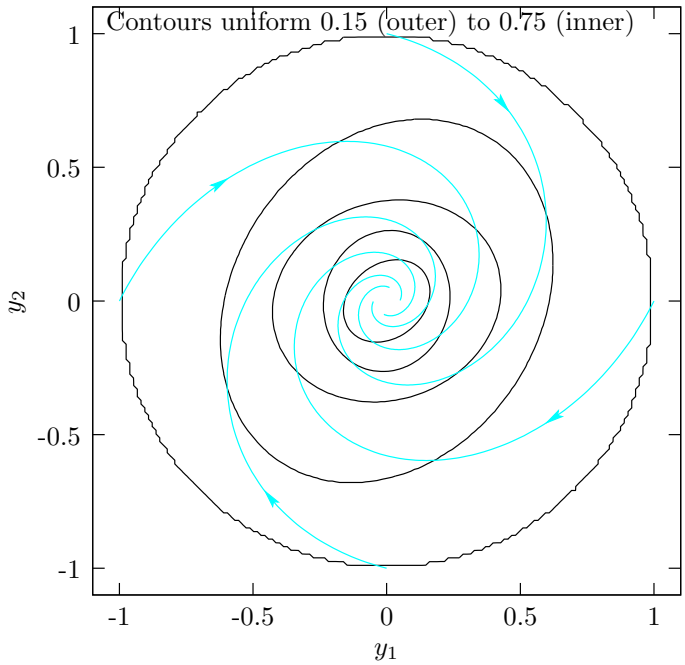

Figure 6.2: Contours of $\rho_{\text{asymptoticapproach}}(\mathbf{y})$ for system (6.1), with trajectories. The density increases along trajectories, from a boundary value of $\frac{1}{2\pi}$ to infinity at the origin. The singularity at the origin is integrable, however, and the probability of observing the system in its infinitesimal neighborhood approaches zero.

and so

$$\rho_{\text{asymptoticapproach}}\left(\mathbf{Z}\left(\mathbf{Z_0}, s\right)\right) = \frac{3}{8\pi}\left(s + \frac{4}{3}\right) \tag{6.4}$$

On the boundary (where $s = 0$), $\rho_{\text{asymptoticapproach}}(\mathbf{y})$ has the constant value $\frac{1}{2\pi}$. Contours of $\rho_{\text{asymptoticapproach}}(\mathbf{y})$, computed by integration along trajectories, are plotted in Figure 6.2. To obtain $\rho_{\text{asymptoticapproach}}(\mathbf{y})$ explicitly (that is, without invoking the intermediate variable s), one would have to solve characteristics $\mathbf{Z}(\mathbf{Z_0}, s)$ of (6.1), which are

$$\begin{pmatrix} Z_1(\mathbf{Z_0}, s) \\ Z_2(\mathbf{Z_0}, s) \end{pmatrix} = \exp\left(-\frac{3}{8}s\right) \begin{pmatrix} Z_{01}\cos\left(\sqrt{\frac{63}{64}}s\right) - \sqrt{\frac{1}{63}}\left(Z_{01} - 8Z_{02}\right)\sin\left(\sqrt{\frac{63}{64}}s\right) \\ Z_{02}\cos\left(\sqrt{\frac{63}{64}}s\right) - \sqrt{\frac{1}{63}}\left(Z_{02} - 8Z_{01}\right)\sin\left(\sqrt{\frac{63}{64}}s\right) \end{pmatrix} \tag{6.5}$$

analytically for s. Because $\partial\Omega$ is a unit circle, $Z_{01}^2 + Z_{02}^2 = 1$. The inversion would not be trivial.

At this point, application of the theory is essentially complete. One can compute any desired observable by taking the moment of its phase function against whatever $\rho(\mathbf{y})$ is appropriate (6.2

or 6.4), possibly making use of the streamtube change of variables described in Appendix A. For example, the covariance matrix based on $\rho_{\mathrm{asymptoticapproach}}(\mathbf{y})$ is

$$\begin{pmatrix} < y_1 y_1 > & < y_1 y_2 > \\ < y_2 y_1 > & < y_2 y_2 > \end{pmatrix} = \begin{pmatrix} 0.184 & 0.005 \\ 0.005 & 0.192 \end{pmatrix} \tag{6.6}$$

Again, other ways of bounding (3.5) would have yielded somewhat different values.

6.3 Reduced-order model

A more interesting application is based on the methods introduced in Chapter 4: using $\rho(\mathbf{y})$ to construct a reduced-order model. The system is only two-dimensional to begin with, but we can reduce the order from two to one.

A reasonable choice for the model variable in this case is $H(\mathbf{y})$, the Hamiltonian of the *undamped* system (that is, if both of the diagonals in (6.1) were zero), given by

$$H(\mathbf{y}) = \frac{1}{2}\left(y_1^2 + y_2^2\right) \tag{6.7}$$

One might guess *a priori* that $H(\mathbf{y})$ would be a good choice because it is monotone in time along trajectories, and because at fixed H, $\partial H(\mathbf{Y}(\mathbf{Y_0}, t))/\partial t$ does not vary too much, particularly at low damping.

Following the steps of Chapter 4:

1. Because we are modeling the decay process, the density $\rho(\mathbf{y})$ will be $\rho_{\mathrm{asymptoticapproach}}(\mathbf{y})$ from (6.4).

2. The vector $\boldsymbol{\varphi}_{\mathbf{w}}(\mathbf{y})$ has only one component. $\varphi_{w_1}(\mathbf{y}) = H(\mathbf{y})$, given by (6.7). For notational simplicity, it will be denoted $\varphi_w(\mathbf{y})$.

3. In this case, $\partial\varphi_w/\partial t$ is $\mathbf{f} \cdot \nabla H$, or $-\frac{1}{2}y_1^2 - \frac{1}{4}y_2^2$. Because the original system is linear, it would be possible to compute the conditional probability $\langle \partial\varphi_w/\partial t \mid \varphi_w(\mathbf{y}) = W \rangle$ analytically. In the

interest of demonstrating a more general technique, however, a numerical approximation is applied below.

4. The model system is then

$$\frac{dW}{dt} = \left\langle -\frac{1}{2}y_1^2 - \frac{1}{4}y_2^2 \;\middle|\; \frac{1}{2}\left(y_1^2 + y_2^2\right) = W \right\rangle \tag{6.8}$$

with initial condition $W(W_0, 0) = W_0 = H(\mathbf{Y_0})$. $W(W_0, t)$ is a modeled approximation to the full undamped system's Hamiltonian.

5. The expected deviation of $-\frac{1}{2}y_1^2 - \frac{1}{4}y_2^2$, either conditioned on W or globally, measures uncertainty in the model's prediction.

Analysis begins by computing $\rho(\mathbf{y})$ at every point on a grid in y_1, y_2 space that is also inside Ω. The grid is chosen to avoid $\mathcal{R}$; in the example below, its spacing is 0.014 in both y_1 and y_2. The lattice extends over a rectangle from $(-1.1, -1.1)$ to approximately $(1.1, 1.1)$, but the computational grid consists only of lattice points inside the unit circle.

Next, $H(\mathbf{y})$ is computed at every gridpoint, and the grid maxima and minima are established (in this case, 0 and 0.5). The minimum and maximum $H(\mathbf{y})$ define a range, which is then partitioned uniformly into bins. Within each bin, $H(\mathbf{y})$ is approximately constant, and the bins have small ΔH, so conditional expectation over a bin approaches the desired limit as the bin size approaches zero (provided the lattice remains fine enough to keep a large number of gridpoints in each bin). In this case, the partition consists of 40 uniformly H-spaced bins, which are concentric annuli. (The innermost bin is a disk.)

To work out the required conditional probability involves taking a limit, as indicated in (4.3). Numerically approximating a limit involves computing a sequence of solutions having smaller and smaller bin size. In the interest of clarity, however, one solution of a single, uniformly-small bin size is investigated here.

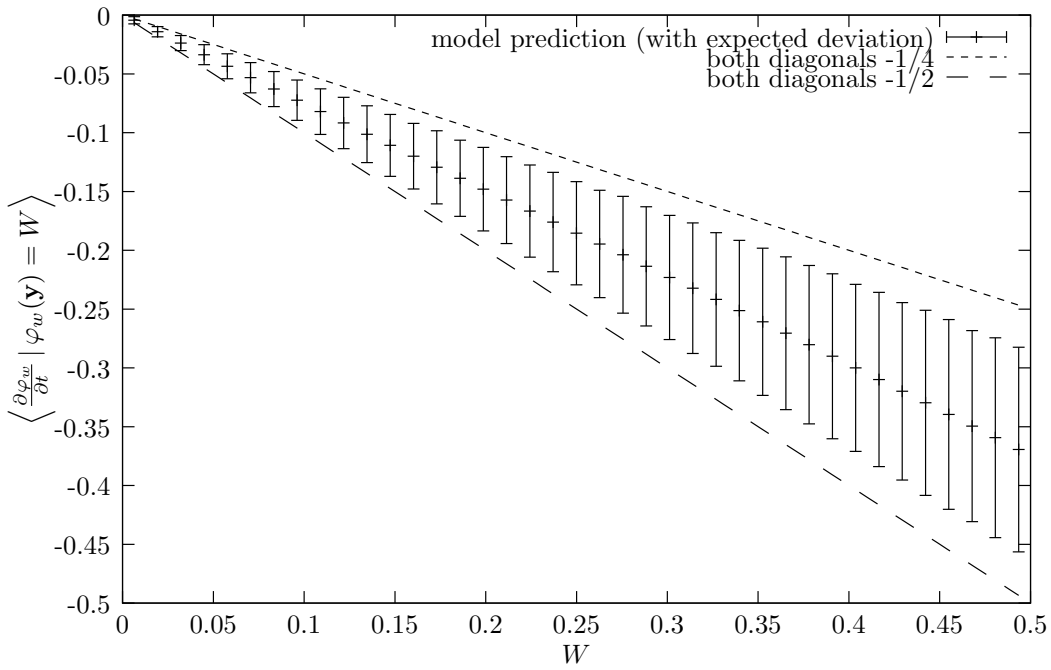

Figure 6.3: Binned conditional expectations $\left\langle \frac{\partial \varphi_w}{\partial t} \,\middle|\, \varphi_w(\mathbf{y}) = W \right\rangle$, the modeled rate of decay of the (undamped system's) Hamiltonian for (6.1). Top and bottom curves indicate analytical decay rates for systems that are like (6.1) but whose diagonals are both $-1/2$ or $-1/4$, respectively. The predicted decay rate falls between the two. Error bars indicate the uncertainty, in dimensions of the ordinate.

The expected value of $\partial \varphi_w / \partial t$ over each bin is then approximated as:

$$\langle \partial \varphi_w / \partial t \mid \varphi_w(\mathbf{y}) \text{ in bin } i \rangle \approx \frac{\sum \left(-\frac{1}{2} y_{1_j}^2 - \frac{1}{4} y_{2_j}^2 \right) \rho_j}{\sum \rho_j} \tag{6.9}$$

where sums are taken over all gridpoints j in the ith bin. These conditional expectations are plotted in Figure 6.3. The predicted rate of decay falls somewhere between that of a system whose diagonals are both $-1/2$, and one whose diagonals are both $-1/4$, which is reasonable. Predicted deviations from $g(W)$ are small, showing that the choice of model variables was a good one; the average of nondimensional standard deviation (4.6) over w is 0.253, which is small compared to 1.

Once the approximate (6.9) has been computed, the next step is to use it as a model, numerically integrating (4.4) to obtain the modeled Hamiltonian decay profile. Integration of the numerical function implied in Figure 6.3 is straightforward. It yields approximately a decaying exponential for the modeled Hamiltonian.

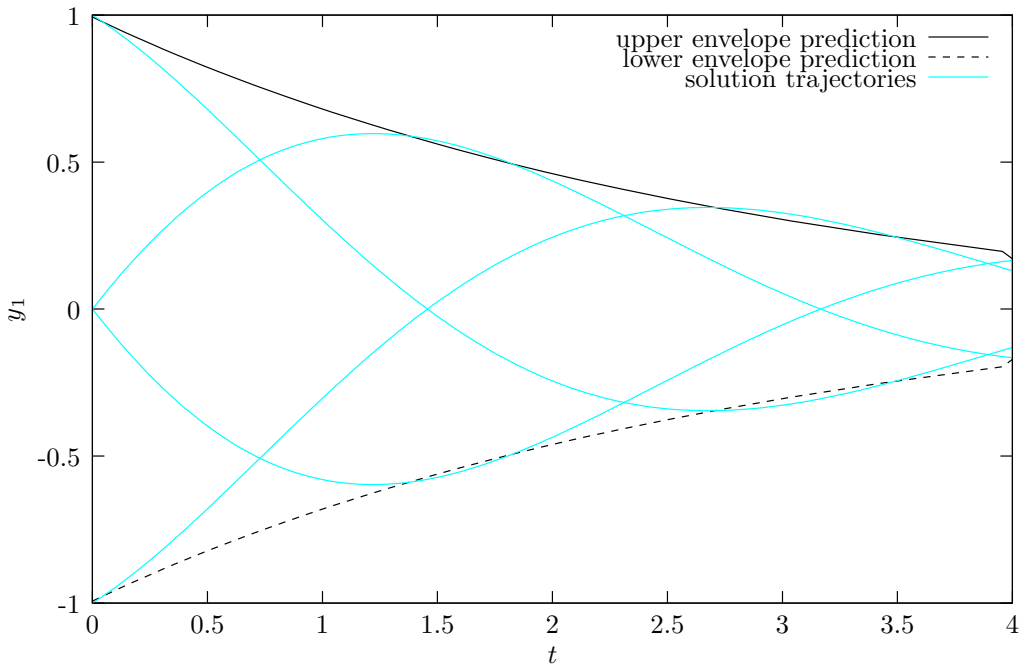

Figure 6.4: Envelope curves. The top and bottom curves predict an envelope based on the reduced-order model. The initial condition for the model is $W_0 = 0.5$. Plotted between the envelope curves are several trajectories. Each starts at a different $\mathbf{Y_0}$, but satisfies $H(\mathbf{Y_0}) = 0.5$.

One way to compare the modeled solution to real trajectories is to derive from it a pair of envelope curves. The solution's envelope in y_1 can be found by solving for y_1 as a function of H while forcing $y_2 = 0$. There are two solutions at each H, hence the pair of curves. In Figure 6.4, envelope curves based on the model prediction are plotted against several solution trajectories.

Chapter 7

Example: Rayleigh-Plesset equation

7.1 Introduction

The Rayleigh-Plesset equation is a nonlinear ordinary differential equation describing how a gas bubble immersed in liquid oscillates under fluctuations in ambient pressure. It serves as a model for many physical applications, including cavitation phenomena, shock-wave lithotripsy, sonoluminescence, and inertial confinement. The isothermal form examined here makes an additional simplifying assumption—temperature variations are negligible—that, although it is quite restrictive, retains essential features of the physics. A nondimensional form of the equation, from the review of Feng and Leal (1997), is

$$xx'' + \frac{3}{2}(x')^2 = \frac{1}{x^3} + 2P - \frac{3}{x} - \nu_0 \frac{x'}{x} \tag{7.1}$$

Here x is a nondimensional bubble radius, P is a physical parameter of the system (involving vapor pressure, surface tension, and a few other factors), and ν_0 is a nondimensional viscosity. The $'$ signifies differentiation with respect to nondimensionalized time. We arbitrarily take the typical values $P = -0.1$ and $\nu_0 = 0.05$ for this example.

Because equation (7.1) is second-order, it can be converted into a two-dimensional system ($N = 2$) of first-order equations. The following choice of variables is known to be canonical—that is, it leaves

a Hamiltonian structure when ν_0 is zero:

$$\begin{aligned} Y_1 &= x \\ Y_2 &= x^3 x' \end{aligned} \tag{7.2}$$

With this change of variables, Y_1 is q, a generalized coordinate, and Y_2 is p, a generalized momentum. In terms of $\mathbf{Y}$, system (7.1) is

$$\frac{d}{dt}\begin{pmatrix} Y_1 \\ Y_2 \end{pmatrix} = \begin{pmatrix} \frac{Y_2}{Y_1^3} \\ \frac{3}{2}\frac{Y_2^2}{Y_1^4} + \frac{1}{Y_1} + 2PY_1^2 - 3Y_1 - \nu_0 \frac{Y_2}{Y_1^2} \end{pmatrix} \tag{7.3}$$

The Hamiltonian of the inviscid ($\nu_0 = 0$) system is given by

$$H(\mathbf{y}) = \frac{Y_2^2}{2Y_1^3} - \log(Y_1) + \frac{3}{2}Y_1^2 - \frac{2}{3}PY_1^3 \tag{7.4}$$

For Ω, we take a surface at which the Hamiltonian of the inviscid system ($\nu_0 = 0$) is constant, because it is a trapping region irrespective of ν_0. The constant, 2.317, has been chosen to give an approximately order-of-magnitude range of bubble radius. A phase portrait appears in Figure 7.1.

The phase-space divergence $\nabla \cdot \mathbf{f}$ of (7.3) is everywhere negative, but it is *not* constant: it is $-\nu_0/y_1^2$. The only contribution to $\nabla \cdot \mathbf{f}$ comes from the viscous term, because the phase-space divergence of a Hamiltonian system in canonical coordinates is zero (Liouville). This expression is singular along the y_2 axis; because Ω lies entirely in the right-half plane, however, $\nabla \cdot \mathbf{f}$ still remains bounded inside it.

There is only one point in Ω that is inaccessible from the boundary—the stationary point at $(a, 0)$, where a is the positive real root of $2Py_1^3 - 3y_1^2 + 1$. Here, $P = -0.1$, so a is approximately 0.5667. This is also the point at which $H(\mathbf{y})$ is a minimum. Thus, as in the previous example, $\mathcal{R}$ consists of only a single stationary point; all other points of Ω belong to its complement, $\mathcal{R}^c$.

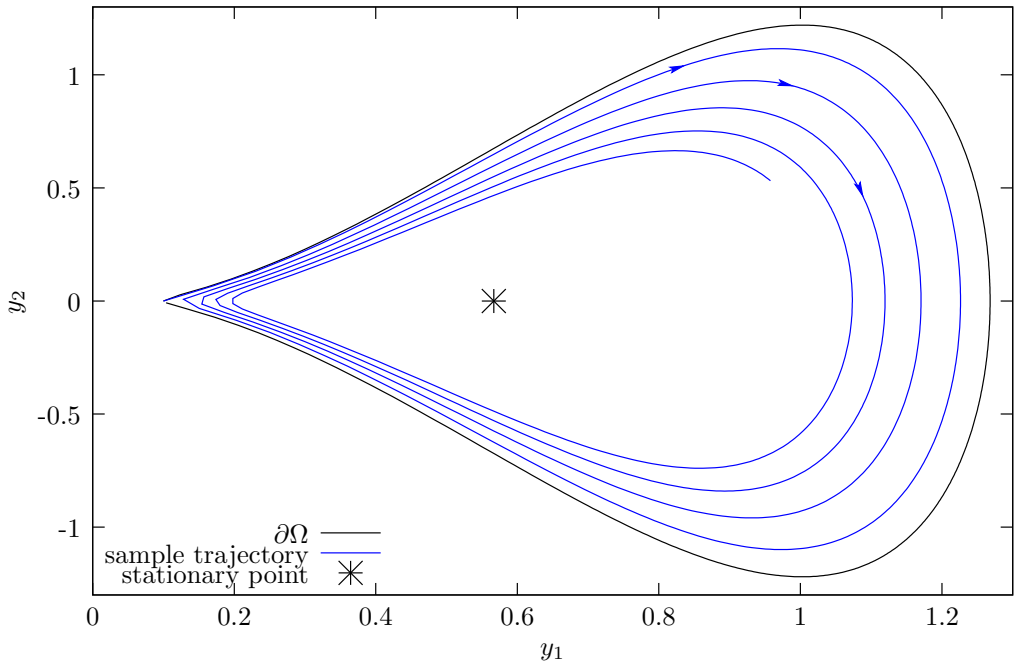

Figure 7.1: Phase portrait of the Rayleigh Plesset system (7.3). The outer boundary coincides with an isosurface of the (corresponding inviscid system's) Hamiltonian. With finite viscosity, trajectories spiral inward toward a stationary point at fixed bubble radius.

7.2 Solutions

In this example, as in previous examples for which $\mathcal{R}^c$ consisted of a single stationary point, $\rho_{\text{stationary}}(\mathbf{y})$ is a Dirac delta function. That is, the expected value of an observable $\varphi(\mathbf{y})$ under stationary conditions is $\varphi(\mathbf{y})$ evaluated at the stationary point $(a, 0)$.

Because $\nabla \cdot \mathbf{f}$ is *not* constant, the asymptotic approach solution must be expressed in the integral form given by (E.13); it does not simplify analytically. That is, along characteristics $\mathbf{Z}(\mathbf{Z_0}, s)$,

$$\rho_{\text{asymptoticapproach}}(\mathbf{Z}(\mathbf{Z_0}, s)) = \frac{\lambda}{2M(\mathbf{Z_0}, s)} \int_s^\infty M(\mathbf{Z_0}, s') s' \, ds' \tag{7.5}$$

where

$$M(\mathbf{Z_0}, s) = \exp\left(\int_0^s \nabla \cdot \mathbf{f}|_{\mathbf{Z}(\mathbf{Z_0}, s')} \, ds' \right) = \exp\left(-\nu_0 \int_0^s \frac{1}{Z_1(\mathbf{Z_0}, s')} \, ds' \right) \tag{7.6}$$

The constant λ must cause the integral over Ω of $\rho_{\text{asymptoticapproach}}(\mathbf{y})$ to be 1, as mandated by (1.4). Finding $\rho_{\text{asymptoticapproach}}(\mathbf{y})$ explicitly from (7.5) would require solving the characteristic equations

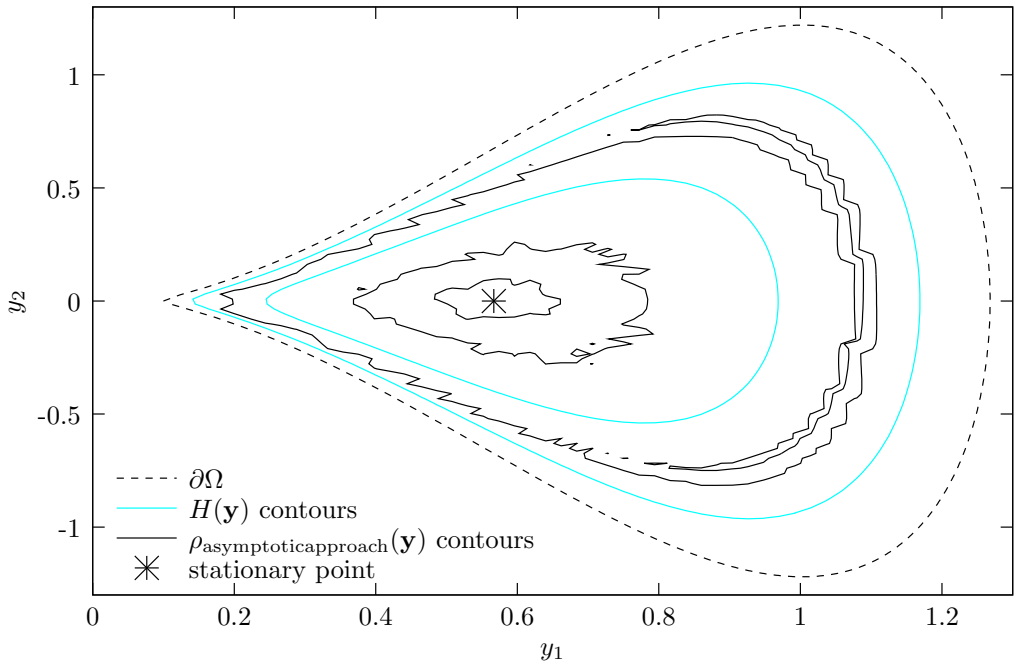

Figure 7.2: Contours of $\rho_{\text{asymptoticapproach}}(\mathbf{y})$ for the Rayleigh-Plesset test case, shown at levels 0.5, 1.0, and 1.5 (outermost to innermost, respectively), and of the inviscid system's Hamiltonian, shown at levels 1.0, 1.5, and 2.0.

for $s_b(\mathbf{Z})$, which would be impractical.

Nevertheless, $\rho_{\text{asymptoticapproach}}(\mathbf{y})$ may be approximated numerically by integrating along trajectories, just as in the previous examples. Contours are plotted in Figure 7.2. Because $\nabla \cdot \mathbf{f}$ is not constant, neither is the boundary condition.

7.3 Reduced-order model

The Rayleigh-Plesset equation presents our first opportunity to address a question of real outside interest. Its sharp cusps present a problem for some applications because they mean that direct numerical integration of (7.3) would be time-consuming. Integrating across the near-singularity at each radius minimum requires significant computational effort, and such effort is wasted when detailed resolution of the cusp is unnecessary, as when it factors only tangentially into a larger process that is only sensitive to (for example) the average energy or frequency.

In his Ph.D. thesis, which principally concerns other aspects of computational bubble dynamics,

Tanguay (2004) briefly explores the possibility of creating such a model for a more complicated analogue of (7.3). Tanguay characterizes the flow of probability mass in action-angle coordinates, but follows a Lagrangian description of an ensemble cloud rather than an (unmoving) sample point density, leading to difficulty as time progresses.

Following Chapter 4, construction of a reduced-order model is a five-step process:

1. Choose the appropriate $\rho(\mathbf{y})$. Because the goal is to model asymptotic decay behavior, $\rho_{\text{asymptoticapproach}}(\mathbf{y})$, given by (7.5), is an appropriate choice.

2. Choose the model variables. As in the simpler example studied in Chapter 6, we make use of the undamped ($\nu_0 = 0$) system's Hamiltonian. Thus $\varphi_{\mathbf{w}}(\mathbf{y})$ has only a single component, $\varphi_w(\mathbf{y})$, which is $H(\mathbf{y})$, given by (7.4).

3. Compute the conditional expected value $\langle \partial\varphi_w/\partial t \mid \varphi_w(\mathbf{y}) = W \rangle$. The phase function corresponding to $\partial\varphi_w/\partial t$ is $\mathbf{f} \cdot \nabla\varphi_w$, which in this case is $-\nu_0 y_2^2/y_1^5$.

4. Solve the model system. Model means are plotted in Figure 7.3.

5. Compute the uncertainty. Predicted standard deviations appear as error bars in Figure 7.3.

A striking feature of Figure 7.3, relative to Figure 6.3 in the previous chapter, is that the error bars are much larger. The expected nondimensional deviation using $H(\mathbf{y})$ as the model variable is approximately 1 to 2, meaning the expected error in phase velocity is typically once to twice as large as the model mean. Hence, $H(\mathbf{y})$ is not nearly as good a choice for the model variable $\varphi_w(\mathbf{y})$ as it was in Chapter 6. Of course, no other reduced-order model having $H(\mathbf{y})$ as its model variable could give a smaller average deviation. It would benefit the modeler to choose a different model variable, particularly if he or she is interested in behavior near the stationary point, where the predicted deviation is particularly large.

Nevertheless, the model solution may be applied, as it was in the previous chapter, to predicting envelope curves. It works reasonably well for short times, where the expected deviation remains comfortably less than 1. Predicted top and bottom envelopes are plotted in Figure 7.4.

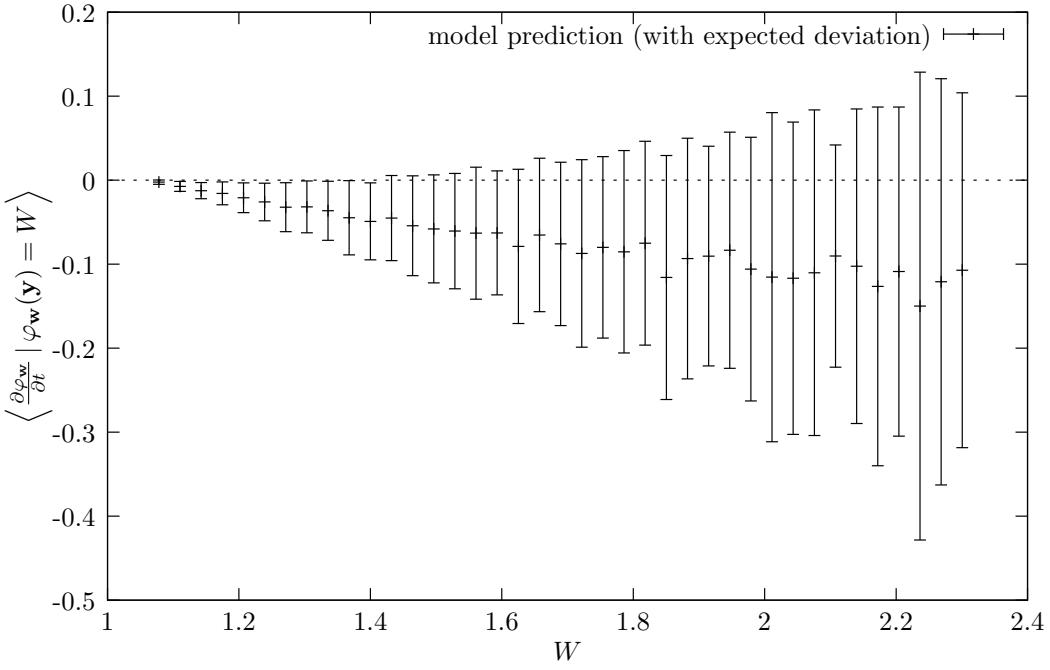

Figure 7.3: Binned conditional expectations $\left\langle \frac{\partial \varphi_w}{\partial t} \,\middle|\, \varphi_w(\mathbf{y}) = W \right\rangle$, the decay rate of the Hamiltonian of the inviscid ($\nu_0 = 0$) Rayleigh-Plesset example system (7.3). Error bars show the predicted *dimensional* standard deviation, which is typically 1–2 times the mean.

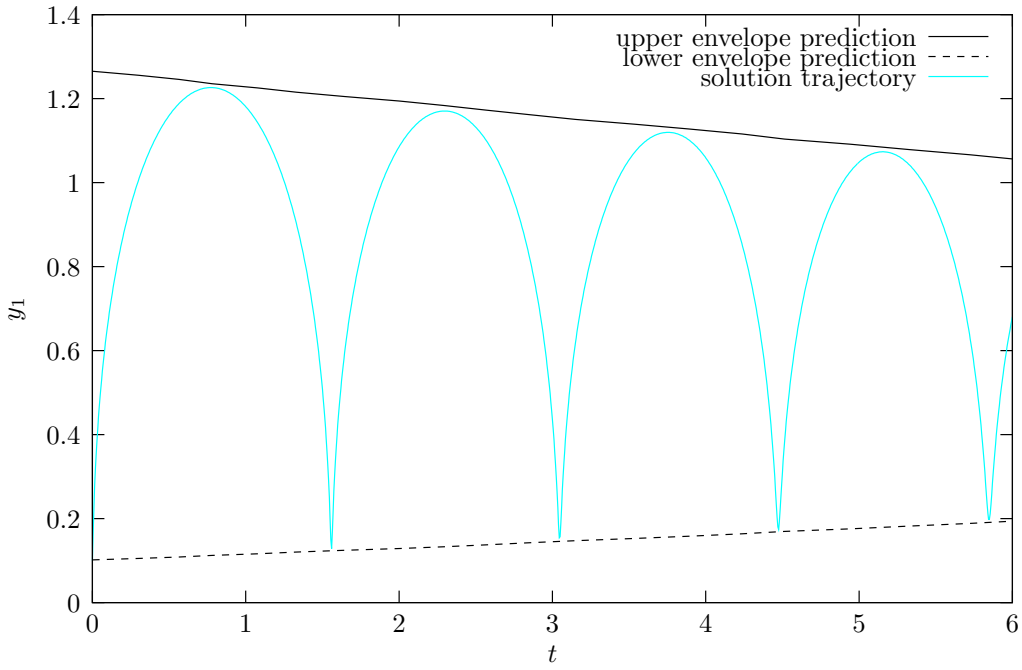

Figure 7.4: Envelope curves for the Rayleigh-Plesset example system (7.3). The top and bottom curves demarcate the predicted envelope. The initial condition for the model is $W_0 = 2.317$. Plotted between the envelope curves is the same trajectory shown in Figure 7.1, which satisfies $H(\mathbf{Y_0}) = 2.317$.

Chapter 8

Example: Lorenz equation

8.1 Introduction

Prior to the early 1960s, conventional wisdom—based mostly on experience with linear and nearly linear systems—divided differential equations into two major categories: stochastic or deterministic. Parameters of the former, such as forcing and damping, were random, whereas those of the latter were predictable. Stochastic systems, it was believed, gave rise to stochastic solutions, and deterministic systems gave rise to deterministic solutions. Barring singularities, a differential equation that was not stochastic could be assumed to have a regular, predictable solution for all time.

The apparent dichotomy became important to early efforts at weather prediction, which had finally begun a transition from empiricism to first-principles analysis. While it might not have been practical to measure the temperature, wind speed, humidity, and so forth everywhere on Earth's surface at once, such quantities were at least knowable in principle. As measuring technology and computers improved, it followed that the remaining unknowns would become progressively less important, allowing for ever-longer range forecasts. Limits on the march of progress—if indeed there were any—would be imposed externally by such fundamentally unpredictable forcings as the solar radiation level.

A major intellectual challenge to this mode of thinking arrived in the form of a paper by Edward Lorenz, then and still a meteorologist at the Massachusetts Institute of Technology. The paper, *Deterministic Nonperiodic Flow* (Lorenz, 1963), rose to landmark status by demonstrating,

by way of a uniquely simple example, that nonlinear problems can be fundamentally different. Even a deterministic three-dimensional system with a simple quadratic nonlinearity—a crude model of thermal convection in the atmosphere—gives rise to fundamentally unpredictable, stochastic behavior through strong dependence on infinitesimal details of the initial condition. Any quasi-periodic[1] solution, Lorenz demonstrated, cannot be stable. If indeed weather systems resemble Lorenz's model, then there are fundamental limits on how far into the future weather can be predicted, regardless of advances in measuring or computation technology.

The phenomenon of strong dependence on initial conditions in a bounded system has come to be called chaos, and it is now believed to be a critical feature of many physical processes, including turbulence. Lorenz's original system remains popular among researchers due to its simplicity, and much has been discovered about it in the intervening decades.

Lorenz's original three-dimensional model equation is given by

$$\frac{d}{dt}\begin{pmatrix} Y_1 \\ Y_2 \\ Y_3 \end{pmatrix} = \begin{pmatrix} \alpha\,(Y_2 - Y_1) \\ \beta Y_1 - Y_2 - Y_1 Y_3 \\ Y_1 Y_2 - \gamma Y_3 \end{pmatrix} \tag{8.1}$$

where α is the Prandtl number, β is related to the Rayleigh number, and γ is a third parameter involving geometry. The so-called classical case, which was originally cited by Lorenz, takes $\alpha = 10$, $\beta = 28$, and $\gamma = 8/3$. The phase vector $\mathbf{Y}(\mathbf{Y_0}, t)$ represents the state of a small two-dimensional fluid-filled cell, periodic in one direction, which is simultaneously heated at bottom and cooled on top. Heat causes the fluid density to decrease, leading to an unstable arrangement of heavier fluid atop lighter. If the system is perfectly balanced—analogous to a long stick being perfectly balanced on its tip—then it can remain in that state indefinitely: Zero is a stationary point of (8.1).

At the slightest perturbation, however, two counter-rotating rolls develop. The direction of their rotation is arbitrarily sensitive to details of the initial perturbation. Rotation and the subsequent heat transfer tend to correct the imbalance after a few cycles, but continued heating prevents stability

[1] In Lorenz's terminology, a trajectory that returns arbitrarily close to its starting point is called quasi-periodic; strictly periodic solutions are a subset of quasi-periodic ones.

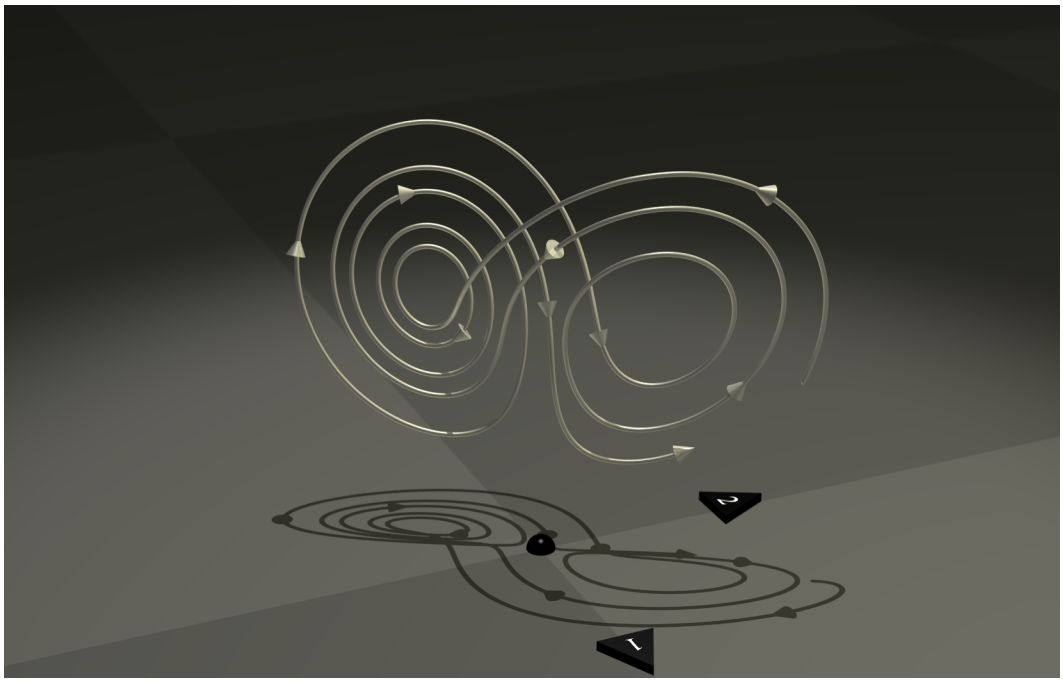

Figure 8.1: Finite segment of a typical trajectory of Lorenz's equations (8.1), computed by numeric integration and rendered as a metal wire. Conical beads indicate the direction of travel. The black hemisphere marks the origin, and directions of the positive y_1 and y_2 axes are as indicated (triangles marked 1 and 2, respectively; the base of each triangle is 20 units from the origin). The positive y_3 axis points upward; the highest point on the wire is approximately 45 units above the $y_1 - y_2$ plane. Shadows on the $y_1 - y_2$ plane are cast by a spotlight high on the $+y_3$ axis.

from ever being achieved. After some time, the system comes to another unstable equilibrium and reverses, only to repeat the same pattern again later.

A typical trajectory of Lorenz's system is shown as a wire model (to illustrate its three-dimensional structure) in Figure 8.1; a more traditional view appears in Figure 8.2, which includes projections onto the three coordinate planes. The phase-space behavior of Lorenz's system has the rare feature of being recognizable to many laypeople: Its trajectories approach the famous Lorenz butterfly, a strange attractor (Tucker, 2002) that has become something of a icon for chaos theory. Long-time solutions are dominated by two large counter-rotating whorls. Typically, the system orbits around one whorl or the other for an unpredictable number of cycles, after which, having landed on the wrong side of an inscrutable divider, it reverses, veering to the opposite side. The divider is so complicated and so fine that it is practically impossible to predict the state of the system more than a few cycles into the future.

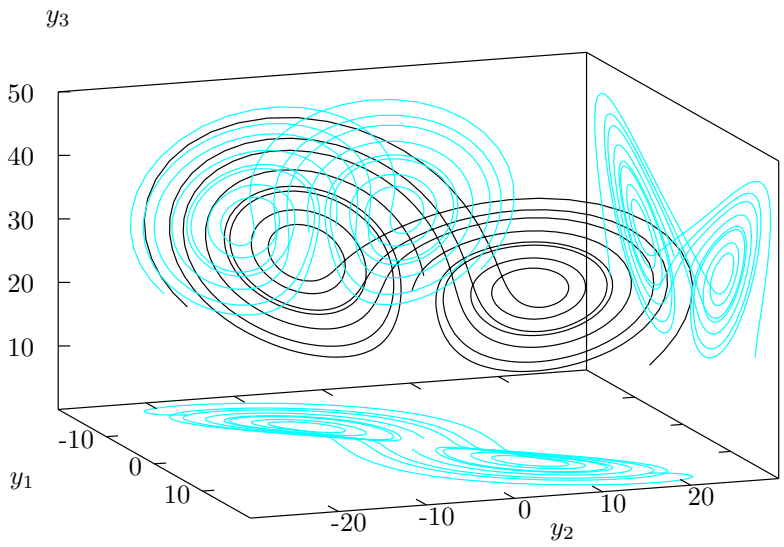

Figure 8.2: Two additional trajectories of the Lorenz dynamical system (8.1), rendered in a more traditional way, with projections on the three coordinate planes. The trajectories eventually approach a fractal strange attractor resembling a butterfly.

Equation (8.1) has three stationary points: one at the center of each whorl and one at the origin. None is stable. However, the motion is bounded; it is possible (though nontrivial) to construct trapping regions for the system. See Pogromsky et al. (2003) for a discussion.

The phase-space divergence $\nabla \cdot \mathbf{f}$ is constant and negative at $-(\alpha + 1 + \gamma)$, which in the classical case works out to $-41/3$. Thus the system is a candidate for analysis by our methods. However, it is unlike previous examples in several important ways. First, it does not approach a stationary point after infinite time, but rather it approaches a strange attractor of fractal dimension. This marks the first example for which stationary and steady solutions differ. A system on the attractor (that is, on $\mathcal{R}$) is statistically stationary, but it is not steady; a system on any of the three stationary points is both stationary and steady. The invariant density $\rho_{\text{stationary}}(\mathbf{y})$ will be singular everywhere on the attractor, and zero everywhere else (that is, all points of $\mathcal{R}^c$).

Asymptotic approach also has a different meaning in this chapter: it signifies asymptotic approach to the attractor set, with its attendant motion, rather than to any particular fixed point. A model for Lorenz's system in asymptotic approach would describe its approach to the attractor. One might be interested in a reduced-order system, or the answers to such obvious questions as, "What is the

root mean square rotation rate under stationary conditions?" The latter is given by a moment of $\rho_{\text{stationary}}(\mathbf{y})$, specifically:

$$\text{RMS rotation rate} = \left(\int_{\Omega} y_1^2 \, \rho_{\text{stationary}}(\mathbf{y}) \, dV \right)^{\frac{1}{2}} \tag{8.2}$$

One difficulty we encounter with Lorenz's system is that although trapping regions exist, none is a canonical (in the sense of being an isosurface of some Hamiltonian) choice. We have too much flexibility in choosing Ω, and that means $\rho_{\text{asymptoticapproach}}(\mathbf{y})$ is not uniquely determined. The stationary density, however, remains invariant under such changes (discussion in Section 2.6), and more realistic model systems do not suffer from this limitation. We will take a somewhat arbitrary implicitly defined Ω and avoid overstating significance of the asymptotic approach density here.

8.2 Solutions

The definition for Ω is implicit: among points in a rectangular prism extending from -20 to 20 in the y_1 direction, -30 to 30 in the y_2 direction, and -2 to 50 in the y_3 direction, those belonging to any trajectory that departs the prism in finite time are *not* members of Ω; all others are members of Ω. Thus Ω is, implicitly, a trapping region. Dimensions of the prism were chosen to contain all points in a typical long-time trajectory of the system; however, it should emphasized that this choice for Ω is arbitrary.

The stationary density $\rho_{\text{stationary}}(\mathbf{y})$ is the SRB measure of (8.1), a probability density that is singular on $\mathcal{R}$, now a fractal set of measure zero, and zero everywhere else. We approximate $\rho_{\text{stationary}}(\mathbf{y})$ below using the conjecture of Section 3.7, under which it is regarded as a long-time conditional limit of the asymptotic approach density. The reader is referred to Froyland and Dellnitz (2003) for a more rigorous alternative.

Because phase-space divergence is constant, the asymptotic approach density is given simply by (E.14), as it was in Chapters 5 and 6. Again, λ can be computed from (E.15). The solution is again on a grid, now 90 units in y_1 by 135 in y_2 by 117 in y_3. Isosurfaces of $\rho_{\text{asymptoticapproach}}(\mathbf{y})$ are

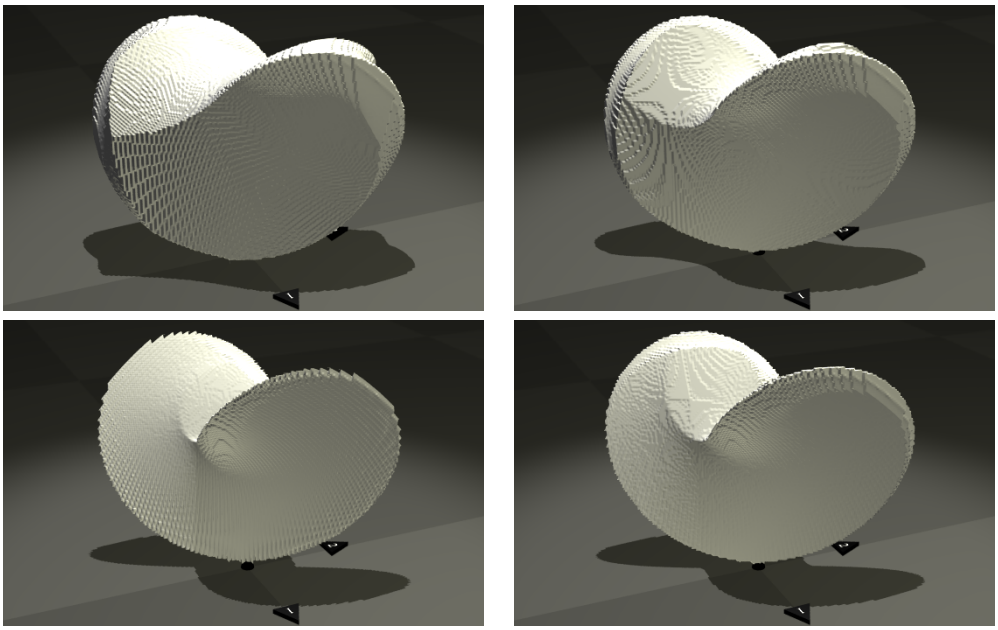

Figure 8.3: Successive isosurfaces of $\rho_{\text{asymptoticapproach}}(\mathbf{y})$ for the Lorenz equations (8.1). Details of the setting are identical to those in Figure 8.1. Isosurface levels, clockwise from the top left, are 0.92×10^{-5}, 1.23×10^{-5}, 1.61×10^{-5}, and 2.00×10^{-5}. The jagged texture is an artifact of numerical isosurface generation.

plotted in Figure 8.3. The density is singular on the attractor set.

8.3 Reduced-order model

In this section, we attempt to apply the reduced-order modeling theory developed in Chapter 4 to Lorenz's equations. Our motivation is not to find a globally acceptable reduced order model for Lorenz's system, but to show how the method fares in an imperfect situation. And the situation is surely imperfect: under the Poincaré-Bendixson theorem, a 2D model system cannot exhibit chaos, so its dynamics will be fundamentally different.

Model construction proceeds via the five-step process outlined in Chapter 4. Step 1 is to choose the appropriate sample point density. In previous examples, the asymptotic approach density was the only logical choice, because stationarity was a trivial situation. Now, however, stationarity is quite interesting: it corresponds to the system's behavior in the long-time limit.

Hence, for Lorenz's equations, under a given set of model variables, two different reduced-order

models can be constructed: one for systems that are undergoing asymptotic approach, and another for systems that have attained stationarity. The appropriate model to use is the one which matches actual experimental conditions.

Next (Step 2), model variables must be selected. The original system is three-dimensional ($N = 3$), so we may construct a reduced-order model of one or two dimensions ($M = 1$ or $M = 2$, respectively). We arbitrarily choose to examine two-dimensional models. The first set of model variables, explained in the following paragraph, is arbitrary and relatively simple; the latter, visited in Section 8.4, is based on principal-component analysis.

For the first set of model variables, consider the trajectory in Figure 8.1. The shadow in the $y_1 - y_2$ plane is nearly $1:1$ with the wire above, except where the wire is close to vertical (i.e., a region that follows a line segment joining the two whorls' center points.) Thus $\varphi_{w_1}(\mathbf{y}) = y_1$ and $\varphi_{w_2}(\mathbf{y}) = y_2$ are a reasonable, though perhaps not optimal, choices of model variables.

The remaining three steps are:

3. Compute the conditional expectation $\langle \partial \boldsymbol{\varphi}_{\mathbf{w}}/\partial t \mid \boldsymbol{\varphi}_{\mathbf{w}}(\mathbf{y}) = \mathbf{W} \rangle$, which has the components $\langle f_1(\mathbf{y}) \mid y_1 = W_1 \cap y_2 = W_2 \rangle$ and $\langle f_2(\mathbf{y}) \mid y_1 = W_1 \cap y_2 = W_2 \rangle$. These are computed by a binning process in two dimensions.

4. Normally, the fourth step would be to solve the model system

$$\frac{d}{dt} \begin{pmatrix} W_1 \\ W_2 \end{pmatrix} = \begin{pmatrix} \langle f_1(\mathbf{y}) \mid y_1 = W_1 \cap y_2 = W_2 \rangle \\ \langle f_1(\mathbf{y}) \mid y_1 = W_1 \cap y_2 = W_2 \rangle \end{pmatrix} \tag{8.3}$$

   for $\mathbf{W}(\mathbf{W_0}, t)$. Here, however, for illustration, we instead plot the right-hand side as a vector field. The stationary model velocity field in appears in Figure 8.4, and the asymptotic approach model velocity field appears in Figure 8.5. Both plots include projected streamlines of the full three-dimensional system for reference.

5. Compute the expected deviation. Contours of the nondimensional standard deviation are plotted in Figure 8.4 for stationarity and in Figure 8.5 for asymptotic approach.

To see how the reduced-order models work, let us walk through their predictions for the behavior of two systems, one undergoing asymptotic approach and another that has reached stationarity.

First, let an experiment be conducted under asymptotic approach conditions. Let its model initial condition (which here is its position in the $y_1 - y_2$ plane) be $\mathbf{W_0} = (0, 20)$. From standard deviation contours in Figure 8.5, one can see that expected deviation is less than 0.5 there, so the model prediction is initially reliable. The model velocity field in Figure 8.5 indicates that the system will travel roughly in the $+w_1$ direction until it approaches the attractor's projection in the $w_1 - w_2$ plane. Along the way, however, it crosses contours of increasing expected deviation. By the time the system approaches the attractor's projection, expected deviation from the model is greater than 1.5; hence, the model is no longer reliable there.

Thus the asymptotic approach model does a reasonable job of describing how a system away from the attractor in the $w_1 - w_2$ plane will approach the attractor. It does not, of course, predict behavior on the attractor reliably.

Now, assume stationarity rather than asymptotic approach. Figure 8.4 is analogous to Figure 8.5. Notice that no information is provided outside the attractor's $w_1 - w_2$ projection, because $\rho_{\text{stationary}}(\mathbf{y})$ is zero there. Logically, this is sensible; the presence of a system outside that region would contradict the assumption of stationarity. Hence we are restricted to initial conditions $\mathbf{W_0} = \boldsymbol{\varphi}_{\mathbf{w}}(\mathbf{Y_0})$ that lie inside the projected domain of the attractor. Consider a system whose $\mathbf{W_0} = (15, 15)$, which is inside the attractor's projection and near the upper-right corner of the model domain. From nondimensional standard deviation contours in Figure 8.4, the predicted deviation there is low—less than 0.5, so the model should initially be a reliable predictor of behavior. From the model velocity field at $\mathbf{W} = (15, 15)$, motion is predicted to be in roughly the $-w_2$ direction, then to continue clockwise around the rightmost whorl. This motion appears likely to continue ($\text{dev}(\mathbf{W}) < 0.5$) until it approaches a line segment joining the two whorl centers, where from standard deviation contours, the expected deviation spikes. Thus, the stationary model's prediction is expected to work reliably when the system is away from the bifurcation region, and to break down when the system is close to it. This is, again, a qualitatively reasonable prediction.

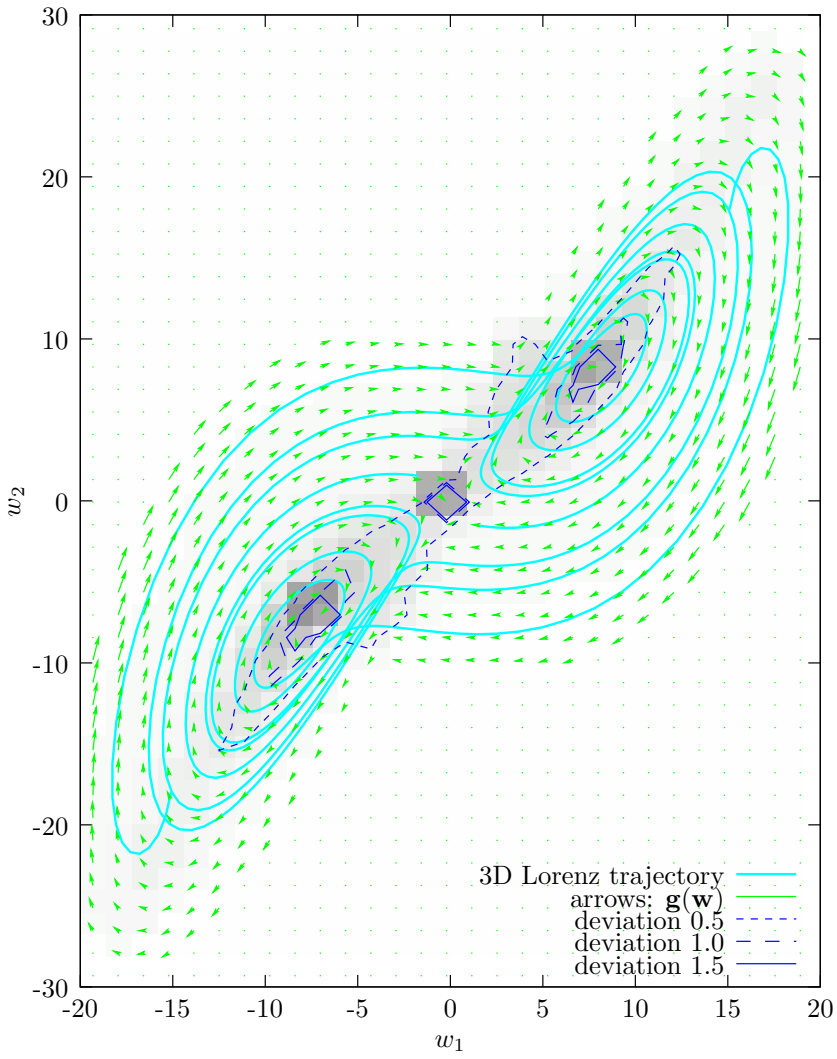

Figure 8.4: Tabulated function representing a reduced order model for Lorenz's equation, under stationarity, with the arbitrary model variables $w_1 = \varphi_{w_1}(\mathbf{y}) = y_1$ and $w_2 = \varphi_{w_2}(\mathbf{y}) = y_2$. Arrows indicate the direction of $\mathbf{g}(\mathbf{W})$; their lengths are proportional to its magnitude. Also shown for references are two trajectories of the full three-dimensional system, as well as contours and shading to indicate the local expected nondimensional standard deviation. The model is only defined where the density is nonzero—that is, where the probability of finding the system under stationary conditions is nonzero.

8.4 Reduced-order model on principal component modes

The choice $\varphi_{w_1}(\mathbf{y}) = y_1$, $\varphi_{w_2}(\mathbf{y}) = y_2$ in the previous section was simple but arbitrary; one might expect model variables based on physical attributes of the system to perform better (in the sense of having a lower average nondimensional standard deviation). In this section, we construct a two-dimensional reduced order model for Lorenz's equations based on the two largest-eigenvalue principal

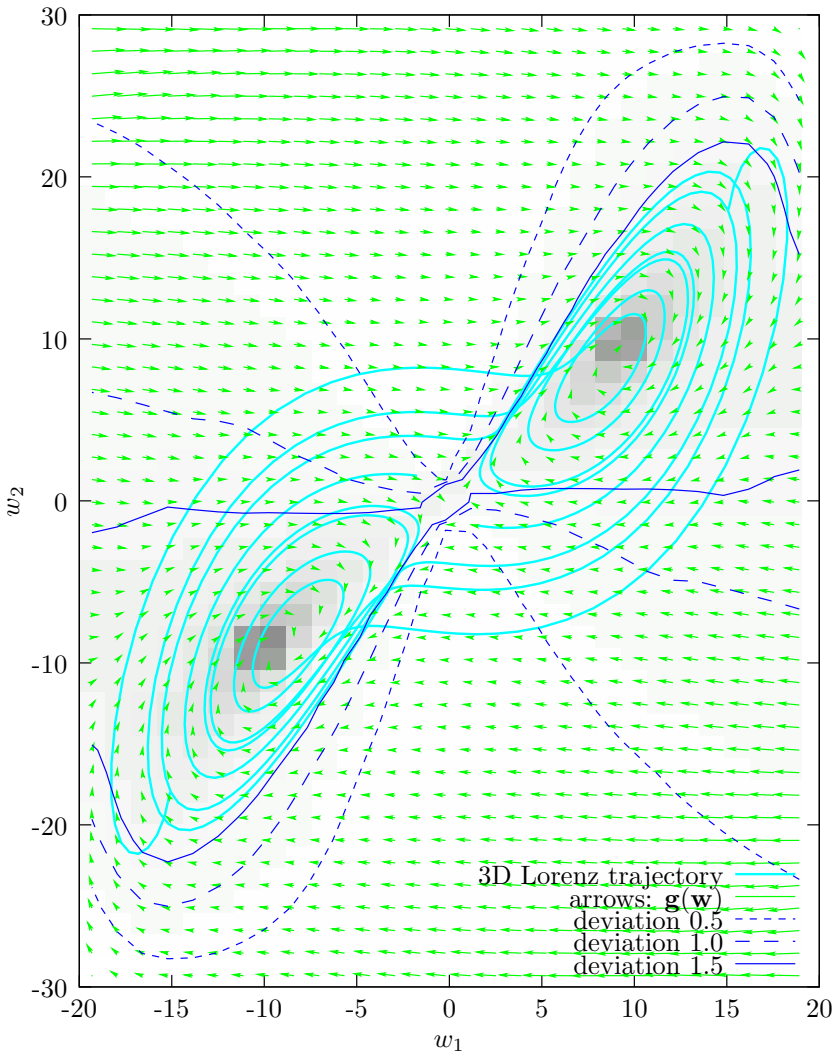

Figure 8.5: Tabulated function representing a reduced order model for Lorenz's equation, under asymptotic approach, with the arbitrary model variables $w_1 = \varphi_{w_1}(\mathbf{y}) = y_1$ and $w_2 = \varphi_{w_2}(\mathbf{y}) = y_2$. Arrows indicate the direction of $\mathbf{g}(\mathbf{W})$; their lengths are proportional to its magnitude. Also shown for reference are two trajectories of the full three-dimensional system, as well as contours and shading to indicate the local nondimensional standard deviation.

component modes. These are the modes which, for experimental data, might have been derived with Karhunen-Loevé theory.

As before, it would be possible to compute a model for stationarity or asymptotic approach, but we restrict attention to stationarity here.

Principal component analysis, which sometimes goes by the name proper orthogonal decomposition, is a tool for finding reduced-order subspaces for a problem—or in our terminology, model

variables. It identifies orthogonal directions in which the sample points (or in this case, the sample point density) have maximum variance. These are simply the principal eigenvectors of the mean-centered covariance matrix—those whose corresponding eigenvalues are largest.

One may compute the covariance matrix by taking appropriate moments of the sample point density. Let $\upsilon_i = y_i - < y_i >$. The mean-centered covariance matrix under stationarity is approximately:

$$\begin{pmatrix} <\upsilon_1\upsilon_1> & <\upsilon_1\upsilon_2> & <\upsilon_1\upsilon_3> \\ <\upsilon_2\upsilon_1> & <\upsilon_2\upsilon_2> & <\upsilon_2\upsilon_3> \\ <\upsilon_3\upsilon_1> & <\upsilon_3\upsilon_2> & <\upsilon_3\upsilon_3> \end{pmatrix} = \begin{pmatrix} 79.38 & 61.32 & 0.00 \\ 61.32 & 84.36 & 0.05 \\ 0.00 & 0.05 & 83.48 \end{pmatrix} \tag{8.4}$$

The eigenvalues and corresponding eigenvectors are, in order from largest magnitude to smallest:

$$\begin{array}{r|ccc} 143.24 & -0.693 & -0.721 & 0.000 \\ 83.48 & 0.000 & 0.000 & 1.000 \\ 20.50 & 0.721 & -0.693 & 0.000 \end{array} \tag{8.5}$$

The first two eigenvectors together account for more than 90% of the stationary density's variance, and thus should be a better choice for model variables than the naïve choice (y_1, y_2). We therefore take $M = 2$, $\varphi_{w_1}(\mathbf{y}) = 0.693y_1 + 0.721y_2$ (sign does not matter) and $\varphi_{w_2}(\mathbf{y}) = y_3$.

The resulting reduced order model appears in Figure 8.6. There are dark areas of high nondimensional standard deviation in the bifurcation region and near the origin, but over most of the plane the standard deviation is small.

It was expected that the average deviation would be smaller for principal-component model variables than for the naïve choice (y_1, y_2), but both are small and in fact the naïve model performs slightly better, with an average deviation over w of 0.103, versus 0.119 for the principal component model variables.

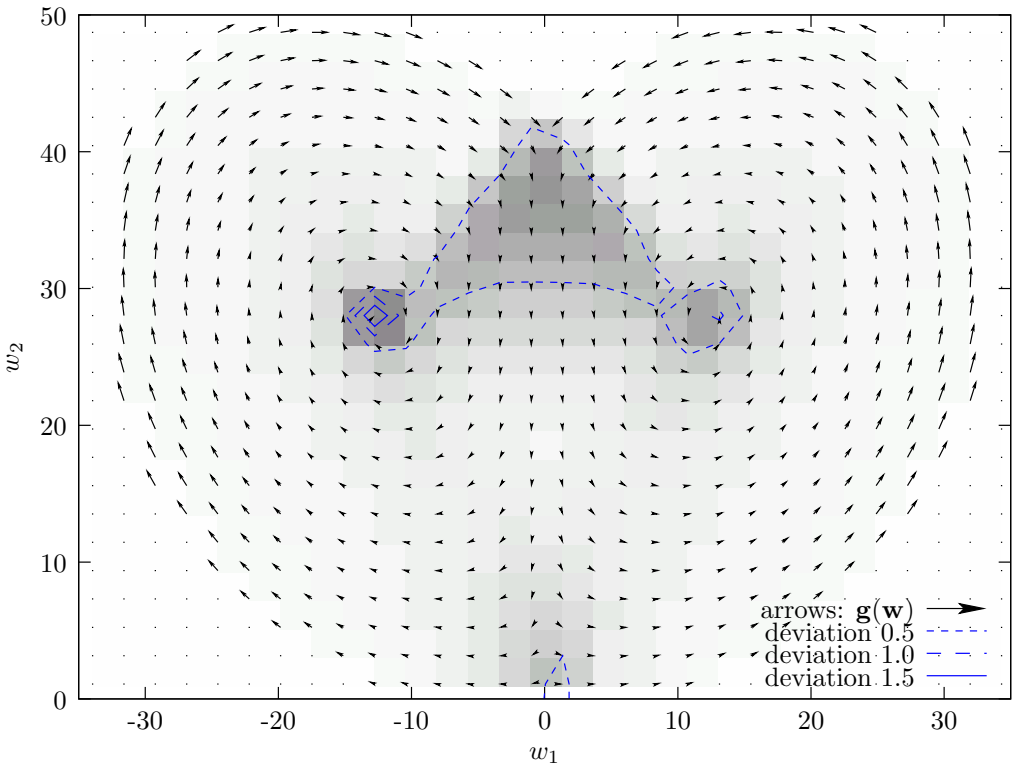

Figure 8.6: Tabulated function represeting a reduced order model for Lorenz's equation under stationarity. Model variables $w_1 = \varphi_{w_1}(\mathbf{y}) = 0.693y_1 + 0.721y_2$ and $w_2 = \varphi_{w_2}(\mathbf{y}) = y_3$ are unit eigenvectors associated with the two largest-magnitude eigenvalues of the covariance matrix—the modes which would have been chosen by Karhunen-Loevé theory. Arrows indicate the direction of $g(\mathbf{W})$; their lengths are proportional to its magnitude. Also shown are contours and shading of the local nondimensional standard deviation.

8.5 On the conjectured relationship between densities

In Section 3.7, it was conjectured that the stationarity density is equivalent to a particular limit of the asymptotic approach density. Mathematically, several plausibility arguments were given for that conjecture; physically, it meant that the statistics of asymptotic approach, after a sufficiently long period of time, should approach those of stationarity.

The conjecture was applied in this section to obtain an approximate $\rho_{\text{stationary}}(\mathbf{y})$. In Table 8.1, the conjecture's predictions for covariance statistics are compared to those obtained by long-term time averaging. Convergence appears plausible, but not certain.

source	$< v_1 v_1 >$	$< v_1 v_2 >$	$< v_1 v_3 >$	$< v_2 v_2 >$	$< v_2 v_3 >$	$< v_3 v_3 >$
$\rho_{\text{cutoff}} = 1.23e-05$	95.3	107	0.07	166	0.08	128
$\rho_{\text{cutoff}} = 1.42e-05$	99.8	103	0.09	147	0.09	121
$\rho_{\text{cutoff}} = 1.61e-05$	99.3	93.3	0.12	126	0.12	113
$\rho_{\text{cutoff}} = 1.80e-05$	94.2	80.7	-0.01	107	0.02	99.8
$\rho_{\text{cutoff}} = 2.00e-05$	84.9	67.2	0.06	90.8	0.18	87.8
$\rho_{\text{cutoff}} = 2.10e-05$	79.4	61.3	0.00	84.4	0.05	83.5
time avg 2e+05	68	67	0.17	84	0.19	59
time avg 4e+05	68	67	0.51	84	0.53	59

Table 8.1: Convergence of mean-centered covariance statistics for $\rho_{\text{asymptoticapproach}}|\rho > \rho_{\text{cutoff}}$, compared to those obtained by long-time averaging. The first six rows give results for six different values of ρ_{cutoff}; the largest value of $\rho_{\text{asymptoticapproach}}(\mathbf{y})$ on the grid was $7.70e-05$. Values were chosen to coincide with those depicted in Figure 8.3 and points in between, as well as the larger value $2.10e-05$ (which is at the 90th percentile of grid values) used to approximate $\rho_{\text{stationary}}(\mathbf{y})$ in this chapter. The bottom two rows provide the same statistics computed via time averaging two trajectories over 1e+05 and 2e+05 time units, respectively, and thus approximate the true stationary statistics. Convergence does appear to be plausible, although there are relatively large numerical errors in the y_3 direction, which seems reasonable given the relatively larger mean in the y_3 direction. Further refinement might increase error as the number of grid points inside the cutoff isosurface decreases.

8.6 Implications for turbulence modeling

The reduced-order modeling analysis above, although far simpler than what would be required for forced turbulence, highlights several features a turbulence model based on Chapter 4 should possess.

Foremost, no guesswork was involved, except perhaps in the choice of model variables. Construction of a turbulence model typically involves both art and science, but the method applied here is straightforward and boring. All concepts have clear and unambiguous meanings and transparent limitations.

For a given set of conditions and choice of model variables, the model equation derived in Chapter 4 is ideal. No other model on the same variables deviates less, on average, from the true N-dimensional behavior. Still, there may be regions of the model's phase space where a high standard deviation means the model (and indeed any model having the same model variables) will perform poorly.

Cast into our terminology, large eddy simulation is a rule for creating model variables and an assumption of stationarity. Therefore, a given grid and set of boundary conditions admits exactly one ideal LES model. There may be regions of the model phase space where it predicts poorly;

in those regions, all models predict poorly. The ability to establish local confidence estimates is a feature missing from contemporary LES, and should be a helpful development.

Chapter 9

Example: Burgers' equation in one spatial dimension

9.1 Introduction

This chapter presents our first application to a partial differential equation. Burgers' equation is a simplified model equation for turbulence. It is identical to the Navier-Stokes equations in every way except for the pressure term, which is omitted to make analysis easier. It fact, Burgers' equation can be solved exactly: a clever change of variables (the Cole-Hopf transformation) recasts it into a heat equation. Decaying Burgers' turbulence has been examined by, e.g., Gotoh and Kraichnan (1993), but we will examine a simple nonturbulent case known as the Stokes limit.

In one dimension, Burgers' equation is given by

$$\frac{\partial u}{\partial t} + u\frac{\partial u}{\partial x} = \nu\frac{\partial^2 u}{\partial x^2} \tag{9.1}$$

where $u(x,t)$ is velocity and $\nu \geq 0$ is viscosity. We take periodic boundary conditions in physical space; the domain is $x \in [-\pi, \pi)$ and $u(-\pi, t) = u(\pi, t)$. When $\nu = 0$, the equation is said to be *inviscid* and develops singularities (shock waves) in finite time. The inviscid equation also conserves energy, as may be verified by multiplying (9.1) by u, integrating over x, and setting $\nu = 0$.

Similarly, an average of (9.1) over x (even with finite viscosity) eliminates the convective and viscous terms, showing that the average remains constant over time. The average is therefore

arbitrary—choosing it amounts to selecting an inertial frame of reference. Hence, we may take

$$\int_{-\pi}^{\pi} u(x,t)\,dx = 0 \tag{9.2}$$

without loss of generality.

One way to characterize decaying systems such as this one is by the energy spectrum. That is, at an arbitrary time (or energy) of decay, how are the energies at each wavenumber related? We will attempt to answer this question for the Stokes limit, a regime in which viscous forces dominate.

In order to obtain a system of ordinary differential equations, the partial differential equation (9.1) must be discretized. Let $u(x,t)$ be represented by the Fourier series

$$u(x,t) = \sum_{j=1}^{N/2} \left(Y_{2j-1}\left(\mathbf{Y_0},t\right)\cos\left(jx\right) + Y_{2j}\left(\mathbf{Y_0},t\right)\sin\left(jx\right)\right) \tag{9.3}$$

which is sufficiently general, provided the average of $u(x,t)$ over x is assumed to be 0 (9.2), and $N \to \infty$. To fill each wavenumber completely, finite N should be even. Components can be extracted from the resulting sum by integrating against the basis functions, which are orthogonal over the x domain.

The $N \to \infty$ limit has not yet been considered, so we restrict attention to truncations at finite wavenumber. This is consistent with DNS practice, and in any case is a prerequisite for exploring the $N \to \infty$ limit.

Substituting (9.3) into (9.1) leaves, for the convective term, a double sum involving products of the $\mathbf{Y}(\mathbf{Y_0},t)$ components and basis functions. The latter can be combined via trigonometric identities. Thus the convective term in (9.1) makes a quadratic contribution to $\mathbf{f}(\mathbf{Y})$. For the viscous term, a single sum remains, with every term identical to its corresponding term in the original series, except multiplied by $-\nu$ times the square of the wavenumber j. Thus the viscous term in (9.1) makes a linear contribution to $\mathbf{f}(\mathbf{Y})$.

Before taking the Stokes limit, then, the right-hand side is the sum of quadratic and linear terms:

$$f_i(\mathbf{y}) = y_j Q_{jik} y_k + L_{ij} y_j \tag{9.4}$$

where the Q and L components are constants determined by integrating the convective and viscous terms of (9.1), respectively, with $u(x,t)$ given by Fourier series (9.3), against basis functions. Conveniently, L_{ij} is diagonal. When $\nu = 0$, the L term vanishes.

To find a suitable Ω, consider isosurfaces of energy for the inviscid system. By Parseval's identity, these are spherical shells centered on the origin. Indeed, when ν is zero, the rate of change of $Y_j Y_j$ (sum implied) is zero, as may be verified by direct substitution; its trajectories remain on spheres of constant radius. That is, $Q_{jik} Y_j Y_i Y_k = 0$. Thus a sphere of any radius, centered on the origin, is an appropriate choice for Ω. We denote the square of the radius by E.

In the Stokes limit, convection is negligible compared to viscous dissipation; although the convective term determines Ω, it plays no part in $\mathbf{f}(\mathbf{y})$. Because L_{ij} is diagonal, what remains is a completely decoupled linear system:

$$\frac{dY_i}{dt} = -\nu k_i^2 Y_i \qquad (\textit{no summation implied}) \tag{9.5}$$

where k_i^2 is the square of the wavenumber affiliated with the ith mode Y_i:

$$k_i^2 = \lfloor \frac{i+1}{2} \rfloor^2 \tag{9.6}$$

The phase-space divergence of (9.5) is a constant:

$$\nabla \cdot \mathbf{f} = -\nu \sum_{i=1}^{N} k_i^2 \tag{9.7}$$

Crucially, (9.5) has a simple analytical solution. Trajectories are given by

$$Y_i(\mathbf{Y_0}, t) = Y_{0i} \exp(-\nu k_i^2 t) \tag{9.8}$$

The motion is bounded, and $\mathcal{R}$ consists of a single stationary point at the origin. All other points in Ω belong to $\mathcal{R}^c$.

9.2 Solutions

The stationary density is trivial: it is a Dirac delta function at the origin. Physically, that means the only stationary solution to (9.5) is the trivial $u(x,t) = 0$.

For the state of asymptotic decay, however, $\rho_{\text{asymptoticapproach}}(\mathbf{y})$ is appropriate, and it is non-trivial. From (E.14) the asymptotic approach density along characteristics is

$$\rho_{\text{asymptoticapproach}}(\mathbf{Z}(\mathbf{Z_0}, s)) = \frac{\lambda}{2(-\nabla \cdot \mathbf{f})} \left(s + \frac{1}{(-\nabla \cdot \mathbf{f})} \right) \tag{9.9}$$

where λ is given by (E.15):

$$\lambda = \frac{(\nabla \cdot \mathbf{f})^3}{\int_{\partial\Omega} \mathbf{f} \cdot \hat{\mathbf{n}} \, dS} \tag{9.10}$$

Characteristics $\mathbf{Z}(\mathbf{Z_0}, s)$ coincide with trajectories (9.8) whose initial points $\mathbf{Z_0}$ lie on the surface of the boundary sphere:

$$Z_{0_1}^2 + Z_{0_2}^2 + Z_{0_3}^2 + \cdots = E \tag{9.11}$$

Thus,

$$Z_1^2 \exp(2\nu k_1^2 s) + Z_2^2 \exp(2\nu k_2^2 s) + Z_3^2 \exp(2\nu k_3^2 s) + \cdots = E \tag{9.12}$$

Although it cannot be explicitly solved for s, (9.12) allows $\rho_{\text{asymptoticapproach}}(\mathbf{y})$ to be constructed implicitly from (9.9).

9.3 The energy spectrum

We now attempt to calculate the energy spectrum at an arbitrary characteristic time $s^\star$ of decay. That is, we are interested in moments of a probability density which is conditional on $s = s^\star$. By (9.9), this condition corresponds to examining an isosurface of $\rho_{\text{asymptoticapproach}}(\mathbf{y})$; by (9.12), such

an isosurface is an ellipsoidal shell in $\mathbf{y}$. The ellipsoid is centered on the origin and aligned with coordinate axes.

That is, the density $\rho(\mathbf{y})$ is

$$\delta\left(y_1^2 \exp(2\nu k_1^2 s^\star) + y_2^2 \exp(2\nu k_2^2 s^\star) + y_3^2 \exp(2\nu k_3^2 s^\star) + \cdots - E\right) \tag{9.13}$$

The energy in mode Y_i is $\left\langle y_i^2 \right\rangle$. When reporting spectra, one conventionally adds the energies at each wavenumber; in this case, that means adding contributions from the sine and cosine components. (In more than one spatial dimension, shell summation might also be required.) Thus by "expected energy spectrum," we mean the set of expected values $\left\langle y_1^2 + y_2^2 \right\rangle$ for wavenumber 1, $\left\langle y_3^2 + y_4^2 \right\rangle$ for wavenumber 2, $\left\langle y_5^2 + y_6^2 \right\rangle$ for wavenumber 3, and so on up to wavenumber $N/2$. Each of these must be normalized in some way; we choose to normalize by $\left\langle y_1^2 + y_2^2 \right\rangle$, which is the energy in the first wavenumber. That is,

$$E_k = \frac{\left\langle y_{2k-1}^2 + y_{2k}^2 \right\rangle}{\left\langle y_1^2 + y_2^2 \right\rangle} \tag{9.14}$$

By symmetry of (9.13), the integral of $\rho(\mathbf{y})$ against any term of the form $y_i^2 \exp(2\nu k_i^2 s^\star)$, over all space, is the same. The integral over all space is equal to the integral over Ω, because the ellipsoid is a strict subset of Ω. Hence the ratio of expected values of any two components is

$$\frac{\left\langle y_i^2 \right\rangle}{\left\langle y_j^2 \right\rangle} = \frac{\exp(2\nu k_j^2 s^\star)}{\exp(2\nu k_i^2 s^\star)} = \frac{\exp(-2\nu k_i^2 s^\star)}{\exp(-2\nu k_j^2 s^\star)} \tag{9.15}$$

The expected energies in sine and cosine components of the same wavenumber are therefore equal. Finally, then,

$$E_k \propto \exp(-ck^2) \tag{9.16}$$

where c is a positive constant. The form holds irrespective of $s^\star$ and is our predicted energy spectrum for Burgers' equation in the Stokes limit during asymptotic approach.

9.4 Remark: from the Stokes limit to Navier-Stokes

The preceeding discussion concerned Burgers' equation, but as interest is ultimately in turbulence, the full three-dimensional constant-density Navier-Stokes equations will eventually need to be analyzed. Although Navier-Stokes trajectories cannot be solved analytically, there are several similarities to the preceeding situation which should help. This section's aim is to briefly draw attention to those similarities that might be exploited.

First, Navier-Stokes, when discretized on the same kind of truncated Fourier series as above, leads to a similarly quadratic system of ordinary differential equations that has negative constant divergence. The pressure term makes no change in this respect, and viscous dissipation is not altered. Further, the interiors of spheres of constant energy remain appropriate choices for the trapping region Ω.

However, the equation of continuity makes for an important change: under three-dimensional Navier-Stokes, $\mathbf{Y}$ has only two degrees of freedom for each wavenumber triplet.

Applying the numerical method used in previous chapters would amount to doing DNS repeatedly (albeit with non-arbitrary initial conditions), which is not computationally feasible. Fortunately, there is reason to hope certain approximations will be possible. These will be the subject of future work.

Chapter 10

Conclusions

The present work sought to address two questions regarding the influence of experimental conditions on the statistics and reduced-order behavior of dissipative ordinary differential equations. First, what do experimental conditions such as stationarity and asymptotic approach imply about the distribution of sample points in phase space? Second, how do they ultimately influence results, particularly with regard to reduced-order behavior?

The experimental condition of stationarity, it was shown, requires that the distribution of sample points be singular on $\mathcal{R}$, a subset of phase space that is not accessible from any boundary-crossing trajectory in finite time. When $\mathcal{R}$ consists of a single stationary point, as it did in the one-dimensional linear example (Chapter 5), the damped linear oscillator example (Chapter 6), the unforced Rayleigh-Plesset equation example (Chapter 7), and the Burgers' equation example (Chapter 9), the appropriate density is a Dirac delta function at that point. When $\mathcal{R}$ contains a single periodic attractor, the density is singular along it; when it contains a single strange attractor, as for Lorenz's equations (Chapter 8), the density approaches an SRB measure. When $\mathcal{R}$ contains two or more of the above, the stationarity density is a linear combination. Proportions are arbitrary so long as the sum is unity.

Asymptotic approach, on the other hand, led to a sample point density that grows algebraically along trajectories. Like the stationarity density, it is singular on $\mathcal{R}$; unlike the stationarity density, however, the total probability mass there is negligible. The asymptotic approach density is greater than zero throughout the domain. The variational condition used to derive the asymptotic approach

density also provides a boundary condition, leaving a unique solution even when multiple attractors are present. In Chapter 5, it was shown that for the trivial one-dimensional linear example, the asymptotic approach density might correspond to a set of experiments of exponentially decaying duration.

Construction of explicit stationarity and steady decay densities served to answer the first question posed above: experimental conditions impose a specific structure on the distribution of sample points in phase space. The second question concerned how to apply it.

For most kinds of observables, the answer is simply to take an appropriate moment of the sample point density, as expressed in equation (1.5). The phase function $\varphi(\mathbf{y})$ should match the observable of interest. It was shown in Chapter 4 that by judicious choice of observables, one can systematically construct reduced-order models, along with deviation estimates. Such models create predictions based on conditional expectation of reduced-order behavior, which can be obtained directly from the sample point density. The deviation estimates are corresponding second-order moments.

For a given set of model variables, therefore, each experimental condition yields a different model, and a model only makes sense in the context of its experimental condition. It was discussed in Chapter 4 how this observation might explain, and suggest a way to resolve, the closure problem.

Reduced-order models of $M = 1$ were computed for the two-dimensional systems of Chapters 6 and Chapter 7, and of $M = 2$ for the three-dimensional system of Chapter 8. The latter featured separate models for stationarity and asymptotic approach, as well as a stationarity model based on principal component analysis.

Future topics of interest include moving to *nonautonomous* systems—those for which t appears explicitly on the right-hand side—and approximate solution techniques (particularly for large N). The latter are necessary to make progress on three-dimensional DNS of the Navier-Stokes equations; a $\rho(\mathbf{y})$ appropriate for these could lead to theoretically clean turbulence models. Also of interest are alternative formulations for asymptotic approach (based on alternative bounding strategies), and deeper connection to ergodic theory. A clear proof or disproof of the conjecture in Section 3.7 would be helpful.

Finally, earlier versions of this study attempted to unify the conditions of stationarity and asymptotic approach under the common rubric of reproducibility. It was argued that such experimental conditions are of interest because they lead to reproducible behavior, which suggested creating a measure of reproducibility and maximizing it with respect to $\rho(\mathbf{y})$. In that theoretical framework, stationarity and asymptotic approach are simply maxima under different constraints. Such a unified treatment, although based on less familiar concepts, might ultimately prove simpler.

Appendix A

Integration over streamtubes

We have frequently encountered the need to integrate a function of $\mathbf{y}$ over a volume $\mathcal{R}^c$, which is that portion of the trapping region Ω accessible along trajectories $\mathbf{Z}(\mathbf{Z_0}, s)$ (which cross $\partial\Omega$ at $\mathbf{Z_0}$, where $s = 0$) in finite s. Recall that Ω and $\mathcal{R}^c$ differ only on $\mathcal{R}$, a set of measure zero (proof in Appendix C). Such integrals may benefit from a change of variables in which differential elements dV are aligned with streamtubes; that change of variables is the subject of this appendix.

By definition, each point in $\mathcal{R}^c$ belongs to exactly one trajectory that entered Ω at a finite time in the past, and each trajectory crosses $\partial\Omega$ exactly once (since Ω is a trapping region). Thus a partition of $\partial\Omega$ into differential surface elements dS defines a set of streamtubes that fills the entire volume of $\mathcal{R}^c$ without overlap, and every point in $\mathcal{R}^c$ belongs to exactly one of the streamtubes.

The goal is therefore to replace an integral dV with one over $ds\,dS$, where ds is a differential unit of time along a trajectory contained by the streamtube whose intersection with $\partial\Omega$ is the differential area dS at the point $\mathbf{Z_0}$ (Figure A.1). This transformation naturally requires a Jacobian determinant, which will be denoted $\mathcal{J}(\mathbf{Z_0}, s)$. Thus a more precise statement of the goal is to find $\mathcal{J}(\mathbf{Z_0}, s)$ such that

$$\int_{\mathcal{R}^c} h(\mathbf{y})\, dV = \int_{\partial\Omega} \int_0^\infty h(\mathbf{Z}(\mathbf{Z_0}, s))\mathcal{J}(\mathbf{Z_0}, s)\, ds\, dS \tag{A.1}$$

for any Lebesgue-integrable function $h(\mathbf{y})$ on $\mathcal{R}^c$.

Consider the small volume dV_0 subtended by a typical differential area element dS, extruded inward along the vector $\mathbf{f}(\mathbf{Z_0})\, ds$ (Figure A.1, right). From geometry, the volume of dV_0 is $-\,\mathbf{f} \cdot \hat{\mathbf{n}}|_{\mathbf{Z_0}}\, ds\, dS$.

Now consider a partition of the streamtube into sections of length ds (in time, along trajectories),

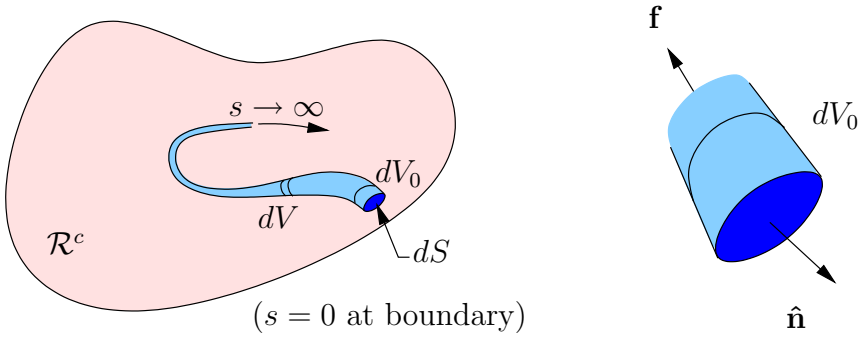

Figure A.1: Integrating over the volume of $\mathcal{R}^c$ by integrating over its streamtubes. On the left: a typical streamtube. It intersects the surface $\partial\Omega$ over a small area dS at $\mathbf{Z_0}$ (label omitted for clarity), then proceeds inward toward $s \to \infty$. It can be partitioned into volumes whose length in time is ds; two such volumes are shown. On the right: a closeup of dV_0, the differential volume nearest the wall.

starting from $s = 0$ at the boundary. The endcaps of partitions deep inside Ω may become highly distorted, but because their edges remain on the surface of the streamtube, all volume remains accounted for. The section nearest the wall is dV_0; the next section is exactly the volume that would have been occupied by dV_0 if it were allowed to convect down the streamtube under the influence of $\mathbf{f}$ during ds, and similarly for subsequent sections. The volume of each section is therefore $J(\mathbf{Z}(\mathbf{Z_0}, s))\, dV_0$, where

$$\frac{dJ}{ds} = (\nabla \cdot \mathbf{f})\, J \tag{A.2}$$

along streamlines. (This is a basic property of Lagrangian flow descriptions; see for example Majda and Bertozzi (2002) for a proof.) If the units of dS square those of $\mathbf{f} \cdot \hat{\mathbf{n}}\, ds$, then $J(\mathbf{Z_0}) = 1$. Thus $dV = -\mathbf{f} \cdot \hat{\mathbf{n}}\, J\, ds\, dS$, and so

$$\mathcal{J}(\mathbf{Z_0}, s) = -\mathbf{f} \cdot \hat{\mathbf{n}}|_{\mathbf{Z_0}} \exp\left(\int_0^s \nabla \cdot \mathbf{f}|_{\mathbf{Z}(\mathbf{Z_0}, s')}\, ds' \right) \tag{A.3}$$

The change of variables of Equation (A.1) works with Jacobian determinant $\mathcal{J}$ from $(A.3)$. Remember that the surface parameterization must be scaled so that units of dS match those of $\mathbf{f} \cdot \hat{\mathbf{n}}\, ds$ squared.

Appendix B

Conditional probabilities

This appendix reviews relevant topics from the theory of conditional probability.

Let A and B be two events. The *conditional probability* $\Pr(A|B)$ is the probability of event A given that event B has already occurred. It is given by

$$\Pr(A|B) = \frac{\Pr(A \cap B)}{\Pr(B)} \tag{B.1}$$

when $\Pr(B) > 0$, and is otherwise undefined. The expression $A \cap B$ refers to the *intersection* of A and B; $\Pr(A \cap B)$ is the probability that both A and B occur.

Conditional probability can be extended to continuum situations. If $\rho(\mathbf{y})$ is a probability density on $\mathbf{y} \in \Omega$, then the expected value, or *expectation*, of some observable function $\varphi(\mathbf{y})$ is

$$\langle \varphi \rangle = \int_\Omega \varphi(\mathbf{y}) \rho(\mathbf{y}) \, dV \tag{B.2}$$

This is the standard, unconditional expected value. One might also inquire about the expected value given that $\mathbf{y}$ is in some subset $\mathcal{S}$ of Ω. This is called the *conditional expectation* of $\varphi(\mathbf{y})$ given that $\mathbf{y} \in \mathcal{S}$, and is written $\langle \varphi | \mathbf{y} \in \mathcal{S} \rangle$. There are a number of ways to express it, but for our purposes the following definition suffices.

The conditional density $\rho(\mathbf{y})$ given that $\mathbf{y} \in \mathcal{S} \subset \Omega$ is

$$\rho(\mathbf{y}|\mathbf{y} \in \mathcal{S}) = \begin{cases} \frac{\rho(\mathbf{y})}{\int_{\mathcal{S}} \rho(\mathbf{y}')\, dV_{y'}} & \mathbf{y} \in \mathcal{S} \\ 0 & \mathbf{y} \notin \mathcal{S} \end{cases} \tag{B.3}$$

Using B.3, the conditional expectation of $\varphi(\mathbf{y})$ given that $\mathbf{y} \in \mathcal{S}$ is

$$\langle \varphi(\mathbf{y}) \,|\, \mathbf{y} \in \mathcal{S} \rangle = \int_{\Omega} \varphi(\mathbf{y}) \rho(\mathbf{y} \,|\, \mathbf{y} \in \mathcal{S})\, dV = \frac{\int_{\mathcal{S}} \varphi(\mathbf{y}) \rho(\mathbf{y})\, dV}{\int_{\mathcal{S}} \rho(\mathbf{y})\, dV} \tag{B.4}$$

A special case of (B.4) occurs when $\mathcal{S}$ has no volume (Lebesgue measure zero). For example, consider the conditional expectation

$$\langle \varphi(\mathbf{y}) \,|\, w < h(\mathbf{y}) < w + \Delta w \rangle \tag{B.5}$$

for some continuous scalar function $h(\mathbf{y})$ and $\Delta w > 0$. In this example, $\mathcal{S}$ is the set $w < h(\mathbf{y}) < w + \Delta w$. If Δw is allowed to approach zero, then the Lebesgue measure of $\mathcal{S}$ approaches zero, causing the numerator and denominator in (B.4) to approach zero.

We can define

$$\langle \varphi(\mathbf{y}) \,|\, h(\mathbf{y}) = w \rangle = \lim_{\Delta w \to 0} \langle \varphi(\mathbf{y}) \,|\, w < h(\mathbf{y}) < w + \Delta w \rangle \tag{B.6}$$

whenever the limit exists. The expression is almost identical when $\mathbf{h}(\mathbf{y})$ is a vector function, except that $\mathbf{w}$ is then also a vector, and the limit must hold as the norm of $\mathbf{\Delta w}$ approaches zero.

Appendix C

Properties of the inaccessible set

In Section 2.2, the trapping region Ω is expressed as the direct sum of two subsets: $\mathcal{R}$, the set of points *not* accessible in finite time from any trajectory crossing $\partial\Omega$, and $\mathcal{R}^c$, its complement. For any $\mathbf{y} \in \mathcal{R}^c$, there is one trajectory that crosses $\partial\Omega$ and reaches $\mathbf{y}$ in a finite period of time. Some properties of $\mathcal{R}$ are derived in this appendix.

C.1 Volume (Lebesgue measure)

First, for strictly dissipative problems ($\nabla \cdot \mathbf{f} < 0$ everywhere), the volume of $\mathcal{R}$ is negligible compared to the volume of Ω. That is, the Lebesgue measure of $\mathcal{R}$, $\lambda(\mathcal{R})$, is zero.

Proof: Let $\mathcal{V}(t)$ be a set of points in phase space satisfying $\mathcal{V}(0) = \Omega$ but that evolves over time under the influence of $\mathbf{f}$. At all finite t, $\mathcal{R} \subset \mathcal{V}(t)$; if there were a point at which the boundaries crossed, that point would be accessible from $\partial\Omega$ in finite time along a trajectory, contradicting the definition of $\mathcal{R}$. Thus $\lambda(\mathcal{V}(t)) \geq \lambda(\mathcal{R})$.

We now show that there is an upper bound on $\lambda(\mathcal{V}(t))$ that approaches zero as t approaches infinity. The volume of $\mathcal{V}(t)$ is the sum of its differential elements, each of which is proportional to a Jacobian satisfying

$$\frac{dJ}{dt} = (\nabla \cdot \mathbf{f})\, J \tag{C.1}$$

along trajectories. (See Appendix A for more about J.) J begins with the value 1 at $t = 0$. Thus

the volume of the shrinking region at any time t is bounded exponentially:

$$\lambda(\mathcal{V}(t)) \leq \lambda(\Omega) \exp\left(\max_{\mathbf{y}\in\Omega} (\nabla \cdot \mathbf{f})\, t\right) \tag{C.2}$$

The divergence of $\mathbf{f}$ was assumed to be everywhere negative, so for large t the volume of $\mathcal{V}(t)$—and therefore $\lambda(\mathcal{R})$—has an upper bound that approaches zero, completing the proof.

C.2 Normal component of the velocity

Also of interest is the behavior of $\mathbf{f} \cdot \hat{\mathbf{n}}$ on $\partial\mathcal{Q}$, the inner boundary of $\mathcal{Q}^c$, as $\min T(\mathbf{Z_0}) \to \infty$, which is to say as $\mathcal{Q}$ approaches $\mathcal{R}$. Recall that the sets $\mathcal{Q}$ and $\mathcal{Q}^c$ were introduced in Section 3.2. We now show that the product of $\mathbf{f}\cdot\hat{\mathbf{n}}$ with a small unit of surface area on $\partial\mathcal{Q}$ decreases at least exponentially.

Consider a streamtube ω traversing $\mathcal{Q}^c$ from the outer surface $\partial\Omega$ to the inner surface $\partial\mathcal{Q}$. By the divergence theorem,

$$\int_{\partial\omega} \mathbf{f} \cdot \hat{\mathbf{n}}\, dS = \int_{\omega} \nabla \cdot \mathbf{f}\, dV \tag{C.3}$$

Denote the intersection of ω and the outer surface $\partial\Omega$ as $dS_{\partial\Omega}$, and that of ω and the inner surface $\partial\mathcal{Q}$ as $dS_{\partial\mathcal{Q}}$. Sides of the streamtube make no contribution to the surface integral of (C.3), and since the ends are differentially small,

$$dS_{\partial\Omega}\, \mathbf{f} \cdot \hat{\mathbf{n}}|_{\mathbf{Z_0}} - dS_{\partial\mathcal{Q}}\, \mathbf{f} \cdot \hat{\mathbf{n}}|_{\mathbf{Z}(\mathbf{Z_0}, T(\mathbf{Z_0}))} = \int_{\omega} \nabla \cdot \mathbf{f}\, dV \tag{C.4}$$

The second term on the left-hand side is negative because $\hat{\mathbf{n}}$ is oriented outward relative to $\mathcal{Q}$, which is inward relative to $\mathcal{Q}^c$.

The right-hand side of (C.4) may be expressed using the streamtube change of variables (Appendix A), leaving

$$\begin{aligned} &dS_{\partial\Omega}\, \mathbf{f} \cdot \hat{\mathbf{n}}|_{\mathbf{Z_0}} - dS_{\partial\mathcal{Q}}\, \mathbf{f} \cdot \hat{\mathbf{n}}|_{\mathbf{Z}(\mathbf{Z_0}, T(\mathbf{Z_0}))} = \\ &- dS_{\partial\Omega}\, \mathbf{f} \cdot \hat{\mathbf{n}}|_{\mathbf{Z_0}} \int_0^{T(\mathbf{Z_0})} \nabla \cdot \mathbf{f}|_{\mathbf{Z}(\mathbf{Z_0}, s)} \exp\left(\int_0^s \nabla \cdot \mathbf{f}|_{\mathbf{Z}(\mathbf{Z_0}, s')}\, ds'\right) ds \end{aligned} \tag{C.5}$$

The integrand on the right-hand side of (C.5) is of the form $\exp(-u)\,du$. After integrating and simplifying,

$$dS_{\partial\mathcal{Q}}\ \mathbf{f}\cdot\hat{\mathbf{n}}|_{\mathbf{Z}(\mathbf{Z_0},T(\mathbf{Z_0}))} = dS_{\partial\Omega}\ \mathbf{f}\cdot\hat{\mathbf{n}}|_{\mathbf{Z_0}} \exp\left(\int_0^{T(\mathbf{Z_0})} \nabla\cdot\mathbf{f}|_{\mathbf{Z}(\mathbf{Z_0},s)}\ ds\right) \tag{C.6}$$

Because the divergence of $\mathbf{f}$ is everywhere negative (the system was assumed to be dissipative), the right-hand side of (C.6) decreases exponentially as $\min T(\mathbf{Z_0}) \to \infty$, completing the proof.

Expression (C.6) only guarantees that the product of $dS_{\partial\mathcal{Q}}$ with $\mathbf{f}\cdot\hat{\mathbf{n}}$ vanishes in the limit; it does not guarantee that the factor $\mathbf{f}\cdot\hat{\mathbf{n}}$ vanishes specifically. The latter property follows from the assumed continuity of $\mathbf{f}(\mathbf{y})$. If the Lebesgue measure of $\mathcal{Q}$ approaches zero, then its thickness—the distance between boundary surfaces—must approach zero almost everywhere. If $\mathbf{f}\cdot\hat{\mathbf{n}}$ did not approach zero almost everywhere on $\partial\mathcal{Q}$, then $\mathbf{f}(\mathbf{y})$ would thus be required to make a discontinuous jump across it, violating the assumption of continuity.

C.3 Limitation on the density growth rate

One application for (C.6) is to eliminate the third possibility for equation (3.3), which was that $\int_{\partial\mathcal{Q}^c} \rho\mathbf{f}\cdot\hat{\mathbf{n}}\,dS = 0$, but $\rho\mathbf{f}\cdot\hat{\mathbf{n}} \neq 0$ over a nonnegligible part of $\partial\mathcal{Q}^c$. The integral over $\partial\mathcal{Q}^c$ is the sum of that over $\partial\Omega$ and that (negated) over $\partial\mathcal{Q}$. Thus if $\int_{\partial\mathcal{Q}^c} \rho\mathbf{f}\cdot\hat{\mathbf{n}}\,dS = 0$, then

$$\int_{\partial\Omega} \rho(\mathbf{Z_0})\ \mathbf{f}\cdot\hat{\mathbf{n}}|_{\mathbf{Z_0}}\ dS_{\partial\Omega} - \int_{\partial\mathcal{Q}^c} \mathbf{f}\cdot\hat{\mathbf{n}}|_{\mathbf{Z}(\mathbf{Z_0},T(\mathbf{Z_0}))}\,\rho(\mathbf{Z}(\mathbf{Z_0},T(\mathbf{Z_0})))\,dS_{\partial\mathcal{Q}} = 0 \tag{C.7}$$

Again, the negative sign is due to the reversed orientation of normals to $\partial\mathcal{Q}$ relative to those of $\mathcal{Q}^c$.

Multiplying both sides of (C.6) by $\rho(\mathbf{Z}(\mathbf{Z_0},T(\mathbf{Z_0})))$ and summing over streamtubes,

$$\begin{aligned}&\int_{\partial\mathcal{Q}} \rho(\mathbf{Z}(\mathbf{Z_0},T(\mathbf{Z_0})))\ \mathbf{f}\cdot\hat{\mathbf{n}}|_{\mathbf{Z}(\mathbf{Z_0},T(\mathbf{Z_0}))}\,dS_{\partial\mathcal{Q}} = \\ &\int_{\partial\Omega} \rho(\mathbf{Z}(\mathbf{Z_0},T(\mathbf{Z_0})))\ \mathbf{f}\cdot\hat{\mathbf{n}}|_{\mathbf{Z_0}} \exp\left(\int_0^{T(\mathbf{Z_0})} \nabla\cdot\mathbf{f}|_{\mathbf{Z}(\mathbf{Z_0},s)}\ ds\right) dS_{\partial\Omega}\end{aligned} \tag{C.8}$$

Substituting from (C.8) into (C.7),

$$\int_{\partial\Omega} \rho(\mathbf{Z_0})\, \mathbf{f}\cdot\hat{\mathbf{n}}|_{\mathbf{Z_0}} \left(1 - \frac{\rho(\mathbf{Z}(\mathbf{Z_0}, T(\mathbf{Z_0})))}{\rho(\mathbf{Z_0})} \exp\left(\int_0^{T(\mathbf{Z_0})} \nabla\cdot\mathbf{f}|_{\mathbf{Z}(\mathbf{Z_0},s)}\, ds\right)\right) dS_{\partial\Omega} = 0 \qquad \text{(C.9)}$$

Region Ω was assumed to be trapping, so on its boundary $\partial\Omega$, $\rho(\mathbf{Z_0})\, \mathbf{f}\cdot\hat{\mathbf{n}}|_{\mathbf{Z_0}}$ cannot be positive. If it differed from zero on a set of finite measure, as was assumed, then for (C.9) to hold, the expression in parentheses would have to be zero almost everywhere on that set. That would require $\rho(\mathbf{Z}(\mathbf{Z_0}, T(\mathbf{Z_0})))$ to grow at least exponentially—which happens to match the rate that the streamtube Jacobian (A.3) decays. Thus the fraction of probability mass beyond any isosurface of fixed s would have to approach unity as $\min T(\mathbf{Z_0}) \to \infty$, violating condition (3.1).

Appendix D

Derivation of the asymptotic approach conditions by variational calculus

D.1 Derivation of the governing equations

This appendix details the constrained minimization of κ, as defined in equation (3.9), with respect to $\rho(\mathbf{y})$. Repeating the definition here for reference,

$$\kappa = \int_{\mathcal{Q}^c} \left(\frac{\partial}{\partial y_i} \left(f_i \left(\mathbf{y} \right) \rho \left(\mathbf{y} \right) \right) \right)^2 dV$$

Our reasoning follows Weinstock (1974).

There is only one constraint that leads to a Lagrange multiplier: that $\rho(\mathbf{y})$ be properly normalized, as mandated by equation (1.4). In a form suitable for minimization, it is

$$\left(\int_{Q_c} \rho(\mathbf{y}) \, dV - 1 \right) = 0 \tag{D.1}$$

At the constrained minimum point, then, the following expression is stationary with respect to both $\rho(\mathbf{y})$ and the Lagrange multiplier λ:

$$\int_{\mathcal{Q}^c} \left(\frac{\partial}{\partial y_i} \left(f_i \left(\mathbf{y} \right) \rho \left(\mathbf{y} \right) \right) \right)^2 dV - \lambda \left(\int_{\mathcal{Q}^c} \rho(\mathbf{y}) \, dV - 1 \right) \tag{D.2}$$

Suppose $\rho(\mathbf{y})$ minimizes expression (D.2). Let $\eta(\mathbf{y})$ be any bounded twice-differentiable function over $\mathcal{Q}^c$. For a given choice of $\eta(\mathbf{y})$, there is a one-parameter family of test functions:

$$P(\mathbf{y};\epsilon) = \rho(\mathbf{y}) + \epsilon\eta(\mathbf{y}) \tag{D.3}$$

Clearly, $P(\mathbf{y};0) = \rho(\mathbf{y})$ irrespective of which test function $\eta(\mathbf{y})$ is chosen.

For notational convenience, let

$$g(y, P, \frac{\partial P}{\partial y_1}, \cdots, \frac{\partial P}{\partial y_N}, \lambda) = \left(\frac{\partial}{\partial y_i}\left(f_i\left(\mathbf{y}\right)P\left(\mathbf{y};\epsilon\right)\right)\right)^2 - \lambda\left(P(\mathbf{y};\epsilon) - \frac{1}{\int_{\mathcal{Q}^c} dV}\right) \tag{D.4}$$

Further, let $I(\epsilon)$ be defined as

$$I(\epsilon) = \int_{\mathcal{Q}^c} g(y, P, \frac{\partial P}{\partial y_1}, \cdots, \frac{\partial P}{\partial y_N}, \lambda)\, dV \tag{D.5}$$

Then for any choice of $\eta(\mathbf{y})$, $I'(\epsilon)$ is zero at the minimum point, which is at $\epsilon = 0$ (where $P(\mathbf{y};\epsilon) = \rho(\mathbf{y})$).

$$I'(0) = 0 \tag{D.6}$$

To find $I'(0)$, we differentiate (D.5), make use of (D.3), and integrate by parts:

$$\begin{aligned} I'(\epsilon) &= \int_{\mathcal{Q}^c} \frac{\partial g}{\partial P}\frac{dP}{d\epsilon} + \frac{\partial g}{\partial(\partial P/\partial y_i)}\frac{d(\partial P/\partial y_i)}{d\epsilon}\, dV \\ &= \int_{\mathcal{Q}^c} \frac{\partial g}{\partial P}\eta(\mathbf{y}) + \frac{\partial g}{\partial(\partial P/\partial y_i)}\frac{\partial \eta}{\partial y_i}\, dV \\ &= \int_{\mathcal{Q}^c} \left(\frac{\partial g}{\partial P} - \frac{\partial}{\partial y_i}\left(\frac{\partial g}{\partial(\partial P/\partial y_i)}\right)\right)\eta(\mathbf{y})\, dV + \int_{\partial\mathcal{Q}^c}\left(\frac{\partial g}{\partial(\partial P/\partial y_i)}\hat{n}_i\right)\eta(\mathbf{y})\, dS \end{aligned} \tag{D.7}$$

From (D.4),

$$\left.\frac{\partial g}{\partial P}\right|_{\epsilon=0} = 2\left(\frac{\partial}{\partial y_j}\left(f_j(\mathbf{y})\rho(\mathbf{y})\right)\right)\frac{\partial f_i}{\partial y_i} - \lambda \tag{D.8}$$

and

$$\left.\frac{\partial g}{\partial(\partial P/\partial y_i)}\right|_{\epsilon=0} = 2\left(\frac{\partial}{\partial y_j}\left(f_j(\mathbf{y})\rho(\mathbf{y})\right)\right)f_i \tag{D.9}$$

Thus

$$
\begin{aligned}
&I'(0) \\
&\quad = \int_{\mathcal{Q}^c} \left(2 \left(\frac{\partial}{\partial y_j} \left(f_j(\mathbf{y}) \rho(\mathbf{y}) \right) \right) \frac{\partial f_i}{\partial y_i} - \lambda - \frac{\partial}{\partial y_i} \left(2 \left(\frac{\partial}{\partial y_j} \left(f_j(\mathbf{y}) \rho(\mathbf{y}) \right) \right) f_i \right) \right) \eta(\mathbf{y}) \, dV \\
&\quad + \int_{\partial \mathcal{Q}^c} \left(2 \left(\frac{\partial}{\partial y_j} \left(f_j(\mathbf{y}) \rho(\mathbf{y}) \right) \right) f_i \hat{n}_i \right) \eta(\mathbf{y}) \, dS
\end{aligned}
\tag{D.10}
$$

which simplifies to

$$
\begin{aligned}
I'(0) = &- \int_{\mathcal{Q}^c} \left(\lambda + 2 f_i \frac{\partial}{\partial y_i} \left(\frac{\partial}{\partial y_j} \left(f_j(\mathbf{y}) \rho(\mathbf{y}) \right) \right) \right) \eta(\mathbf{y}) \, dV \\
&+ 2 \int_{\partial \mathcal{Q}^c} \left(\left(\frac{\partial}{\partial y_j} \left(f_j(\mathbf{y}) \rho(\mathbf{y}) \right) \right) f_i \hat{n}_i \right) \eta(\mathbf{y}) \, dS
\end{aligned}
\tag{D.11}
$$

Equation (D.11) must equal zero for all bounded, twice-differentiable test functions $\eta(\mathbf{y})$ on $\mathcal{Q}^c$, so in particular it must be zero for those $\eta(\mathbf{y})$ that vanish on the boundary $\partial \mathcal{Q}^c$. For these, the volume integral must itself be equal to zero, and so—by a basic lemma of variational calculus—what remains of the integrand vanishes pointwise over $\mathcal{Q}^c$:

$$
f_i \frac{\partial}{\partial y_i} \left(\frac{\partial}{\partial y_j} \left(f_j(\mathbf{y}) \rho(\mathbf{y}) \right) \right) = -\frac{\lambda}{2} \qquad \forall y \in \mathcal{Q}^c \tag{D.12}
$$

We recognize (D.12) as an Euler-Lagrange equation for $\rho(\mathbf{y})$.

If (D.12) holds, then the volume integral in (D.11) vanishes for all $\eta(\mathbf{y})$, including those that are nonzero on $\partial \mathcal{Q}^c$, so the surface integral of (D.11) must separately vanish. Applying the same lemma, but now over $\partial \mathcal{Q}^c$, leaves

$$
\left(\frac{\partial}{\partial y_j} \left(f_j(\mathbf{y}) \rho(\mathbf{y}) \right) \right) \left(f_i \hat{n}_i \right) = 0 \qquad \forall y \in \partial \mathcal{Q}^c \tag{D.13}
$$

Equation (D.12) is a second-order linear partial differential equation for $\rho(\mathbf{y})$, and equation (D.13) is its boundary condition. The Lagrange multiplier λ is determined by enforcing constraint (D.1).

D.2 Parabolicity

Equation (D.12) is second-order and linear; we now show that moreover it is parabolic. Expanding out the left-hand side,

$$f_i f_j \frac{\partial^2 \rho}{\partial y_i \partial y_j} + \cdots = -\frac{\lambda}{2} \tag{D.14}$$

where the $\cdots$ represent terms of first-order and below. The components of any two columns (fixed j) of the dyadic product matrix $f_i f_j$ have a fixed ratio (the ratio of the corresponding f_i components) and thus are linearly dependent. The determinant of a matrix is nonzero if and only if its columns are linearly independent, so the determinant of the $f_i f_j$ matrix is zero. Second-order partial differential equations whose coefficient matrix is zero are called parabolic. Thus equation (D.12) is parabolic.

Appendix E

Solution of the asymptotic approach equations

This appendix provides a detailed solution to the asymptotic approach equations from Section 3.4 along characteristics.

E.1 General solution by the method of characteristics

Along characteristic curves (3.12), equation (3.10) may be written

$$\frac{d}{ds}\left(\frac{d\rho}{ds} + (\nabla \cdot \mathbf{f})\rho\right) = -\frac{\lambda}{2} \tag{E.1}$$

for $\rho(\mathbf{Z}(\mathbf{Z_0}, s))$ with $\mathbf{Z_0}$ held constant. Integrating (E.1) once yields

$$\frac{d\rho}{ds} + (\nabla \cdot \mathbf{f})\rho = -\lambda s/2 + C_1(\mathbf{Z_0}) \tag{E.2}$$

Because the solution takes place over $\mathcal{Q}^c$, each characteristic's $\mathbf{Z_0}$ can be placed on the entrance boundary $\partial\Omega$ (where $s = 0$) without loss of generality. Applying condition (3.11) there reveals the constant $C_1(\mathbf{Z_0})$ to be zero at all $\mathbf{Z_0}$. What remains is an inhomogeneous linear first-order ODE for $\rho(\mathbf{Z}(\mathbf{Z_0}, s))$.

Upon setting $C_1(\mathbf{Z_0}) = 0$, equation (E.2) may be solved via the integrating factor $M(\mathbf{Z_0}, s)$:

$$M(\mathbf{Z_0}, s) = \exp\left(\int_0^s \nabla \cdot \mathbf{f}|_{\mathbf{Z}(\mathbf{Z_0}, s')}\, ds'\right) \tag{E.3}$$

Using $M(\mathbf{Z_0}, s)$, equation (E.2) may then be written

$$\frac{d}{ds}(\rho M) = -\frac{\lambda}{2} M s \tag{E.4}$$

which has the solution

$$\rho(\mathbf{Z}(\mathbf{Z_0}, s)) = -\frac{\lambda}{2M(\mathbf{Z_0}, s)} \int_0^s M(\mathbf{Z_0}, s')\; s'\, ds' + \frac{C_2(\mathbf{Z_0})}{M(\mathbf{Z_0}, s)} \tag{E.5}$$

where the integration constant $C_2(\mathbf{Z_0})$ is not yet determined. On the inner boundary $\partial\mathcal{Q}$, $\mathbf{f} \cdot \hat{\mathbf{n}}$ approaches zero (see Appendix C, Section C.2), so (3.11) provides no new information about it. $C_2(\mathbf{Z_0})$ can be determined, however, by requiring that the solution satisfy (3.1).

In Section 3.2, the sets $\mathcal{Q}$ and $\mathcal{Q}^c$ were created to avoid the mathematically problematic limit set $\mathcal{R}$ of points inaccessible from the boundary in finite time. The location of the border separating $\mathcal{Q}$ and $\mathcal{Q}^c$ was a smooth function $T(Z_0)$ of time elapsed along trajectories entering Ω. As $\min T(\mathbf{Z_0}) \to \infty$, $\rho(\mathbf{y})$ becomes more and more concentrated near $\mathcal{R}$, but cannot be allowed to approach a Dirac delta.

Let $0 < s_1 < \min T(\mathbf{Z_0})$ be a finite intermediate time and let α be the event that a measurement is taken when $s_b(\mathbf{y}) > s_1$. Then constraint (3.1) requires that

$$\lim_{s_1 \to \infty} \left(\lim_{\min T(\mathbf{Z_0}) \to \infty} \Pr(\alpha) \right) = 0 \tag{E.6}$$

But

$$\Pr(\alpha) = \int_{y \in \mathcal{Q}^c : s_b(\mathbf{y}) > s_1} \rho(\mathbf{y})\, dV \tag{E.7}$$

To evaluate (E.7), it is helpful to change variables as described in Appendix A. By a serendipitous

coincidence of equations (E.3) and (A.3),

$$\mathcal{J}(\mathbf{Z_0}, s) = -\mathbf{f}(\mathbf{Z_0}) \cdot \hat{\mathbf{n}}(\mathbf{Z_0})\, M(\mathbf{Z_0}, s) \tag{E.8}$$

Substituting the new Jacobian into E.7,

$$\Pr(\alpha) = \int_{\partial\Omega} -\mathbf{f}(\mathbf{Z_0}) \cdot \hat{\mathbf{n}}(\mathbf{Z_0}) \left(\int_{s_1}^{T(\mathbf{Z_0})} \left(-\frac{\lambda}{2} \int_0^s M(\mathbf{Z_0}, s')s'\, ds' + C_2(\mathbf{Y_0}) \right) ds \right) dS \tag{E.9}$$

On $\partial\Omega$, $\mathbf{f} \cdot \hat{\mathbf{n}} \leq 0$ (since Ω is a trapping region), so for (E.6) to be zero, equation (E.9) requires

$$\lim_{\min T(\mathbf{Z_0}) \to \infty} \left(\lim_{s_1 \to \infty} \left(\int_{s_1}^{T(\mathbf{Z_0})} \left(-\frac{\lambda}{2} \int_0^s M(\mathbf{Z_0}, s')s'\, ds' + C_2(\mathbf{Y_0}) \right) ds \right) \right) = 0 \tag{E.10}$$

In the joint limit, the length of the interval from s_1 to $T(\mathbf{Z_0})$ can be anywhere from zero to infinity depending on the direction of approach, so for the limit to exist and be zero, the integrand must vanish. The upper limit of integration is bounded above and below by ∞. Hence,

$$-\frac{\lambda}{2} \int_0^\infty M(\mathbf{Z_0}, s')s'\, ds' + C_2(\mathbf{Z_0}) = 0 \tag{E.11}$$

and so finally,

$$C_2(\mathbf{Z_0}) = \frac{\lambda}{2} \int_0^\infty M(\mathbf{Z_0}, s')s'\, ds' \tag{E.12}$$

With constraint (3.1) taken into account, (E.5) is therefore

$$\rho(\mathbf{Z}(\mathbf{Z_0}, s)) = \frac{\lambda}{2M(\mathbf{Z_0}, s)} \int_s^\infty M(\mathbf{Z_0}, s')s'\, ds' \tag{E.13}$$

The constant Lagrange multiplier λ is determined by enforcing the normalization constraint (1.4).

E.2 Simplifying when divergence is constant

When $\nabla \cdot \mathbf{f}$ is a negative constant, equation (E.13) simplifies to

$$\rho(\mathbf{Z}(\mathbf{Z_0}, s)) = \frac{\lambda}{2(-\nabla \cdot \mathbf{f})} \left(s + \frac{1}{(-\nabla \cdot \mathbf{f})} \right) \tag{E.14}$$

An immediate consequence of (E.14) is that $\rho(\mathbf{y})$ is constant when s is constant. In particular, $\rho(\mathbf{y})$ has the constant value $\lambda/(2(\nabla \cdot \mathbf{f})^2)$ on boundary $\partial\Omega$. It is also possible to express λ more compactly when $\nabla \cdot \mathbf{f}$ is a constant:

$$\lambda = \frac{(\nabla \cdot \mathbf{f})^3}{\int_{\partial\Omega} \mathbf{f} \cdot \hat{\mathbf{n}} \, dS} \tag{E.15}$$

The numerator and denominator in this expression are both negative. Again, results (E.14) and (E.15) only hold when $\nabla \cdot \mathbf{f}$ is a negative constant; if $\nabla \cdot \mathbf{f}$ varies, then the boundary value may vary as well.

E.3 Bounding alternatives for the asymptotic approach integral

Recall that in Section 3.3, some uncertainty surrounded the choice of bounds for the asymptotic approach integral (3.5). We chose to bound it using the Cauchy-Schwartz inequality, but noted that equally reasonable alternatives exist. For example, a different Hölder inequality could have been applied, or we could have multiplied and divided by a function of $\rho(\mathbf{y})$ first, before splitting the integral. Because the choice was ultimately arbitrary, there remains a lingering uncertainty about the result: What if our choice had been different? Ultimately, how unique an experimental condition is asymptotic approach?

We now demonstrate that a variety of other paths taken at that point would have ultimately led to similar, or even identical, moments.

The partial differential equations and boundary condition for $\rho_{\text{asymptoticapproach}}(\mathbf{y})$, (D.12) and

(D.13), were derived by minimizing κ (3.9) subject to the normalization constraint (1.4).

If some other bounding choice were made, then κ would have taken a different form. The first step in analysis, then, is to identify the other forms it might have taken.

For notational purposes, in this section only:

- Let $\alpha(a)$ be any bounded, continuous, twice-differentiable function of $a \in \mathbb{R}$ satisfying $\alpha(a) > 0$ and $\alpha'(a) > 0$.
- Let $\beta(\rho)$ be any bounded, continuous, differentiable function of $\rho(\mathbf{y})$ satisfying $\beta(\rho(\mathbf{y})) > 0$ for $\mathbf{y} \in \Omega$.
- Let $\nabla \cdot \rho\mathbf{f}$ denote the quantity
$$\frac{\partial}{\partial y_i}\left(\rho(\mathbf{y}) f_i(\mathbf{y})\right)$$

In terms of these, the original κ of (3.9) had the form

$$\int_{\mathcal{Q}^c} \alpha\left(\left(\nabla \cdot \rho\mathbf{f}\right)^2\right) \beta(\rho(\mathbf{y}))\, dV \tag{E.16}$$

with $\alpha(a) = a$ and $\beta(\rho) = 1$.

Critically, many—perhaps all—reasonable bounding choices would have led to this same form, differing only in the functions $\alpha(a)$ and $\beta(\rho)$. How dependent, then, is the solution upon the choices of $\alpha(a)$ and $\beta(\rho)$?

Following the derivation in Appendix D, the first important difference would have been in the definition of g, given in equation (D.4). It would become

$$g(y, P, \frac{\partial P}{\partial y_1}, \cdots, \frac{\partial P}{\partial y_N}, \lambda) = \alpha\left(\left(\frac{\partial}{\partial y_i}\left(f_i\left(\mathbf{y}\right) P\left(\mathbf{y};\epsilon\right)\right)\right)^2\right) \beta(P(\mathbf{y};\epsilon)) - \lambda\left(\cdots\right) \tag{E.17}$$

where the term in parentheses $(\cdots)$ does not differ from its value in (D.4). The next changes occur

in (D.8) and (D.9), which become, respectively,

$$\left.\frac{\partial g}{\partial P}\right|_{\epsilon=0} = 2\,\alpha'\left(\left(\nabla\cdot\rho\mathbf{f}\right)^2\right)\left(\nabla\cdot\rho\mathbf{f}\right)\left(\nabla\cdot\mathbf{f}\right)\beta(\rho) + \alpha\left(\left(\nabla\cdot\rho\mathbf{f}\right)^2\right)\beta'(\rho) - \lambda \tag{E.18}$$

and

$$\left.\frac{\partial g}{\partial(\partial P/\partial y_i)}\right|_{\epsilon=0} = 2\,\alpha'\left(\left(\nabla\cdot\rho\mathbf{f}\right)^2\right)\left(\nabla\cdot\rho\mathbf{f}\right)\left(f_i\right)\beta(\rho) \tag{E.19}$$

The manipulations that follow parallel those of Appendix D; the resulting Euler-Lagrange equation, analogous to (D.12), becomes

$$f_j\frac{\partial}{\partial y_j}\left(\alpha'\left(\left(\nabla\cdot\rho\mathbf{f}\right)^2\right)\left(\nabla\cdot\rho\mathbf{f}\right)\beta(\rho)\right) - \frac{1}{2}\alpha\left(\left(\nabla\cdot\rho\mathbf{f}\right)^2\right)\beta'(\rho) = -\frac{\lambda}{2} \tag{E.20}$$

The effective boundary condition (equation D.13) remains unchanged, having merely been multiplied by a nonzero factor.

The derivative expressions in (E.20) are all of the form $f_i\frac{\partial}{\partial y_i}$. It follows that *characteristics of (E.20) coincide with trajectories* as well. Because equations (D.12) and (E.20) have identical families of characteristics, their solutions exhibit certain similarities.

In particular, when $\nabla\cdot\mathbf{f}$ is a constant, both solutions can only be functions of s. Hence, their isosurfaces coincide. If, when studying the asymptotic approach of a system having constant negative divergence, one considers only moments that are conditioned on s, then alternative choices for the bounds on integral (3.5) will not affect the outcome.

Bibliography

G. D. Birkhoff. Proof of the ergodic theorem. *Proceedings of the National Academy of Sciences*, 17: 656–660, 1931.

R. Bowen and D. Ruelle. The ergodic theory of Axiom A flows. *Invent. Math.*, 29:181–202, 1975.

M. Dellnitz and O. Junge. On the approximation of complicated dynamical behavior. *SIAM Journal on Numerical Analysis*, 36:491–515, 1999.

Z. C. Feng and L. G. Leal. Nonlinear bubble dynamics. *Annual Review of Fluid Mechanics*, 29: 201–243, 1997.

G. Froyland and M. Dellnitz. Detecting and locating near-optimal almost-invariant sets and cycles. *SIAM Journal of Scientific Computing*, 24:1839–1863, 2003.

G. Gallavotti and E. G. D. Cohen. Dynamical ensembles in nonequilibrium statistical mechanics. *Physical Review Letters*, 74:2694–2697, 1995.

T. Gotoh and R. H. Kraichnan. Statistics of decaying Burgers turbulence. *Physics of Fluids A*, 5: 445–457, 1993.

T. J. R. Hughes, L. Mazzei, and A. A. Oberai. The multiscale formulation of large eddy simulation: Decay of homogeneous isotropic turbulence. *Physics of Fluids*, 13:505–512, 2001.

E. T. Jaynes. Information theory and statistical mechanics. *Physical Review*, 106:620–630, 1957.

E. T. Jaynes. *Maximum Entropy and Bayesian Methods*, pages 1–27. Kluwer Academic Publishers, Dordrecht, 1989.

Y. Kaneda, T. Ishihara, M. Yokokawa, K. Itakura, and A. Uno. Energy dissipation rate and energy spectrum in high resolution direct numerical simulations of turbulence in a periodic box. *Physics of Fluids*, 15:L21–L24, 2003.

E. N. Lorenz. Deterministic nonperiodic flow. *Journal of the Atmospheric Sciences*, 20:130–141, 1963.

A. Majda and A. Bertozzi. *Vorticity and Incompressible Flow.* Cambridge University Press, Cambridge, UK, 2002.

P. Moin and K. Mahesh. Direct numerical simulation: A tool in turbulence research. *Annual Review of Fluid Mechanics*, 30:539–578, 1998.

R. D. Moser, J. Kim, and N. N. Mansour. Direct numerical simulation of turbulent channel flow up to $Re_\tau = 590$. *Physics of Fluids*, 11:943–945, 1999.

S. A. Orszag and G. S. Patterson, Jr. Numerical simulation of three-dimensional homogeneous isotropic turbulence. *Physical Review Letters*, 28:76–79, 1972.

A. Y. Pogromsky, G. Santoboni, and H. Nijmeijer. An ultimate bound on the trajectories of the Lorenz system and its applications. *Nonlinearity*, 16:1597–1605, 2003.

D. Ruelle. A measure associated with Axiom A attractors. *Amer. J. Math.*, 98:619–654, 1976.

D. Ruelle. Conversations on nonequilibrium physics with an extraterrestrial. *Physics Today*, 57: 48–53, 2004.

C. E. Shannon. A mathematical theory of communication. *The Bell System Technical Journal*, 27: 379–423, 1948.

Y. G. Sinai. Gibbs measures in ergodic theory. *Russ. Math. Surv.*, 27:21–69, 1972.

J. Smagorinsky. General circulation experiments with the primitive equations. *Mon. Weather Rev.*, 91:99–164, 1963.

M. Tanguay. *Computation of bubbly cavitating flow in shock wave lithotripsy*. Ph.D. thesis, California Institute of Technology, May 2004.

R. Temam. Approximation of attractors, large eddy simulations and multiscale methods. *Proceedings: Mathematical and Physical Sciences*, 434:23–29, 1991.

W. Tucker. A rigorous ODE solver and Smale's 14th problem. *Foundations of computational mathematics*, 2:53–117, 2002.

L. van Veen and S. Kida. Periodic motion in high-symmetric flow. In Shigeo Kida, editor, *IUTAM Symposium on Elementary Vortices and Coherent Structures: Significance in Turbulence Dynamics*, pages 93–103. Springer, 2006.

R. Weinstock. *Calculus of Variations*. Dover Publications, Inc., Mineola, NY, USA, 1974.

L.-S. Young. What are SRB measures, and which dynamical systems have them? *Journal of Statistical Physics*, 108:733–754, 2002.